The Role of Superoxide Dismutase 2 in Modulating Sickle Cell Disease Pathology

by

Atinuke Oyinkansola Modupe Aramide Dosunmu-Ogunbi

Bachelors of Science, University of Pittsburgh, 2014

Submitted to the Graduate Faculty of the

School of Medicine in partial fulfillment

of the requirements for the degree of

Doctor of Philosophy

University of Pittsburgh

2021

UNIVERSITY OF PITTSBURGH
SCHOOL OF MEDICINE

This dissertation was presented

by

Atinuke Oyinkanosla Modupe Aramide Dosunmu-Ogunbi

It was defended on

October 14, 2021

and approved by

Sruti Shuva, Professor, Department of Pharmacology & Chemical Biology

Enrico Novelli, Associate Professor, Department of Pharmacology & Chemical Biology

Bruce Freeman, UPMC/Irwin Fridovich Distinguished Professor and Chair, Department of Pharmacology & Chemical Biology

Cheryl Hillery, Professor, Department of Pediatrics

Dissertation Director: Adam Straub, Associate Professor, Department of Pharmacology & Chemical Biology

The Role of Superoxide Dismutase 2 in Modulating sickle Cell Disease Pathology

Atinuke Oyinkansola Modupe Aramide Dosunmu-Ogunbi, PhD

University of Pittsburgh, 2021

Sickle cell disease (SCD) is an inherited hemoglobinopathy resulting from a point mutation in the β-globin gene. This substitution leads to polymerization of sickle hemoglobin (HbS) under deoxygenated conditions and sickling of red blood cells (RBCs). Sickled RBCs can block the microvasculature causing vaso-occlusions and hemolyze releasing free hemoglobin and heme into the intravascular space. These processes cause an increase in the production of reactive oxygen species (ROS). Despite there being an increase in ROS production, there is a decrease in the antioxidant defense system. Superoxide dismutase 2 (SOD2) is an enzymatic antioxidant found only within the mitochondria which functions to dismutate superoxide to hydrogen peroxide. Given the decrease in antioxidants in SCD and that SOD2 is a known regulator of vascular function, this thesis project sought to identify whether SOD2 could modify SCD pathology.

In aim 1, we identified that a common polymorphism of SOD2, SOD2 V16A, is strongly associated with clinical indicators of pulmonary hyper`tension in SCD patients. In human pulmonary arterial endothelial cells (HPAECs), we found that this polymorphism pathologically associates with complex IV of the respiratory chain leading to a decrease in complex activity and mitochondrial respiration. HPAECs transduced with SOD2 V16A also had increased ROS production which was exacerbated with inhibition of complex III of the respiratory chain. In aim 2, we found that SOD2 protein expression is decreased in the pulmonary endothelium of SCD patients. In addition to this, we discovered that SOD2 protein expression was decreased in whole

lung tissue of transgenic sickle mice. Given its significant decrease in sickle conditions, we went on to further define the function of SOD2 in the pulmonary endothelium using human pulmonary microvascular endothelial cells (HPMVECs). In HPMVECs, SOD2 deficiency led to a disruption in barrier function as well as a decrease in migration and proliferation. We found that these reduced functions were linked to a reduction in adhesion stemming from dysregulation of fibronectin processing. Altogether, we are the first to thoroughly investigate the role of SOD2 within the endothelium, and our findings can aide in the development of new therapeutics in the treatment of SCD patients.

Table of Contents

List of Tables

List of Figures

Preface

I would like to dedicate this work to my grandparents and parents, I am proud to continue the line of Dosunmu-Ogunbi scientists and physicians.

Acknowledgements

I am very grateful to Dr. Richard Steinman and the University of Pittsburgh/Carnegie Mellon University Medical Scientist Training Program (MSTP) for giving me the opportunity to develop the skills and acquire the knowledge to become a physician scientist.

I would also like to acknowledge the American Society of Hematology for helping fund this project and to show my appreciation for the opportunities that I have been afforded as a recipient of their training awards.

To my mentor—Dr. Adam Straub—your passion for research has been motivating and inspiring in some of the most frustrating times. Thank you for guiding me throughout this process and teaching me how to be a good scientist.

I would also like to thank the members of my committee, Drs. Enrico Novelli, Sruti Shiva, Cheryl Hillery, and Bruce Freeman, thank you for your expert advice and support for this project.

To all the members of the Straub lab past and present, I could not have done this without you. Megan, there is no way the lab could function without your organization skills. Scott, your prowess as a mouse surgeon made all my animal experiments possible. Katherine and Heidi, thank you for being the only other two people in the lab studying SCD and helping me with bone marrow transplants. Sanker, you are truly a whiz at molecular biology, thank you for helping me design and make plasmid constructs. Brittany and Joe, you both impressed me every day with your knowledge and your excitement for all things scientific, thank you for your inciteful feedback. To my self-proclaimed postdoc mini-mentor, Shuai, you have taught me so much in

this short time we've spent together. I am infinitely grateful for the new techniques you have taught me and your help in editing my manuscripts.

To my father and mother—Drs. Adedoyin and Sesi Dosunmu-Ogunbi—I thank you for your guidance throughout my life and demonstrating every day a passion for medicine and your patients.

To my brother and sister—Olu and Wami—the dedication you demonstrate in chasing after your dreams and goals in life is inspiring.

To my husband, soulmate, and best friend—Joshua Willliam Tashman, PhD—I am so blessed to have you in my life. Having you as someone I can talk to and confide in every day has helped me keep focused on my goals in life.

To my dogs—Raphael and Cassie—this is all for you.

And most of all for God—"Your word is a lamp to guide my feet, and a light for my path." Psalm (119:105)

.

1.0 Introduction

Hemoglobinopathies are one of the most common inherited diseases worldwide afflicting more than 330,000 infants born annually and attributing to 3.4% of deaths in children less than 5 years of age[1]. Hemoglobinopathies encompass all inherited diseases of hemoglobin. There are two categories of hemoglobinopathies: variants of structural hemoglobin and thalassemia syndromes. Within these two categories there is further subcategorization: HbS, HbE, and HbC are the most common structural hemoglobin abnormalities[1] while α- and β-thalassemias encompass the majority of thalassemias[1-3]. Within these groups there are further subtypes and combined types[2]. Sickle cell disease (SCD) is a type of structurally abnormal hemoglobinopathy[4,5].

There are three types of structurally normal hemoglobin, HbA(2), HbA (adult hemoglobin), and HbF (fetal hemoglobin)[6], each is a tetramer composed of two α-globins and either two δ-, β-, or γ-globins[6,7]. Fetal hemoglobin (α(2)γ(2)) is the dominant hemoglobin form found in neonates[8] and its high affinity for oxygen plays an essential role for the transport of oxygen between maternal and fetal circulations[9,10]. In older children and adults HbA (α(2)β(2)) predominates with HbA(2) (α(2)δ(2)) found at low levels throughout the life cycle[8]. Structural hemoglobinopathies occur when there are mutations in the genes responsible for the regulation of the structure of α-, δ-, β-, or γ-globins[7]. SCD is caused by a point mutation in β-globin[5] which results in polymerization of sickle hemoglobin (HbS) and sickling of red blood cells (RBC)[5,11].

1.1 Sickle Cell Disease

Worldwide 112 per 100,000 children are born with SCD[12]. Although Africa holds the highest disease burden at 1,125 per 100,000 live births[12], in the United States SCD is the most common genetic disorder afflicting 1 in 500 African Americans[13]. SCD has a large economic impact with nearly $3 billion spent annually on outpatient, inpatient, and emergency room visits[14]. In addition to this direct cost, there is an indirect economic burden of $15,000 lost annually per person due to unpaid work productivity[15]. Furthermore, individuals with SCD have a reduced life expectancy of 54 years compared to sex and race/ethnicity matched controls[16]. Throughout this diminished life span, SCD patients suffer from vascular damage resulting in chronic painful crises, organ damage, and repeated hospital visits[16].

SCD affects the RBCs which are found throughout the body, meaning no organ system is spared from the effects of the disease pathology. For instance, there is an increased risk of development of neurological complications such as silent and overt strokes, cognitive difficulties, and microstructural injuries[17]. Increased vascular proliferation within the eye can lead to visual impairment and blindness[18]. In the pulmonary system, acute chest syndrome and pulmonary hypertension result in the highest rates of mortality in SCD[19]. The major cardiovascular complications consist of left ventricular diastolic heart disease, sudden death, and dysrhythmia[20]. Renal complications such as chronic kidney disease, hematuria, impaired urine concentrating, acute kidney injury, hypertrophy, altered hemodynamics, and distal nephron dysfunction contribute significantly to shortened life expectancy of SCD patients[21]. Lastly, involvement of the bones and joints are the most common cause of chronic pain with bone destruction in the femoral head and avascular necrosis and involvement of the hip being most typical[22]. All these chronic

complications contribute to the diminished quality of life of SCD patients. While recent advancements in care have greatly reduced infant mortality, there is still a paucity of treatment options[23] highlighting the need for further study into disease modifying pathways.

SCD is the consequence of a single nucleotide substitution (GTG for GAG) at the sixth amino acid of the β-globin gene which is located on the short arm of chromosome 11[24]. This nucleotide change inserts nonpolar, hydrophobic valine in place of negatively charged glutamic acid on the surface of the β-globin chain, leading to the polymerization of deoxygenated, abnormal sickle hemoglobin (HbS)[5]. HbS polymerization deforms the RBC into a sickle, crescent-like shape. Repeated sickling of RBCs results in membrane fragility and hemolysis, occlusion of post-capillary venules, ischemia-reperfusion, and infarction. Vaso-occlusions are the result of decreased capability of deformed RBCs to pass through the blood vessels as well as increased adherence of blood cells to the endothelium[25,26] due to the increased activation of adhesion molecules such as vascular cell adhesion molecule-1 (VCAM-1) and integrin $\alpha_V\beta_3$[27]. These pathological events augment the generation of free radicals through activation of pro-oxidant enzymes, disruption of mitochondrial respiratory chain activity[28], hemolysis induced release of free hemoglobin and heme that catalyze the Fenton reaction, and RBC autooxidation[29-34]. Thus, the overproduction of free radicals contributes to increased oxidative stress in endothelial cells, RBCs, neutrophils, and platelets, which manifests as multi-organ vasculopathy [29-34].

1.2 Oxidative Stress in Sickle Cell Disease

Oxidative stress is defined as the imbalance between reactive oxygen species (ROS), reactive nitrogen species (RNS), and antioxidants. ROS are the reduced metabolites of molecular oxygen. These products are superoxide anion radical ($O_2^{\cdot -}$), hydrogen peroxide (H_2O_2), hydroxyl anion (OH^-), and hydroxyl radical ($^{\cdot}OH$)[35,36]. RNS are the overproduction of nitric oxide ($^{\cdot}NO$) and nitrogen dioxide ($^{\cdot}NO_2$) or peroxynitrite ($ONOO^-$) which is formed from the interaction between nitric oxide and superoxide. To combat ROS and RNS, both non-enzymatic and enzymatic defense mechanisms have evolved[29]. The enzymatic antioxidants include superoxide dismutase (SOD), catalase, glutathione peroxidase, and peroxiredoxins[29]. The non-enzymatic antioxidants include carotenoids, ascorbic acid, zinc, and riboflavin[29]. Thus, if an imbalance between reactive species is not neutralized by these defense mechanisms, oxidation of biological molecules such as DNA, lipids, proteins, and carbohydrates persists, leading to cell dysfunction and death[29].

Despite high oxidative stress, levels of both non-enzymatic[37] and enzymatic antioxidants are reduced in SCD[38,39]. A wide range of non-enzymatic antioxidants have been found to be deficient in RBCs, platelets, and mononuclear cells of SCD patients including vitamin E and C, beta-carotene, omega-3 fatty acids, and plasma retinol[37,40]. Serum and plasma levels of the enzymatic antioxidants SOD, catalase, and glutathione peroxidase are also diminished[38-40]. The reduction of the antioxidant defense system has been associated with increased oxidative damage as measured by plasma lipid and RBC membrane peroxidation, DNA damage markers, and protein carbonylation[38,40]. Therapeutic treatments with antioxidants have shown beneficial effects in both *in vitro* [41-43]and *in vivo* [42,44] models of SCD. Validating the preclinical studies, the only two Food and Drug Administration (FDA) approved drugs for the treatment of SCD, hydroxyurea and L-

glutamine, have antioxidant activity. Hydroxyurea inhibits DNA synthesis, and by complex mechanisms including epigenetic modifications, post-transcriptional and signaling pathways, it increases levels of fetal hemoglobin. As a result, hydroxyurea reduces the occurrence of vaso-occlusive crises in SCD[45]. SCD patients taking hydroxyurea have increased antioxidant capacity and decreased thiobarbituric acid reactive substances (TBARS), a marker of lipid peroxidation, in their plasma[46]. L-glutamine was recently approved by the FDA and reduces pain crises and the number of hospitalizations due to SCD related complications[47]. The mechanism of action of L-glutamine is currently not fully understood, but is presumed to reduce oxidative damage in RBCs[48]. Glutamine supplementation is also able to improve antioxidant capacity through regeneration of glutathione[49]. The improvement in pathology with antioxidant supplementation underscores the importance of maintenance of the antioxidant defense system in the management of SCD.

1.3 Endothelial Cell Dysfunction in Sickle Cell Disease

The endothelium is a primary site of damage in SCD. Hemoglobin, released from hemolyzed RBCs, aggravate and activate the endothelium resulting in organ and tissue injury[50]. Autooxidation of free hemoglobin to methemoglobin releases free heme which is also able to incite injury to the endothelium[51]. Free hemoglobin scavenges nitric oxide ($^{\cdot}NO$) decreasing its bioavailibity resulting in vascular dysfunction[52,53] and aberrant activation of endothelial cells[54]. Free heme, which acts as a damage-associated molecular pattern molecule (DAMP), binds and activates toll-like receptor 4 (TLR4) causing systemic sterile inflammation[55,56]. Heme binding to TLR4 results in the release of inflammatory cytokines which stimulates the production of ROS[57]. Free heme can also trigger the release of neutrophil extracellular traps (NETs) through the

activation of neutrophils[58] promoting vaso-occlusions[55]. Under normal conditions, cell free hemoglobin and heme are scavenged by haptoglobin and hemopexin, respectively, however in SCD this system is overwhelmed[50,59,60]. Endothelial damage is also caused by the hemolytic release of other RBC DAMPs including heat shock protein (Hsp) 70[61], ADP[62], and RBC microvesicles[11].

The vascular endothelium consists of a monolayer of endothelial cells and provides a barrier between the blood and organ tissues. The structural heterogeneity of endothelial cells allows for the formation of three distinct types of endothelium: continuous, fenestrated, and discontinuous[63,64]. Endothelial cells found in the continuous endothelium are tightly coupled by tight junctions and secured to a continuous basal membrane[65,66]. Only water and small solutes (molecular radius, <3nm) are able to pass in between endothelial cells that make up the continuous endothelium[66]. Muscle, lung, skin, heart, and most arteries, veins, and capillaries of the brain contain continuous endothelium[65]. Fenestrated endothelium also has a continuous basal membrane, but in addition contain 50-60 nm wide transcellular pores which are needed in tissues where filtration occurs such as kidney glomeruli, some renal tubules, gastrointestinal tract, endocrine and exocrine glands, and the choroid plexus[65,67]. The discontinuous endothelium is the most permeable due to the presence of 100-200 nm wide fenestrations and a disconnected basal membrane[65,68]. Discontinuous endothelium is found mostly in the sinusoidal beds of the liver, but also can be found in bone marrow and in the spleen[65,68]. The endothelium performs multiple functions some more specific to certain vascular beds and organs than others; however in general all endothelial cells are involved in regulation of hemostasis[69] and vascular tone[70], permeability[71,72], leukocyte trafficking[73,74], angiogenesis[75,76], and immunity[65]. All these endothelial functions are dysregulated in SCD.

Hemostasis refers to the physiologic process by which bleeding at a site of injury can be stopped while simultaneously maintaining blood flow in other parts of the circulation[77]. Normally, the anticoagulant surface of endothelial cells maintains blood in its fluid state[78]. Upon injury to the endothelium, exposure of the subendothelial cell matrix triggers a cascade of events which initiates formation of a blood clot[77,79]. Hemostasis is broken into two main components: primary hemostasis and secondary hemostasis. In primary hemostasis, platelets self-aggregate and adhere to the site of injury to stem blood flow[77,80]. In secondary hemostasis, a proteolytic coagulation cascade generates insoluble fibrin which forms a mesh around the platelet plug to further stabilize it[77,81]. In SCD, both components of hemostasis are increasingly activated.

Elevated wall shear stress, the force per unit area applied by the wall to the fluid tangential to the flow of blood[82], disrupts connections between endothelial cells, exposing the underlying extracellular matrix (ECM)[83]. Exposure of the ECM allows for the adhesion of platelets either directly via platelet glycoproteins such as glycoprotein (GP) VI and GP Ia/IIa receptors[84] or through formation of a bridge mediated by von Willebrand factor and platelet membrane receptor complex GP Ib-IX-V[84,85]. This adhesion to the ECM, directly or indirectly, is the first step of primary hemostasis[85]. Wall shear stress and overall vascular tone is regulated by endothelium derived nitric oxide[86].

Nitric oxide, a primary regulator of vasoactivity, is produced by the enzymatic degradation of L-arginine to L-citrulline in the presence of nicotinamide adenine dinucleotide phosphate (NADPH) and molecular oxygen by endothelial nitric oxide synthase (eNOS)[87,88]. In SCD, hemolytic release of hemoglobin, arginase 1, and asymmetric dimethylarginine (ADMA) depletes and inhibits nitric oxide[54], L-arginine[89], and eNOS[90], respectively[11]. Depletion of this vital vasodilator impairs maintenance of normal vascular tone resulting in an inability to respond to

changes of blood flow which culminates in an increase in wall shear stress in SCD patients[86]. With this increase in wall shear stress, there is increase exposure of the ECM, activation of platelets, and primary hemostasis.

Injury of the endothelium also exposes the blood to the extravascular space which contain tissue factor[77]. Tissue factor starts the coagulation cascade, and therefore secondary hemostasis, by cleaving factor X to factor Xa which then cleaves prothrombin to thrombin which can further activate platelets as well as generate fibrin promoting clot formation[77,91]. There is increased expression of tissue factor on the SCD endothelium[92] and tissue factor procoagulation activity is increased in whole blood of SCD patients[93]. This chronic activation of the coagulation cascade leaves SCD patients prone to thrombotic complications[94]. Therapeutic targeting of the coagulation system has shown to be beneficial in reducing short term consequences of SCD, but the benefits of long term anticoagulation therapy on reducing end organ damage have yet to be examined[95].

Within the blood vessel the endothelium physically separates the blood from the tissue in order to maintain protein and water balance between the interstitial and intravascular compartments[96,97]. The integrity of this barrier varies between organs and even amongst the vascular segments of a particular organ[96]. The barrier is formed laterally through cell-cell junctions and baso-laterally through binding to the basement membrane[97]. The paracellular junction is composed of adherens junctions, gap junctions, and tight junctions[98,99]. In addition to modulating the flow of water and solutes between the extravascular and the intravascular compartments, these adhesive structures are also involved in signaling cell growth and polarity as well as communicating with smooth muscle cells and pericytes[97]. Adherens junctions mostly consist of vascular endothelial (VE)-cadherin whose main function is to regulate permeability through the closure of the paracellular space[97,100]. Gap junctions, formed by proteins in the connexin family[101],

permit cell to cell communication by organizing into intercellular channels to connect the cytoplasm of adjacent cells[97,101]. Tight junctions, compromised of claudins, occludin, junctional adhesion molecules, and zona occludins, form a semipermeable barrier that is size and charge selective depending on its composition[102]. Endothelial cells bind to fibronectin, collagen, actin, laminin, and glycosaminoglycans which are proteins found within the ECM[103,104]. Binding of the endothelial cell to the ECM is mediated by focal adhesions which utilize integrins[97,105]. Members of the integrin superfamily are essential for the maintenance of the endothelial monolayer and the vascular endothelial lining[106].

Exposure of the vasculature to free heme induces an increase in vascular permeability through the catalysis of ROS[107,108]. Increased ROS production induces cellular damage and dysfunction, and the upregulation of inflammatory pathways, which reduce barrier function through the histamine mediated formation of intercellular gaps and the weakening of paracellular junctions[96,108,109]. Ghosh et al found that in transgenic sickle mice the vascular endothelium deteriorates with age[110]. The increased permeability of the vascular endothelium, measured by Evan's blue dye, was increased in multiple organs and aged sickle mice also developed pulmonary edema reminiscent of a chronic permeability clinical phenotype seen in SCD patients[110]. This increase in pulmonary vascular permeability also leaves the sickle mice more susceptible to viral infection, a contributing factor to acute chest syndrome[111]. SCD patients have also been found to have increased gut permeability inducing intestinal injury and permitting bacteria to enter within the systemic circulation[112].

Endothelial cells play active roles in innate and adaptive immunity through their detection of foreign pathogens in the bloodstream[113]. The innate immune system regulates non-specific immunity and responds immediately to foreign pathogens[114]. In response to detection of a foreign

pathogen, innate immune cells release cytokines and chemokines to induce recruitment of phagocytes to the site of injury to destroy the pathogen[114]. The adaptive immune system relies on interaction with cells of the innate immune system[115]. Antigen presenting cells present peptide antigens via major histocompatibility complex (MHC) class I and class II molecules to lymphocytes which then carry out antibody or cell-mediated immune responses[113,115].

Endothelial cells express toll-like receptors (TLRs) and nucleotide oligomerization domain (NOD)-like receptors (NLRs) which are pattern recognition receptors that identify pathogen-associated molecular patterns[113]. Endothelial cells also express chemokine receptors[116] and secrete pro-inflammatory cytokines interleukin-8 (IL-8) and IL-1 via activation of TLR4[117,118]. Endothelial cells can also participate in the adaptive immune system by acting as antigen presenting cells. Endothelial cells upregulate expression of MHC I and induce expression of MHC II upon stimulation[113]. Expression of these MHC molecules allows endothelial cells to influence migration of lymphocytes to sites of inflammation[119].

In SCD, there is an increased incidence of bacterial infections such as osteomyelitis[120,121], meningitis[121,122], urinary tract infections[121,123], and pneumonia[121,124]. While defect of splenic function due to damage from having to filter sickled RBCs is the major contributing factor[125], endothelial cells contribute to the chronic inflamed state through their increased activation by free heme and hemoglobin, hypoxia-induced ROS, and direct contact with sickled RBCs[11]. Free heme acts as a DAMP activating TLR4 receptors on endothelial cells[125] and triggering NFkB signaling and increased expression of adhesion molecules[57]. Reduced NO bioavailibity by free hemoglobin scavenging also induces the expression of endothelial adhesion molecules[11]. An increase in the endothelial adhesion molecules, which include intercellular adhesion molecule 1 (ICAM1), vascular cell adhesion protein 1 (VCAM1), E-selectin, P-selectin, leukocyte surface antigen CD47

and $\alpha_V\beta_3$ integrin, are implicit in adherence of erythrocytes and leukocytes[11,27]. Activated endothelial cells also contribute to the chronic inflammatory state by producing the inflammatory mediators IL-1β, IL-6 and tumor necrosis factor[11,126].

Angiogenesis refers to the development of new blood vessels from pre-existing blood vessels[65]. While angiogenesis is an essential physiological process during development, repair, and reproduction, it can also be pathological[65]. Endothelial cells normally have a turnover rate of over one hundred days; however once activated by angiogenic factors they proliferate rapidly degrading ECM and migrating towards the angiogenic cues to create tubular structures[65,127]. Breakdown of the basal lamina and ECM is regulated by matrix metalloproteinases, plasminogen activators and inhibitors, and several proteinase families[65,128]. Upon degradation, the ECM releases numerous growth factors which promote angiogenesis, simultaneously inhibitors of angiogenesis are also released to tightly control the process[65,129]. Vascular endothelial growth factor (VEGF) is an essential growth factor during the formation of blood vessels and in the newly formed vessel[65,129].

Hypoxic conditions in SCD are generated by vaso-occlusive events as well as by an insufficiency in the number of RBCs able to carry oxygen[130,131]. Hypoxia stimulates the upregulation of endothelial hypoxia inducible factor 1 (HIF-1)[132], which upregulates the transcription of angiogenic genes, including VEGF[130]. Additionally, other angiogenic mediators such as erythropoietin[133], placental growth factor[134], and angiopoietin-2[135] are elevated in SCD patients. Clinically, a pro-angiogenic state is associated with pulmonary hypertension, moyamoya syndrome, leg ulcers, and proliferative retinopathy[136]. Hydroxyurea, the first Food and Drug Administration (FDA) approved drug for SCD, can downregulate *HIF1A* expression reducing vessel assembly[136].

1.4 Superoxide dismutase 2 and Sickle Cell Disease

Superoxide dismutases are a family of enzymatic antioxidant proteins that include three isoforms, all with similar activities, that have been identified and described in mammals: copper-zinc superoxide dismutase (Cu/ZnSOD, SOD1), manganese superoxide dismutase (MnSOD, SOD2), and extracellular superoxide dismutase (ECSOD, SOD3). These enzymes specialize in eliminating oxidative stress through the rapid (catalytic efficiency of 10^9 M^{-1} s^{-1}) dismutation of superoxide anion radicals ($O_2^{\cdot -} + O_2^{\cdot -} + 2H^+ \rightarrow O_2 + H_2O_2$)[137,138] (**Figure 1**). Hydrogen peroxide is then further catalyzed to water by catalase, peroxiredoxins, or glutathione peroxidases. The three isoforms differ in chromosomal position, gene encoding, protein structure, cellular localization, and co-factor requirements (reviewed in detail in [138]). SOD2 is transcribed from *sod2* and translated as a ~23 kDa homotetramer symmetrically assembled from pairs of *N*-terminal helical hairpins. The helical hairpins along with the C-terminal α/β domains contribute ligands to the formation of the catalytic manganese site within each subunit[139]. SOD2 is synthesized in the cytoplasm and localizes to the mitochondrial matrix where it scavenges and accelerates the dismutation of superoxide anion generated by respiratory chain enzymes[140]. During normal erythropoiesis, RBCs lose their mitochondria and other organelles as they mature. This process may be impaired in SCD. A study by Jagadeeswaran *et al* using reticulocyte-identifying fluorescence conjugated CD71 and RNA dye thiazole orange showed increased levels of mitochondria in RBCs [141]. This finding was interpreted as increased retention of mitochondria in sickle RBCs, resulting from disrupted hematopoiesis [141]. Increased ROS production from RBC mitochondria was also observed [141]. It is possible that what was observed in the study by Jagadeeswaran *et al* was not a retention of mitochondria, but a stimulation of erythropoiesis by the

severe hemolytic anemia resulting in an increase in the production of many young erythroid precursors which retain membrane bound organelles such as mitochondria.

Given the importance of SOD2 in modulating mitochondrial ROS, an understanding of how it is regulated, particularly in the context of increased oxidative states, can lead to better insights regarding where therapeutic intervention may be beneficial. The human *sod2* gene is located on the q25.3 band of chromosome 6 and contains many sites for transcriptional modification: GC rich motifs, a Foxoa3 binding site, a NF-kB regulatory element and several specific protein 1 (SP1) and activator protein 2 (AP-2) sites[138]. Transcriptional activation of early growth response 1 (Egr-1) upregulates mRNA expression of SOD2 through the induced expression of platelet-derived growth factor (PDGF)[142]. Additionally, a variety of proinflammatory cytokines such as interleukin (IL)-1, IL-4, IL-6, tumor necrosis factor (TNF)-α, interferon (IFN)-γ, and the bacterial endotoxin lipopolysaccharide (LPS) are robust SOD2 activators [143]. In particular, IL-1 and TNF-α transcriptionally upregulate expression of MnSOD (SOD2) in rat pulmonary endothelial cells, a response that was exacerbated by the addition of LPS [144]. Developmental regulation of SOD2 was found in mouse kidneys and is associated with mpv17-like protein (M-LP). Expression levels of both SOD2 and M-LP increase during embryogenesis, peaking in adulthood before decreasing with age [145,146]. An incidental side effect of microtubule formation inhibitor anti-cancer drugs (vinblastine, taxol, and vincristine) is transcriptional upregulation of SOD2 through activation of protein kinase C, shown in a human lung adenocarcinoma cell line (A549)[147]. Downregulation of SOD2 is elicited by the AP-2 family transcription factors [148,149]. Enzymatic activity of SOD2 is regulated post-translationally, with phosphorylation at serine 106 by Cdk1 increasing enzymatic activity and cell survival,[150,151] while loss of SIRT3 leads to acetylation of lysine 122 and lysine 68 and inhibition of enzymatic activity[152,153].

SOD2 expression is also regulated by ROS and RNS. Increased peroxynitrite can cause nitration at tyrosine 34 leading to enzymatic inhibition [154], while superoxide radicals upregulate SOD2 expression through activation of redox sensitive transcription factors NFκB and Nrf2[155,156]. The antagonistic roles that peroxynitrite and superoxide radicals have in regulating SOD2 expression and activity aides in understanding why mitochondrial antioxidant response in SCD is particularly dysregulated. In addition to ROS and RNS having opposed regulatory functions, SOD2 activation by superoxide radicals in SCD is impaired. While NFκB is activated in SCD, [57,157] there is diminished Nrf2 activation in transgenic mouse models of SCD, suggesting a dysfunctional response by the sickle antioxidant system. Pharmacological activation of the Nrf2 pathway by treatment with dimethylfumarate (DMF) in transgenic sickle mice is able to increase antioxidant expression (hemoxygenase-1 (HO-1), haptoglobin, hemopexin, and ferritin heavy chain (FHC)) in the liver and kidneys, as well as prevent progression of disease pathology in the liver[158]. In a study examining the neuroprotective effects of DMF following oxidative stress from hydrogen peroxide, DMF significantly upregulated gene expression of SOD2 in rat neural stem/progenitor cells[159]. The positive results obtained with pharmacological activation of the Nrf2 antioxidant pathway, and specifically upregulation of SOD2, holds promise for the development of Nrf2 activators such as DMF for clinical use in SCD.

SOD2 has been shown to be a vital enzyme in the maintenance of vascular function. Low levels of intracellular and extracellular hydrogen peroxide and superoxide contribute to physiological biochemical processes such as defense against microorganisms and cell signaling[160,161]. In diseases such as SCD, hypertension, and diabetes, where there is an excess of superoxide, regulation of the SOD enzymes plays an important role in attenuating oxidative damage to the mitochondria and endothelium. Specifically, adjustments in levels of superoxide

have been shown to modulate cell growth, apoptosis, inflammation, gene expression, and vascular tone via oxidation of signaling molecules and activation of redox sensitive transcription factors[140]. SOD2 overexpression and excess generation of hydrogen peroxide has been implicated in angiogenesis through increased oxidation of phosphatase and tensin homolog deleted from chromosome 10 (PTEN)[162], cell differentiation through prolonged extracellular signal-regulated kinase (ERK1/2) signaling[163], and pulmonary hypertension through the activation of hypoxia inducible factor (HIF)-1α-O_2 sensitive pathways[164]. A deficiency of SOD2 in Apo E deficient mice results in mitochondrial damage and impaired vascular relaxation in response to acetylcholine[165]. The endothelial and mitochondrial damage resulting from SOD2 deficiency could not be rescued by 4,5-dihydroxy-1,3-benzene disulfonic acid mediated scavenging of superoxide, supporting the vital role of SOD2 in maintaining vascular function[165]. In vascular aging, disruption of vascular homeostasis and functional deterioration results from imbalances between pro- and anti-oxidants. This vascular aging-related dysfunction is more pronounced in heterozygous SOD2 mice, and is associated with increased levels of mitochondrial ROS production and mitochondrial damage [166]. It has been noted that SCD patients have reduced peripheral blood SOD2 expression[167]. In SCD, increased oxidative scavenging of the vasodilator nitric oxide (NO) is likely a contributory factor in accelerating deterioration of vascular function.

SOD2 expression and activity must be maintained at a balance in order to avoid (1) excess superoxide and (2) overproduction of hydrogen peroxide [168]. Excess superoxide disrupts cellular activity by reacting with NO and targeting iron sulfur clusters [169-171], which can impair NO-mediated vasodilation, [29] activate mitochondrial uncoupling proteins, and modify complex I of the electron transport chain for diminished proton motive force and decreased ATP production[169] [170,171]. On the other hand, increased hydrogen peroxide through the upregulation of SOD2

stimulates prooxidants involved in apoptosis[169], as well as targets thiol groups on proteins and provides a substrate for oxidant production by Fenton chemistry. The deleterious consequences of abnormal SOD2 activity highlights the importance of balance in maintaining healthy vascular function and the need for careful patient selection when considering SOD2 therapies.

In SCD, ischemia-reperfusion increases ROS and RNS generation through the upregulated enzymatic activity of xanthine oxidase[172-174], NADPH oxidases (NOXs)[175-177], and nitric oxide synthase, both coupled and uncoupled [178]. Limited oxygen availability during ischemia-reperfusion impairs metabolism and increases mitochondrial ROS production [179]. Electron transfer between heme iron and oxygen[29] occurs at a faster rate in sickle hemoglobin than in non-sickle hemoglobin [180,181], predisposing sickle RBCs to autooxidation and lysis. Hemolysis releases excess amounts of hemoglobin into plasma, which saturate the scavenging molecules haptoglobin and CD163[55,182]. Unscavenged hemoglobin is free to react with hydrogen peroxide, forming hydroxide radicals via Fenton chemistry. It also scavenges NO, limiting its bioavailability [54,55]. In the proinflammatory milieu of SCD, sickled RBCs have increased adhesion to the vascular endothelium via vascular adhesion molecule-1 (VCAM-1), intracellular adhesion molecule-1(ICAM-1), E-selectin, and P-selectin[29,183-185]. RBC adhesion to vascular endothelium activates the NF-kB pathway and increases oxidative stress as measured by TBARS formation [186]. SOD and catalase were shown to reduce expression of VCAM-1, decreasing oxidative stress as measured by TBARS, in cultured human umbilical vein endothelial cells (HUVEC)[186]. SOD2 mRNA levels are reduced in the peripheral blood of SCD patients, affecting SOD2 protein levels that correlate with RBC count, reticulocyte count, platelet count, C-reactive protein, ferritin, brain natriuretic peptide values and echocardiographic indications of pulmonary hypertension[167]. Considering the beneficial effect of SOD supplementation on oxidative stress and adhesion *in vitro* and the

deficiency of SOD2 in patients with SCD, the potential for SOD therapy in SCD takes on greater meaning. While SOD2 supplementation has the potential to offer great benefit for those SCD patients deficient in SOD2, it is important to note that SOD2 overexpression upregulates angiogenesis through hydrogen peroxide meditated oxidation of PTEN[162]. Angiogenic mediators such as vascular endothelial growth factor (VEGF), placental growth factor (PGF), and erythropoietin (EPO) are reportedly elevated in SCD[130]. Given the role of SOD2 in promoting angiogenesis and the pathological angiogenesis that contributes in some cases to sickle pathology[130], it is vital to screen potential recipients of SOD2 therapy for markers of increased angiogenesis such as VEGF, PGF, and EPO in order to avoid propagating pathological angiogenesis.

The function of SOD2 has been well studied in global and cell type-specific knockout models. In mice, complete global deficiency of SOD2 results in early lethality with the development of severe cardiomyopathy, anemia, and neural degeneration[187]. In order to study the effect of SOD2 deficiency in hematopoietic cells *in vivo* over long periods of time, Friedman *et al* transplanted murine fetal liver stem cells deficient in SOD2 into gamma-irradiated metabolically normal mice[188]. $Sod2^{-/-}$ liver stem cells were able to rescue irradiated mice, but unlike $Sod2^{+/-}$ and $Sod2^{+/+}$ liver stem cells, erythrocyte development was impaired, and mice were persistently anemic[188]. SOD2 deficiency resulted in an increased accumulation of oxidized RBC protein, decreased RBC survival, and decreased RBC membrane deformability[188]. Increased rate of hemoglobin oxidation, increased heme degradation products, and reduced deformability of RBCs [189] were also found in a hematopoietic stem cell transplant model of SOD2 deficiency. All of these RBC pathologies are characteristic of hemolytic anemias such as SCD[188], providing further evidence of the antioxidant's vital role in SCD and other hemolytic anemias. Interestingly, while

Friedman *et al* have shown that SOD2 deficiency is detrimental for RBCs, SOD2 seems nonessential for platelet functioning. Fidler *et al* observed increased mitochondrial ROS in a platelet-specific SOD2 knockout mouse model but the increase in ROS did not affect platelet activation[190]. Even in pathological platelet centered immune mechanisms, such as sepsis and autoimmune inflammatory arthritis, there was no phenotypic difference between the SOD2 knockout and wild type models[190]. These studies indicate that RBCs and not platelets would be a target for therapies centered on SOD2 in SCD.

Several SOD2 gene polymorphisms and their clinical implications have been described [143,191,192]. A valine-16 to alanine (Val-16-Ala) polymorphism associates with clinical complications for SCD patients. This polymorphism is correlated with decreased SOD2 activity as well as increased vaso-occlusive crises and acute splenic sequestration in children with SCD[193]. Decreased SOD2 enzymatic function with the Val16Ala polymorphism has also been observed in cryopreserved human hepatocytes[194] and isolated human erythrocytes[195]. The Val-16-Ala polymorphism occurs at a high frequency among various ethnic groups: 0.4521 in Africans, 0.6492 in Latinos, 0.5375 in South Asians, 0.5162 in Europeans (non-Finnish), 0.1596 in East Asians[196], and 0.4902 in others. The high frequency of the Val16Ala SOD2 polymorphism and reported associations with sickle complications emphasizes the significant role that Val-16-Ala may play in contributing to the phenotypic spectrum of SCD. Recently, Ganini et al. have shown that when cells and animals are exposed to a high iron/manganese ratio, SOD2 incorporates iron more so than manganese, creating a prooxidant peroxidase[197]. This aberrant iron-bound SOD2 leads to oxidative stress and mitochondrial dysfunction both *in vitro* and *in vivo*[197]. In SCD, frequent blood transfusions, decreased RBC survival, and increased intravascular hemolysis increase iron levels[198], thus increasing the iron/manganese ratio. The role of endothelial SOD2 in SCD has yet

to be established. Further investigation into the Val-16-Ala SOD2 polymorphism's antioxidant capacity and how the potential incorporation of iron into SOD2 may contribute to different sickle pathologies (e.g. pulmonary hypertension, stroke, renal failure, leg ulcers) and response to therapeutics will aid in the development of more personalized clinical care.

While the implications of SOD2 regulation in hemolytic disorders is still a new area of investigation, there is an abundance of literature investigating how redox status, and in particular SOD2 expression and activity levels, play a role in response to pharmacological treatment of leukemias and lymphomas. In adult patients with acute lymphoblastic leukemia (ALL), the Val-16-Ala SOD2 polymorphism is associated with increased hepatotoxicity following asparaginase-based treatment[199]. This increased hepatoxicity with the Val-16-Ala polymorphism suggests that asparaginase-based therapies should be used with caution in ALL patients with the polymorphism. In cell line models of acute myeloid leukemia (AML), treatments targeting ROS production and expression levels of SOD2 have shown efficacy [200,201]. Specifically, disulfiram/copper was able to increase ROS in AML cell lines by inducing SOD2 and suppressing catalase, therefore increasing hydrogen peroxide production[200]. This suggests that SOD2 induction-based therapy may be effective as an AML therapeutic. A phase 2 clinical trial investigating the use of Imexon for relapsed follicular and aggressive lymphomas revealed that redox related genes such as glutathione peroxidase and SOD2 correlate with clinical responses[202]. This indicates that analysis of pretreatment markers of oxidative stress may aide in identifying patients most likely to benefit from treatment with Imexon[202]. These studies show that SOD2 holds promise as a prognostic biomarker in leukemia and lymphoma and suggest it may play a role in the pathogenesis of hematologic malignancies.

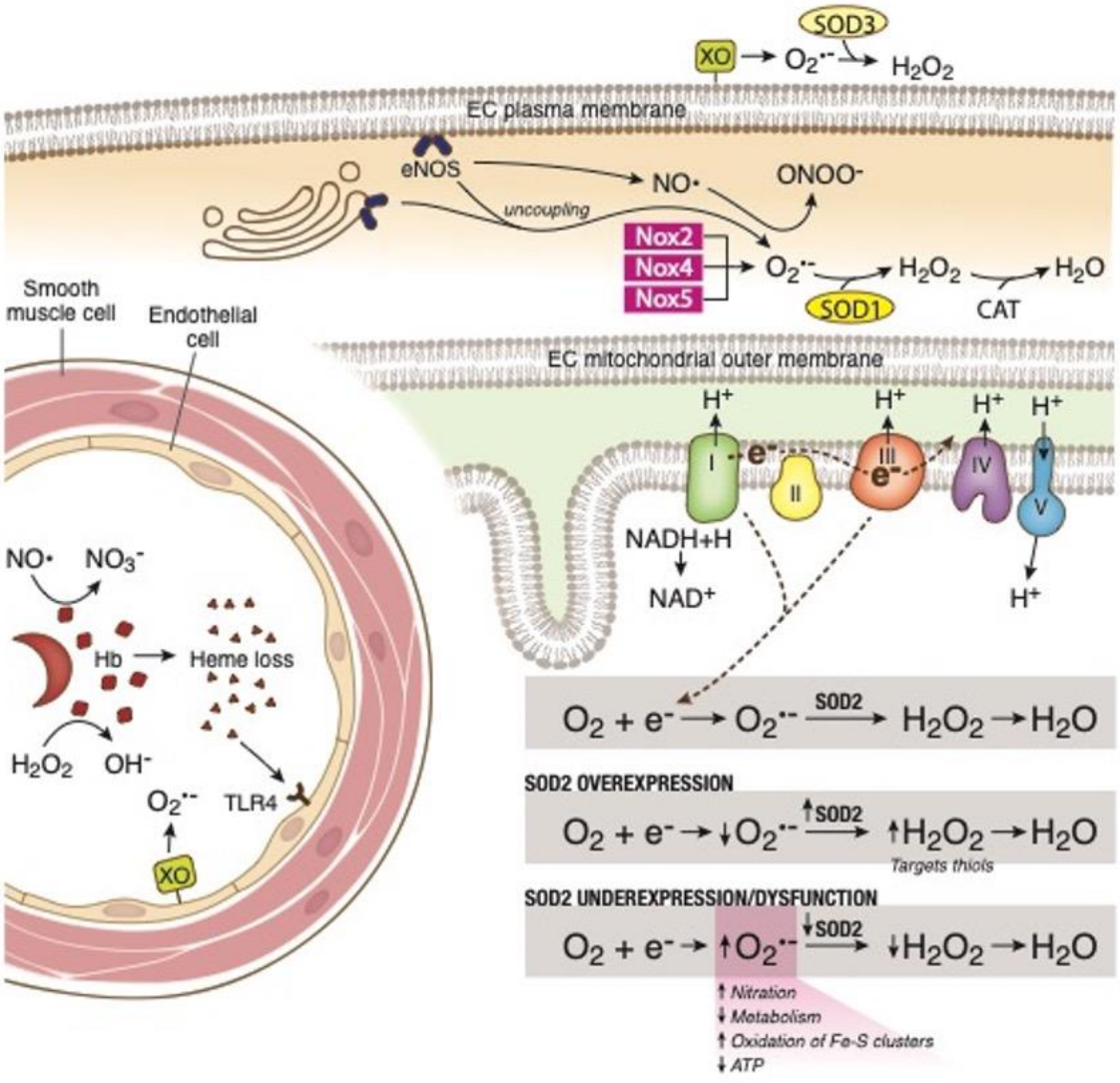

Figure 1

Sickled red blood cells (RBCs) undergo hemolysis releasing hemoglobin (Hb) and heme. Hemoglobin reacts with 1) nitric oxide ($NO^{\cdot}$) forming nitrate (NO_3^-) and 2) hydrogen peroxide (H_2O_2) producing hydroxide (OH^-). Endothelial bound xanthine oxidase (XO) generates superoxide ($O_2^{\cdot-}$) and H_2O_2. Free heme binds to toll like receptor 4 (TLR4) producing reactive species through the activation of the NFκB pathway. Superoxide Dismutase (SOD) 3 is found in the extracellular compartment and transforms $O_2^{\cdot-}$ to H_2O_2.

In the endothelial cell cytoplasm, endothelial nitric oxide synthase (eNOS) uncoupling and NADPH oxidase (NOX) 2, 4, and 5 produce $O_2^{\cdot-}$ which is dismutated by SOD1. eNOS normally generates $NO^{\cdot}$ which is capable of reacting with $O_2^{\cdot-}$ forming peroxynitrite ($ONOO^-$). In the mitochondrial matrix, electrons leaked from complexes I and III of

the respiratory chain react with oxygen (O_2) forming $O_2^{\cdot-}$. SOD2 dismutates $O_2^{\cdot-}$ to H_2O_2 which is further broken down to water by catalase. SOD2 expression and activity is maintained at a precise balance. Overexpression of SOD2 decreases $O_2^{\cdot-}$ levels and increases H_2O_2 levels which are then free to target protein thiols. SOD2 underexpression or dysfunction increase $O_2^{\cdot-}$ levels, increasing nitration and oxidation of iron sulfur clusters and decreasing metabolism and ATP production.

1.5 The Purpose of this Dissertation

We hypothesized that SOD2 is a genetic modifier of SCD. To test this hypothesis, we had two aims. In Aim 1 we determined the function of SOD2 V16A in SCD and in Aim 2 we elucidated the role of SOD2 in the endothelium. The goal for this dissertation is to inform the reader of our discovery that SOD2 is a novel biomarker regulating SCD pathology. SOD2 has been shown to be vital for survival in knockout mouse models with mice succumbing by 3 weeks of age due to neuronal degeneration, dilated cardiomyopathy, and severe anemia[187]. Additionally, SOD2 is fundamental for the preservation of vascular tone. Dikalova et al. found that patients with essential HTN had a 2.6-fold increase in acetylation of SOD2 attributable to a 1.4-fold decrease in Sirtuin 3 (SIRT3) expression[203]. Increased SIRT3 mediated acetylation of SOD2 was found to decrease SOD2 enzymatic activity and further elevate blood pressure in an angiotensin II induced HTN rodent model[203]. Additionally, heterozygous knockout of SOD2 in mice has been shown to produce spontaneous HTN by 2 years of age[204], which can be accelerated to 6 months of age with a high salt (2%) diet [204]. Moreover, aortas isolated from aged SOD2 deficient mice have shown decreased vasorelaxation in response to acetylcholine that associates with increased mitochondrial reactive oxygen species formation[166]. Considering the vascular endothelium is a primary target for damage

in SCD and that SOD2 has been shown to regulate vascular tone, we inquired whether SOD2 could play a role in further modulating SCD pathology.

Herein we present our original research currently in revision and review detailing the role of SOD2 in the sickle pulmonary endothelium. Studies in Chapter 2 outline our results where we show that the common polymorphism for SOD2 which substitutes Valine for Alanine at the 16th amino acid position (SOD2^{V16A}) is associated with clinical markers of endothelial dysfunction in a cohort of 410 SCD patients. We also show that in cultured human pulmonary arterial endothelial cells, SOD2^{V16A} overassociates with Complex IV of the respiratory chain, decreasing its activity and oxygen consumption, while also increasing production of mitochondrial O_2^- and extracellular H_2O_2. In Chapter 3, we go on to show that SCD patients have a significant reduction of SOD2 in both pulmonary endothelial and smooth muscle cells. *In vitro* experiments using cultured human pulmonary microvascular endothelial cells demonstrated that depletion of SOD2 results in an increase in cell adhesion and permeability, a decrease in proliferation and migration, and dysregulation of integrin proteins. We also found that this endothelial cell dysfunction was mediated by disruption in fibronectin processing. In Chapter 4, I discuss what questions remain unanswered, future directions for those wishing to continue these studies, and the implications of our findings in the management and treatment of SCD patients.

2.0 SOD2 V16A Amplifies Vascular Dysfunction in Sickle Cell Patients by Curtailing Mitochondria Complex IV Activity

Atinuke Dosunmu-Ogunbi[1,2,3], Shuai Yuan[3], Michael Reynolds[3], Luca Giordano[3,4], Subramaniam Sanker[3], Mara Sullivan[5], Donna Beer Stolz[5], Brett A. Kaufman[3,4], Katherine C. Wood[3], Yingze Zhang[6], Sruti Shiva[2,3], Seyed Mehdi Nouraie[6], Adam C. Straub[2,3,7]

1 Medical Scientist Training Program, University of Pittsburgh School of Medicine, Pittsburgh, PA, USA

2 Department of Pharmacology and Chemical Biology, University of Pittsburgh School of Medicine, Pittsburgh, PA, USA

3 Heart, Lung, Blood and Vascular Medicine Institute, University of Pittsburgh, Pittsburgh, PA, USA

4 Center for Metabolism and Mitochondrial Medicine, Department of Medicine, University of Pittsburgh School of Medicine, Pittsburgh, Pennsylvania, USA

5 Center for Biologic Imaging, Department of Cell Biology, University of Pittsburgh Medical Center, Pittsburgh, PA, USA

6 Division of Pulmonary, Allergy, and Critical Care Medicine, University of Pittsburgh School of Medicine, Pittsburgh, PA, USA

7 Center for Microvascular Research, Department of Medicine, University of Pittsburgh School of Medicine, Pittsburgh, Pennsylvania, USA

2.1 Summary

Superoxide dismutase 2 (SOD2) catalyzes the dismutation of superoxide to hydrogen peroxide in mitochondria limiting mitochondrial damage. The SOD2 amino acid valine-to-alanine

substitution at position 16 (V16A) in the mitochondrial leader sequence is a common genetic variant among patients with Sickle Cell Disease (SCD). However, little is known about the cardiovascular consequences of $SOD2^{V16A}$ in SCD patients or its impact on endothelial cell function. Here, we show $SOD2^{V16A}$ associates with increased tricuspid regurgitant velocity (TRV), systolic blood pressure, right ventricle area at systole and declined 6-minute walk distance in 410 SCD patients. Plasma lactate dehydrogenase, a marker of oxidative stress, significantly associated with higher TRV. To define the impact of $SOD2^{V16A}$ in endothelium, we introduced the $SOD2^{V16A}$ variant into endothelial cells. $SOD2^{V16A}$ increases hydrogen peroxide and mitochondrial reactive oxygen species (ROS) production compared to controls. Unexpectedly, the increased ROS was not due to $SOD2^{V16A}$ mislocalization but was associated with mitochondrial Complex IV and a concomitant decrease in basal respiration and Complex IV activity. In sum, SOD^{V16A} is a novel clinical biomarker of cardiovascular dysfunction in SCD patients through its ability to decrease mitochondrial Complex IV activity and amplify ROS production in the endothelium.

2.1.1 Graphical Summary:

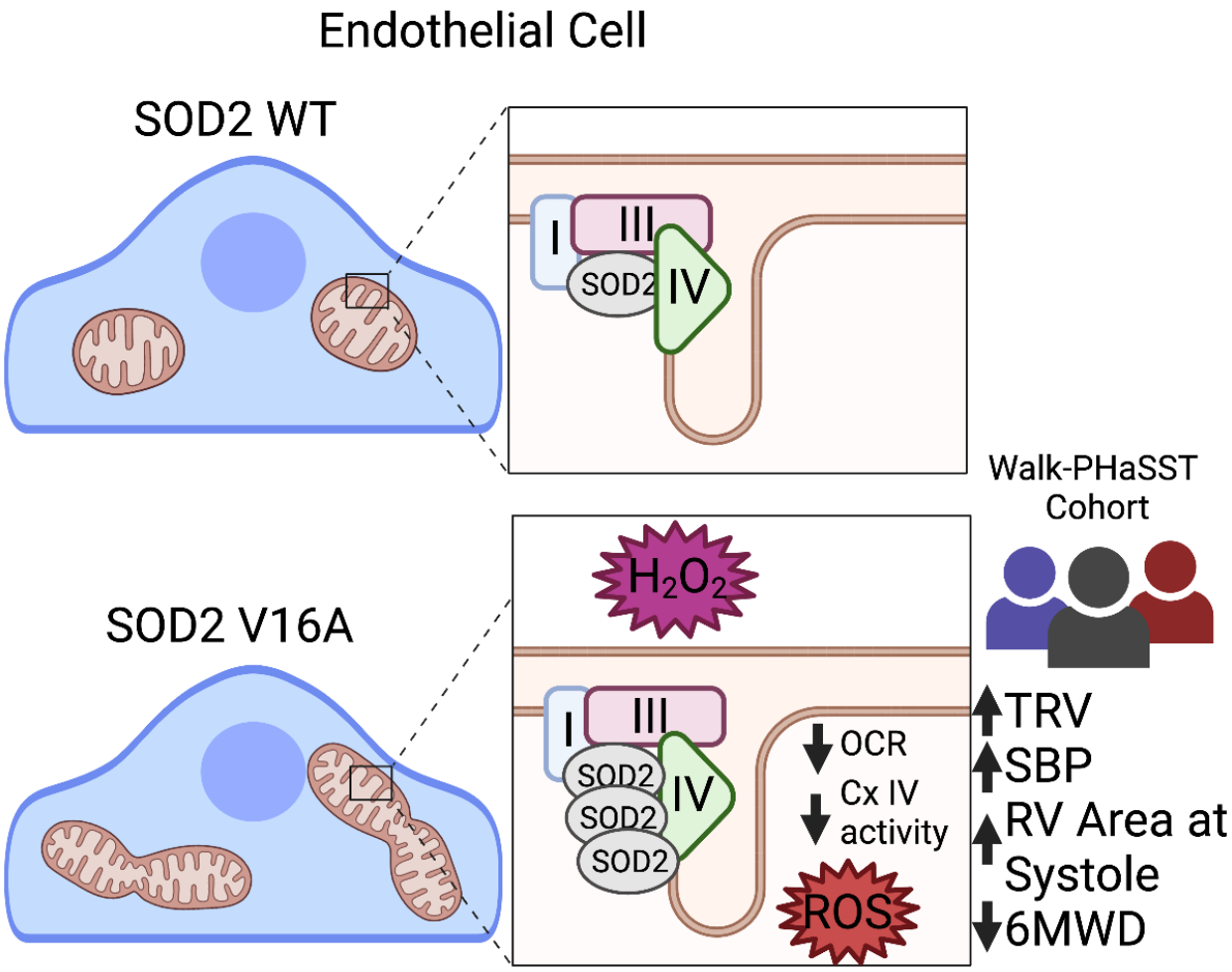

2.2 Introduction

Although sickle cell disease (SCD) is ascribed to a single point mutation in β-globin gene, the cardiovascular presentation among patients remains highly variable. For example, pulmonary hypertension occurs in 6-11% of adult SCD patients and predicts early death[205,206] whereas 24% of patients exhibit signs of stroke by 45 years of age[207]. While several factors contribute to

cardiovascular deviation among SCD patients, genetic variability, and oxidative stress are key elements driving phenotype heterogeneity.

Mitochondria dysfunction contributes to SCD pathogenesis by increasing reactive oxygen species (ROS)[28]. Mitochondria uncoupling increases superoxide ($O_2^{\bullet-}$) formation which is managed by superoxide dismutase 2 (SOD2), a mitochondrial matrix protein that catalyzes dismutation of superoxide to hydrogen peroxide (H_2O_2). A valine-to-alanine substitution ($SOD2^{V16A}$, rs4880) in the mitochondria leader sequence (MLS), is found in 45% of people with African ancestry, 65% of Latinos, 54% of South Asians, and 52% of Europeans[196]. In SCD, $SOD2^{V16A}$ associates with acute splenic sequestration and vaso-occlusive crises in children[193] and increased risk of stroke in adults[208]. However, the impact of $SOD2^{V16A}$ on cardiovascular severity remains unclear and rigorous functional studies defining the impact of $SOD2^{V16A}$ remain elusive. This stems from contradictory results suggesting enzymatic activity of $SOD2^{V16A}$ can be increased[209] or decreased[193]. We hypothesized that $SOD2^{V16A}$ drives mitochondria dysfunction, increases mitochondrial ROS production, and can be used as a prognostic genetic biomarker for vasculopathy in SCD patients.

2.3 Materials and Methods

Cohort and Genetic Analysis

SCD patients from the Treatment of Pulmonary Hypertension and Sickle Cell Disease With Sildenafil Therapy (walk-PHaSST) trial were recruited for molecular genetic analysis (approved under University of Pittsburgh Institutional Review Board Protocol STUDY19060255)[210].

Genotyping of rs4880 was performed using Taqman genotyping assay (C___8709053_10) and methods were performed as described and adjusted for age, gender, BMI, hemoglobin, pulse rate, antihypertensive treatment, α-globin deletion and study site[211].

HPAEC Transduction and Transfection with APEX

Polyhistidine-tagged human SOD2 rs4880 (A) encoding Valine on the 16th amino acid position ($SOD2^{WT)}$ or SOD2 rs4880 (G) encoding Alanine on the 16th amino acid position ($SOD2^{V16A}$) was placed on a bicistronic lentiviral vector that also co-expressed GFP as previously described[212]. HPAECs were incubated with the lentivirus and 1 ug/mL polybrene for 8 hours in a 6 well plate (250,000 cells/well) to achieve a 2-fold increase over endogenous SOD2. Experiments were performed 72 hours post lentiviral transduction. HPAECs were transfected with 0.5 ug $SOD2^{WT}$ or $SOD2^{V16A}$ conjugated with APEX2 using Nucleofector™ (Lonza) according to manufacturer's instructions, experiments were conducted 24 hours post transfection. APEX2 assays were performed as previously described[213].

Respiratory Complex and Oxygen Consumption Assays

Complex I activity was determined by monitoring the rate of oxidation of 5mM NADH in the presence of 5mM coenzyme Q2 at 340 nm in the presence and absence of 1mM rotenone. Complex III activity was determined by monitoring the rate of reduction of 15μM cytochrome c at 550nm in the presence of 8mM ubiquinol. Complex IV activity was determined by measuring oxidation of cytochrome c at 550nm. Complex V activity was determined by measuring oxidation of 300μM NADH at 340nm in the presence and absence of 250μM oligomycin. Complex I, II, and IV activities were normalized to Complex V activity. Oxygen consumption was performed using a Seahorse as previously described[28].

Cell Culture and Reagents

Human pulmonary arterial endothelial cells (HPAECs) were obtained from Lonza. Cells were cultured in Endothelial Basal Medium^{TM}-2 supplemented with Endothelial Growth Medium^{TM}-2 SingleQuots^{TM} (Lonza) at 37°C and 5% CO_2

Primers Used for Plasmid Construction

SOD2^{WT} primers: ATCCGCTAGCGCCAGCATGTTGAG (forward) and TTGAGCTCGAGCTTAATGGTGATGGTGATGATGAGCGGCCGCCTTTTTGCAAGCCA (reverse).

SOD2^{V16A} primers: CAGCTGGCTCCGGCTTTGGGGTATC (forward) and GATACCCCAAAGCCGGAGCCAGCTG (reverse).

Hydrogen Peroxide Measurement

HPAECs were transduced with 20 μL lentivirus in a 6 well plate then replated onto a 96 well plate (~10,000 cells/well). The next day cells were placed in assay buffer (25nM HEPES, 10μM EDTA, 100μM L-NAME (N(G)-Nitro-L-arginine methyl ester), 1mM Taurine and 0.01% BSA in HBSS without phenol red). Catalase (500μg/mL) was added to select wells as a negative control. Cells were pretreated with 2mM antimycin A with or without 10nm aminotriazole and then 20μM coumarin boronate (Cayman) was added to all wells and fluorescence (350/450 nm) was measured kinetically for four hours. Automatic gain adjustment was set to scale to low wells using the wells treated with catalase. The slope of the linear portion of the curve was used to determine the rate of hydrogen peroxide production. The slope was calculated after removing production detected from catalase negative controls. Following the assay, cells were fixed in 2%

PFA for 10 minutes and stained with 0.5% Crystal Violet for 15 minutes. The wells were then washed with water to remove excess dye. 1% SDS was then added to the wells for 20 minutes. Absorbance was read at 590nm using a BioTek Synergy HT Microplate reader. Slopes calculated from the hydrogen peroxide assay were normalize to the total cell number measured by crystal violet absorbance.

SOD Activity

SOD activity was measured using SOD Activity Assay Kit (Abcam, ab65354). To inhibit SOD1 activity 3mM potassium cyanide was added to the cell lysate for 15 minutes[214] before adding reaction solutions.

Mitochondrial DNA (mtDNA) Measurements

Total DNA was extracted as previously described with minor modifications[215]. Snap-frozen cells were lysed in proteinase K buffer (100 mM Tris-HCl pH 8.5, 5 mM EDTA, 0.2% SDS, 200 mM NaCl), 0.6 mg/mL proteinase K (Fisher Scientific) and 0.01% 2-mercaptoethanol, overnight at 55° C. NaCl (1. 27M) was added to precipitate proteins and cell membranes by centrifugation at 28,000 RCF for 15 minutes at 4℃. The supernatant was collected and mixed to 100% ethanol. The nucleic acids were precipitated by centrifugation at 28,000 RCF for 15 minutes at 4 °C. The pellet was washed with 70% ethanol, air-dried overnight in the dark, and resuspended in DNases-free water. DNA was treated with 0.4 mg/mL RNase A (Sigma-Aldrich) for 2 hours at 37 °C to degrade RNAs, then stored at -20 °C, and successively quantified by AccuBlue Broad Range dsDNA Quantitation kit (Biotium).

Mitochondrial DNA (mtDNA) and nuclear DNA (nDNA) were measured by duplex qPCR using the TaqMan chemistry in a 96-well StepOnePlus™ Real-Time PCR System

(Applied Biosystems, Thermo Fisher Scientific). The reaction contained four ng of DNA template, Luna Universal qPCR Master Mix (New England Biolabs), two probes and primer set (ND1PL for mtDNA and B2M for nDNA, respectively). Thermocycling condition and probes/primer set were previously validated[216].

Mitochondrial DNA was normalized to the nDNA by ΔCt method for each sample. The mtDNA/nDNA in $SOD2^{V16A}$ was calculated as variation of $SOD2^{WT}$ (arbitrary unit=1), by 2-ΔΔCt method for each biological replicate.

Mitochondria Superoxide Measurements

Transduced HPAECs were trypsinized and resuspend in Ca^{2+} and Mg^{2+} free Hank's Balanced Salt Solution (HBSS). 150,000 cells were added to each well of a 96 well plate along with 5 μM MitoSOX Red™ (Invitrogen). After addition of MitoSOX, fluorescent signal (510nm/580nm) was recorded at 37°C for 2 hours. Fluorescent intensities were averaged every 6 minutes to reduce variation before the log phase slope was calculated to express the reaction rate. The results were normalized to protein concentration.

Electron Microscope (EM) Imaging and Affinity Pulldown of APEX2-SOD2 Constructs

Transfected HPAECs cells were rinsed and fixed in 1 volume 2% glutaraldehyde, 1 volume deionized water, and two volumes 0.2M cacodylate on ice for one hour. Following fixation cells were washed with 100 mM cacodylate and then incubated with 20 mM glycine 2 mM $CaCl_2$ in 100mM cacodylate on ice for 5 minutes. After washing cells were incubated in 0.5 mg/mL 3,3'-diaminobenzidine (DAB) for 30 minutes. After incubation with DAB, H_2O_2 was added to a final concentration of 10mM until brown precipitate was observed. Cells were then rinsed with 100mM cacodylate, post-fixed in 1% osmium tetroxide with 1% potassium

ferricyanide, rinsed in PBS, dehydrated through a graded series of ethanol and embedded in Poly/Bed® 812 (Luft formulations). Semi-thin (300 nm) sections were cut on a Leica Reichart Ultracut, stained with 0.5% Toluidine Blue in 1% sodium borate and examined under the light microscope. Ultrathin sections (65 nm) were examined on JEOL 1400 Plus transmission electron microscope (grant #1S10RR016236-01 NIH for Simon Watkins) with a side mount AMT 2k digital camera (Advanced Microscopy Techniques, Danvers, MA) at the Center for Biologic Imaging at the University of Pittsburgh.

For affinity pulldown, transfected cells were incubated with 500μM biotin-phenol (Cayman) for 30 minutes. APEX2 was activated by adding H_2O_2 at a final concentration of 100μM for 60 seconds. The reaction was quenched by repeated washing using 10mM sodium ascorbate, 10mM sodium azide, 5 mM Trolox (Cayman) in phosphate buffered saline, pH 8. Biotinylated proteins were enriched utilizing Dynabeads™ M-280 Streptavidin (Invitrogen) and eluted in 2X Lammeli Buffer by heating the beads before immunoblotting.

Quantification of APEX Imaging

To quantify the localization of the SOD2 variants, regions of interest were drawn within the mitochondrial matrix and the cytoplasm adjacent to the measured mitochondria matrix. The inverse of the raw integrated intensities was taken and the inverse of the intensity within the mitochondria matrix was normalized to the inverse of the intensity measured in the cytoplasm.

Measurement of metabolic pathways

Oxygen consumption rate (OCR) was measured in HPAECs transduced with either SOD2 variant using the Seahorse Extracellular Flux (XF96) Analyzer (Seahorse Bioscience, Inc., North Billerica, MA) as previously described[28,217]. HPAECs were transduced in 6 well dishes and grown

in Endothelial Basal Medium. 72 hours after transduction 2.2 x10^4 cells were loaded into each well of a standard XF24 plate. 24 hours after replating, the Endothelial Basal Medium was replaced with Dulbecco's Modified Eagle's Media (DMEM containing 25mM glucose, 2mM glutamine and 1mM pyruvate). Once the medium was changed, cells were consecutively treated with oligomycin A (2.0 μM), FCCP (carbonyl cyanide-ρ-trifluoromethoxyphenylhydrazone) (0.5 μM), Antimycin-A (Ant A) (2 μM), and Rotenone (2 μM). After addition of each agent the wells were mixed and three measurements of OCR were made. After the end of the experiment, measurements were normalized to cell number using crystal violet staining.

ATP-linked OCR is represented as oligomycin A values subtracted from basal respiration. Proton leak is the difference of oligomycin A and Rotenone/Antimycin values. Non-mitochondrial respiration is the Rotenone/Antimycin values subtracted from basal respiration. Values are expressed in terms of a percentage basal respiration for each run.

Fatty acid oxidation (FAO) was measured by treating cells with 40 mM etomoxir (ETO) and subtracting ETO values from basal respiration. Pyruvate metabolism was measured by treating cells with 10 mM UK5099 and subtracting UK5099 values from basal respiration. Glutamine oxidation was measured by treating cells with 5 mM BPTES and subtracting BPTES values from basal respiration. Basal extracellular acidification rate (ECAR) was measured to determine glycolytic rate.

Western Blot Analysis

Cell lysates were prepared as previously described[218]. Goat anti-GFP polyclonal antibody (Abcam, ab6673), mouse 6X-his tag monoclonal ab (Invitrogen, 37-2900), mouse anti-tubulin monoclonal (Sigma, T5168), mouse anti-ATP citrate synthase polyclonal ab (Santa Cruz,

5F8D11), mouse total OXPHOS human ab cocktail (Abcam, ab110411, Complex I-subunit NDUFB8, Complex II-subunit 30kDa, Complex III-subunit Core 2, Complex IV-subunit II, Complex V-subunit alpha), rabbit anti-catalase monoclonal ab (Cell Signaling, D4P7B), mouse anti-TOM20 monoclonal ab (Santa Cruz, sc17764), rabbit anti-HIF-2α monoclonal ab (Cell Signaling, 7096), mouse anti-eNOS monoclonal ab (BD Transduction Labs, 610308), rabbit anti-peNOS S1177 polyclonal ab (Cell Signaling, 9571), and mouse anti-actin monoclonal ab (Santa Cruz, sc47778) were used in western analyses.

ATP Quantification

ATP was quantified using CellTiter-Glo® Luminescent Cell Viability Assay (Promega, G9241) according to manufacturer's instructions.

Measurement of $\Delta\psi$

Transfected HPAECs were incubated with 10 μg/mL JC-1 probe (ThermoFisher Scientific, T3168) for 20 minutes at 37°C then subjected to 2 color flow cytometry (514/529nm and 585/590nm) to quantify the proportion of cells containing JC-1 green monomer (indicative of low $\Delta\psi$) and JC-1 red aggregates (indicative of high $\Delta\psi$) . The ratio of cells containing red aggregates to green monomer was calculated and expressed relative to $SOD2^{WT}$ transfected HPAECs.

In vitro wound healing assay

HPAECs were plated onto 12 well cell culture plates, transduced and grown to confluence. Scratches were made to the bottom of the well using a pipet tip and then imaged. Cells were then incubated in growth factor free medium for approximately 16 hours and reimaged. Percent wound closure was then calculated. Four measurements were made from three wells on three separate

days. Results from each day were averaged and SOD2 V16A closure was normalized to SOD2 WT closure from the respective day.

Cell Survival

22,000 SOD2 WT or SOD2 V16A cells were seeded onto a cell culture plate. The next day nonadherent cells were washed off and the remaining living cells were fixed and stained with crystal violet. Cells were then dissolved with 1% SDS and protein concentration was measured by absorbance at 590 nm. SOD2 V16A cell survival was normalized to SOD2 WT value from the respective day.

Nitrite Measurement

HPAECs were plated and transduced in 6 well cell culture plates. Cells were scraped and collected in a nitrite preservation buffer (potassium ferricyanide 801.1 mM, N-ethylmaleimide 17.6 mM, NP-40 substitute 6%). Samples were then injected in a glass sparger where nitrite was reduced to nitric oxide using the tri-iodide method [potassium iodide 1.11% (w/v), iodine 0.72% (w/v), acetic acid 77.8% (v/v)][219]. The resultant nitric oxide is carried by helium into Sievers Nitrite Oxide Analyzer 280i (General Electric). The chemiluminescent signal from the reaction between nitric oxide and oxygen was recorded. Nitrite concentrations were calculated using the area under the curve and sodium nitrite standards. SOD2 V16A and Ant A treatment nitrite measurements were normalized to SOD2 WT values from the respective day.

SOD2 Immunoprecipitation

HPAECs were plated onto a 10 cm cell culture dish and then transduced with either SOD2 WT or SOD2 V16A. 72 hours after transduction, cells were split in two and half the cells were treated with 2 μM Ant A for 30 minutes at 37 ºC. Cells were then lysed with immunoprecipitation

(IP) buffer (1% NP-40, 137 mM NaCl, 2 mM EDTA, 20 mM Tris) supplemented with proteinase, phosphatase, and deacetylase inhibitors and rotated at 4 ºC for 20-30 minutes. An aliquot was placed aside for whole cell lysate sample and 50 μL Dynabeads™ His-Tag Isolation and Pulldown (ThermoFisher, 10103D) were added to the rest of the lysate and rotated at 4 ºC overnight. The next day, beads were washed 4 times with 0.1% Tween-20. Protein was eluted in 50 μL 2x Lammeli buffer at 95 ºC for 15 minutes, vortexing every 2-3 minutes. IP samples were run on a gel and transferred. Primary antibodies rabbit anti-SOD2 (Abcam, ab13533) and rabbit anti-Acetylated Lysine (Cell Signaling, 9441) were used in Western analysis.

Statistics

Data was expressed as mean ± standard deviation from the mean unless otherwise specified. The n values represent biological replicates. Student's t-test was used to determine significance using GraphPad Prism version 8 software. A *p*-value below 0.05 was considered significant.

2.4 Results

To evaluate the impact of $SOD2^{V16A}$ on cardiovascular phenotypes, we genotyped 410 SS genotype SCD patients from the walk-PHaSST trial[210]. Using multiple linear regression analysis across genotype we found that increased tricuspid regurgitant velocity (TRV, marker of pulmonary hypertension), systolic blood pressure, and right ventricular area at systole (**Figure 2A-C**) along with decreased 6-minute walk distance (**Figure 2D**) correlated with the rs4880 genotype. These clinical parameters are suggestive of reduced pulmonary and cardiovascular function; and

heightened dysfunctional endothelium. These observations were independent of white blood cell count (**Table 1**). A strong trend towards decreased hemoglobin concentration and a significant increase in the hemolytic index were observed indicating a potential role for anemia and hemolysis **(Table 1)**. Plasma lactate dehydrogenase (LDH), a marker of hemolysis[220], also strongly correlated with TRV in rs4880G homozygous patients **(Figure 2E)**. Extracellular activity of LDH increases due to cell membrane perturbation by lipid peroxidation[221]. Thus, LDH is used as a clinical biomarker of oxidative stress and inflammation[220, 221]. Historically, elevated LDH levels in SCD patients associate with increased TRV and pulmonary hypertension[220]. Although we did not observe increased LDH levels in rs4880G homozygotes (**Table 1**), these data suggest that rs4880G associates with worse cardiovascular outcomes in the presence of oxidative stress and inflammation.

To investigate the impact of endothelial $SOD2^{V16A}$, we co-expressed either valine or alanine SOD2 and green fluorescent protein (GFP) (**Figure 2F**) in HPAECs. Using GFP as an expression control, we found no difference in the exogenous SOD2 protein levels, suggesting that $SOD2^{V16A}$ did not affect protein stability (**Figure 2F, G**). Next, we tested whether $SOD2^{V16A}$ impacted enzymatic activity by measuring H_2O_2 production in HPAECs. While there was no difference in H_2O_2 production at baseline, the $SOD2^{V16A}$ variant exacerbated antimycin A, a Complex III inhibitor, induced H_2O_2 production compared to $SOD2^{WT}$ expressing HPAECs (**Figure 2H**). Inhibiting catalase failed to correct the differences in H_2O_2 levels between SOD2 variants **(Figure 3A)**. Furthermore, $SOD2^{V16A}$ did not alter catalase or SOD1 protein expression **(Figure 3B, C)**, suggesting that the difference in H_2O_2 production was independent of catalase and SOD1. These results indicate that $SOD2^{V16A}$ exacerbates H_2O_2 formation in HPAECs under stressed conditions.

While enzymatic dismutation by SOD is the most efficient method of dismutation, superoxide can spontaneously dismutate to H_2O_2 independent of SOD[222]. Therefore, we evaluated whether an increase in mitochondrial $O_2^{\bullet-}$ production could be the source of increased H_2O_2. We found increased mitochondria $O_2^{\bullet-}$ levels both at baseline and with antimycin A treatment in the $SOD2^{V16A}$ transduced HPAECs (**Figure 2I**). Increased mitochondria $O_2^{\bullet-}$ could indicate compromised SOD2 activity. However, when inhibiting SOD1, the only other intracellular SOD isoform, we found SOD activity remained the same between the two variants, indicating that $SOD2^{V16A}$ did not alter SOD2 activity (**Figure 4A, B**).

Since $SOD2^{V16A}$ retained normal activity, we hypothesized that $SOD2^{V16A}$ mislocalizes within HPAECs, considering that the V16A mutation resides in the MLS. To examine SOD2 subcellular location, we fused APEX2, a peroxidase used for electron microscopy and identifying protein-protein interactions, to the *C*-terminus of the two SOD2 variants[213]. Surprisingly, we observed no difference in localization between SOD2-APEX2 variants within the mitochondrial matrix (**Figure 5A, Figure 4C**). Since neither activity nor localization of $SOD2^{V16A}$ was affected, the most likely explanation for the elevated mitochondrial $O_2^{\bullet-}$ is enhanced production. The respiratory chain is the predominant source of mitochondrial $O_2^{\bullet-}$ generation. Therefore, we investigated whether $SOD2^{V16A}$ disrupted respiratory chain complex formation or activity. Although the protein expression of respiratory chain complexes was not affected by $SOD2^{V16A}$ (**Figure 5B, C**), the variant interacted significantly more with Complex IV (**Figure 5D, E**). Specifically, $SOD2^{V16A}$ interacted more with Subunit 2, part of the catalytic domain of Complex IV and showed significantly lower Complex IV activity (**Figure 5F**). Inhibited Complex IV activity impairs mitochondrial respiration[223]. Indeed, we found that basal oxygen consumption was lower in $SOD2^{V16A}$ expressing HPAECs, indicating suppressed mitochondrial respiration (**Figure**

5G). Additionally, there was a compensatory increase in glycolysis and fatty acid oxidation (**Figure 4D, E**).

Despite the compromised Complex IV activity, $SOD2^{V16A}$ expressing HPAECs maintained normal ATP production and mitochondrial potential (**Figure 6A, B**). However, we observed increased mitochondrial hyperfusion (**Figure 6C, D**). This is consistent with the previous observation that reduced Complex IV activity results in mitochondria hyperfusion as a mechanism to maintain mitochondria function and ATP production[224]. These data suggest that $SOD2^{V16A}$ expressed in HPAECs preserve ATP production by hyperfusing mitochondria but does so at the expense of generating more mitochondrial $O_2^{\bullet-}$. This increase in ROS production however did not result in a change in endothelial cell proliferation and migration, cell survival, or HIF-2α expression. However, we found increased nitrite production and eNOS activation (**Figure 7**) possibly due to increased H_2O_2[225]. Increased NO reacts with mitochondrial $O_2^{\bullet-}$ forming peroxynitrite which may exacerbate mitochondria dysfunction. In summary, we have shown that *in vivo* $SOD2^{V16A}$ is a strong predictor of cardiovascular dysfunction in SCD patients; *in vitro* we have demonstrated that $SOD2^{V16A}$ overassociates with Complex IV of the respiratory chain reducing complex activity and resulting in increased mitochondrial $O_2^-$and extracellular H_2O_2 production.

2.5 Discussion

Mechanistically, one limitation remains unsolved: how does $SOD2^{V16A}$ with normal enzymatic activity and correct subcellular location result in lower Complex IV activity? SOD2 is

embedded within the mitochondria supercomplex I:III:IV, stabilizing and protecting the supercomplex from mitochondrial O_2^- damage[226]. In this supercomplex, Complex IV requires 14 subunits to maintain its activity[227]. Subunit 4 has redox-sensitive cysteine residues that have been proposed to regulate Complex IV conformation and activity under oxidative stress[228]. Elevated mitochondrial O_2^- likely enhances H_2O_2 formation leading to thiol oxidation and possible conformational changes in Complex IV, reducing its activity. Other possible targets of hydrogen peroxide oxidation within Complex IV include heme (a_3) and copper (Cu_B) which make up a catalytic site that is also essential for protein folding and assembly[229]. However, the mechanism driving the interaction between $SOD2^{V16A}$ and Complex IV remain elusive and subject to further investigation. SOD2 acetylation has been shown to increase mitochondrial O_2^- production[230], however we found no increase in acetylation of $SOD2^{V16A}$ expressing HPAECs at baseline or after treatment with antimycin A (**Figure 8**).

An alternative hypothesis is that the MLS, which is cleaved once it is translocated in the mitochondria, may impact Complex IV activity. Like $SOD2^{V16A}$, an alanine-to-valine mutation in the MLS of myofibrillogenesis 1 is associated with paroxysmal nonkinesigenic dyskinesia without affecting protein maturation and mitochondrial localization[231]. The alanine residue in cleaved MLSs may impact composition of amphipathic peptides in the mitochondria and inhibit respiration. The exact mechanism of how alanine containing peptides affect mitochondrial respiration remains to be investigated though disturbances of the ratio between amphipathic peptides and mitochondria have been previously shown to have deleterious effects on mitochondria potential and respiration[232].

Importantly, our study may lead to better-informed management of SCD patients by uncovering $SOD2^{V16A}$ as a genetic biomarker to determine efficacy to therapeutics. As such,

current therapies with antioxidant properties such as L-glutamine[233] and hydroxyurea[234] may be more effective in patients carrying the $SOD2^{V16A}$ polymorphism. Lastly, the $SOD2^{V16A}$ polymorphism may help guide precision medicine approaches for SCD particularly those therapies that reduce mitochondrial O_2^{-}[235].

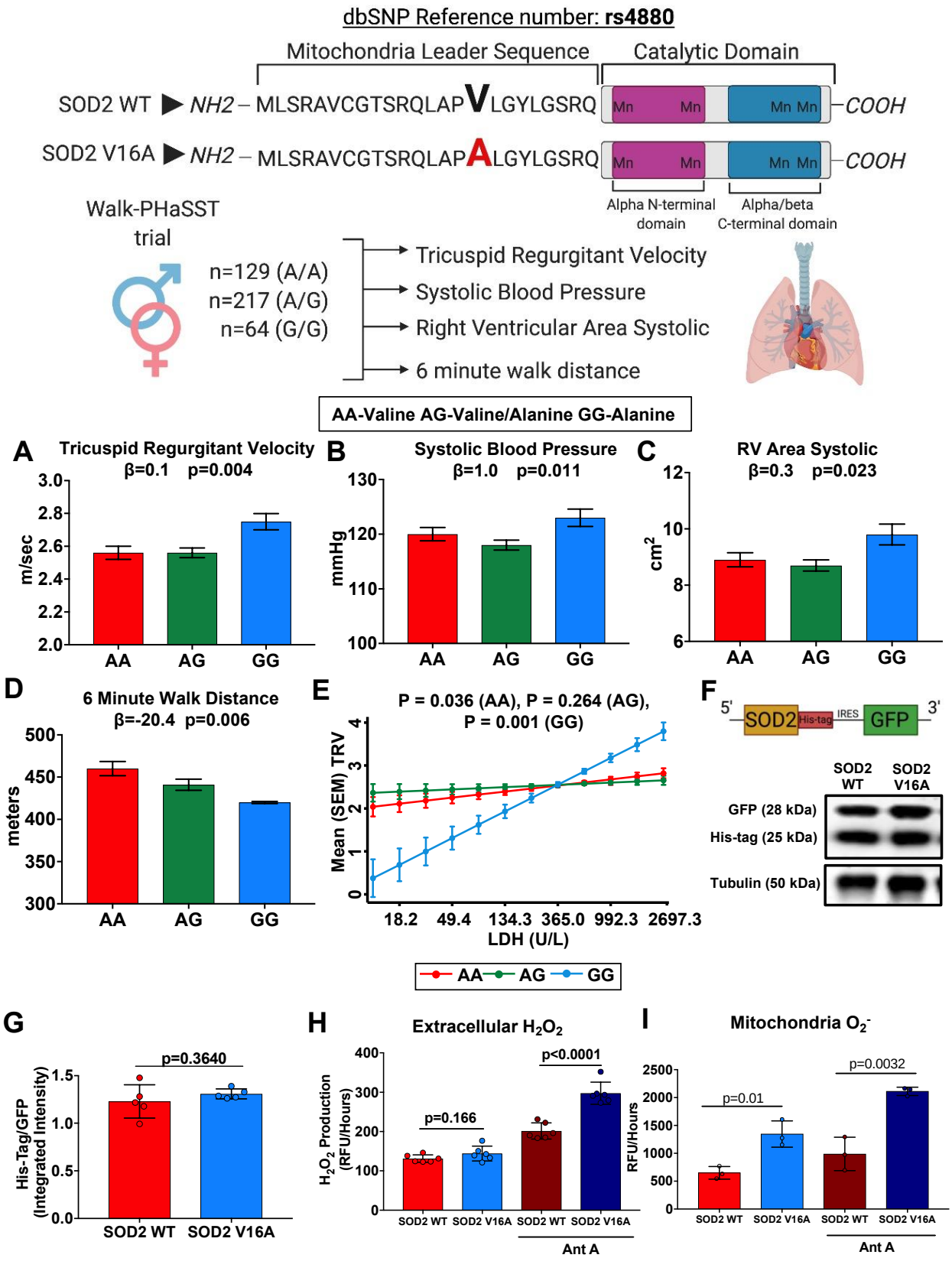
dbSNP Reference number: rs4880
Mitochondria Leader Sequence
Catalytic Domain
SOD2 WT ▶ NH2 – MLSRAVCGTSRQLAP V LGYLGSRQ
SOD2 V16A ▶ NH2 – MLSRAVCGTSRQLAP A LGYLGSRQ
Mn Mn Mn Mn
COOH
Alpha N-terminal domain
Alpha/beta C-terminal domain
Walk-PHaSST trial
n=129 (A/A)
n=217 (A/G)
n=64 (G/G)
Tricuspid Regurgitant Velocity
Systolic Blood Pressure
Right Ventricular Area Systolic
6 minute walk distance
AA-Valine AG-Valine/Alanine GG-Alanine
A
Tricuspid Regurgitant Velocity
β=0.1 p=0.004
m/sec
AA AG GG
B
Systolic Blood Pressure
β=1.0 p=0.011
mmHg
C
RV Area Systolic
β=0.3 p=0.023
cm2
D
6 Minute Walk Distance
β=-20.4 p=0.006
meters
E
P = 0.036 (AA), P = 0.264 (AG),
P = 0.001 (GG)
Mean (SEM) TRV
18.2 49.4 134.3 365.0 992.3 2697.3
LDH (U/L)
AA AG GG
F
5' SOD2 His-tag IRES GFP 3'
SOD2 WT
SOD2 V16A
GFP (28 kDa)
His-tag (25 kDa)
Tubulin (50 kDa)
G
p=0.3640
His-Tag/GFP (Integrated Intensity)
SOD2 WT SOD2 V16A
H
Extracellular H2O2
p<0.0001
p=0.166
H2O2 Production (RFU/Hours)
SOD2 WT SOD2 V16A SOD2 WT SOD2 V16A
Ant A
I
Mitochondria O2-
p=0.0032
p=0.01
RFU/Hours
SOD2 WT SOD2 V16A SOD2 WT SOD2 V16A
Ant A

Figure 2

Superoxide dismutase 2 (SOD2) V16A is associated with clinical markers of endothelial dysfunction and increases extracellular hydrogen peroxide and mitochondrial reactive oxygen species production.

(A) Tricuspid regurgitant velocity (TRV), (B) Systolic blood pressure, (C) right ventricular area at systole, (D) 6-minute walk distance of Walk-PhaSST cohort by SOD2 16^{th} amino acid genotype, and (E) interaction between lactate dehydrogenase and TRV by SOD2 16^{th} amino acid genotype P for interaction of LDH and genotype <0.001. (F) Plasmid schematic of SOD2 lentiviral and (G) protein expression between two SOD2 variants. (H) Extracellular hydrogen peroxide and (I) mitochondrial reactive oxygen species produced by each SOD2 variant with and without antimycin A. Results in (A)-(E) are in mean with standard error of the mean. In (A)-(D), β means measure the change of outcome by each minor allele (additive model) and p values are representing the test for trend. In (E), interaction between SOD genotype and LDH was tested in a linear regression analysis. P values test the correlation between TRV and LDH in each SOD genotype. Results in (G)-(I) are given in mean with standard deviation. AA represents patients with the Alanine variant of SOD2, AG represents patients with the Alanine/Valine variant, and GG represents patients with the Valine variant.

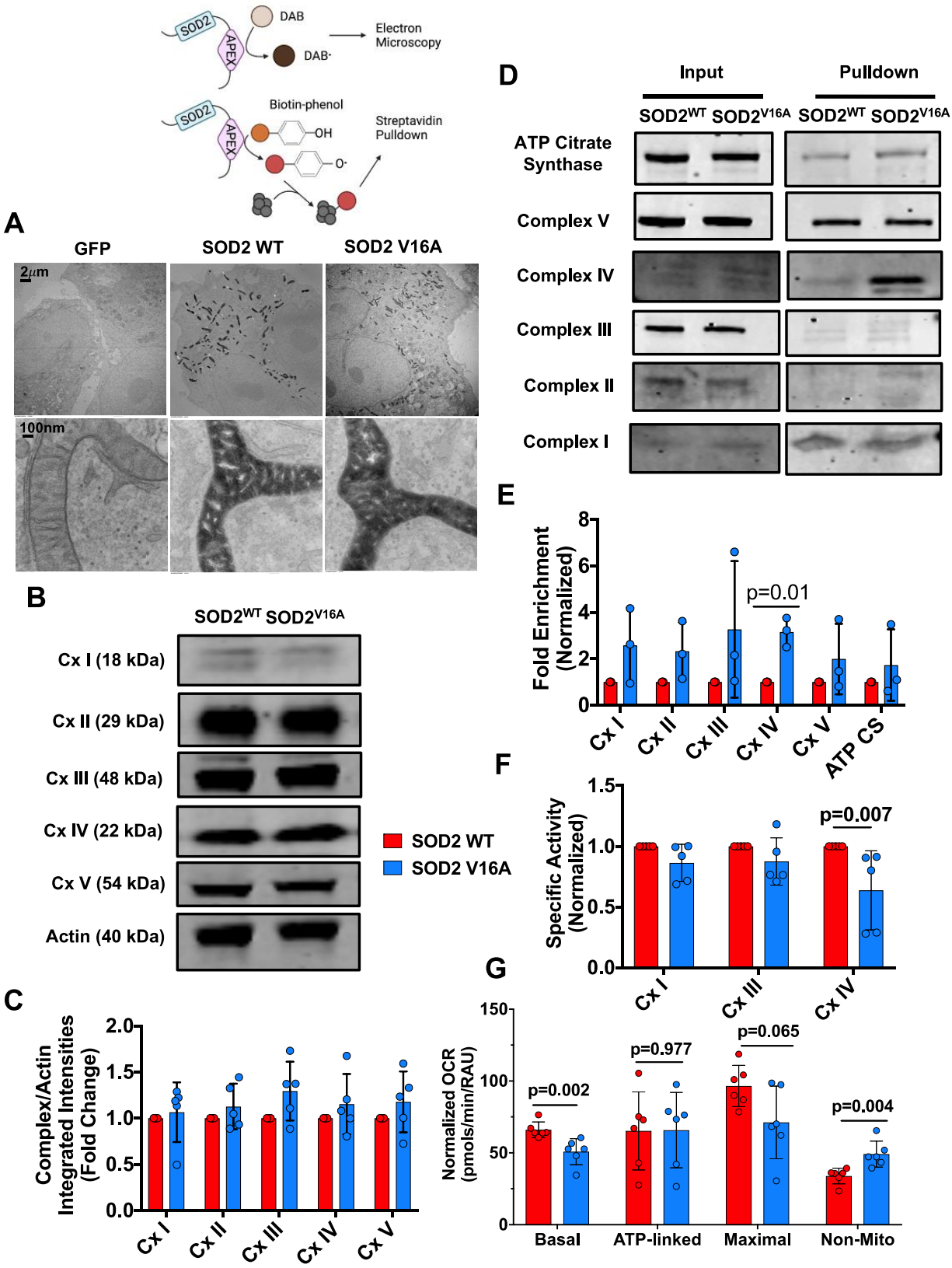
SOD2
APEX
DAB
DAB·
Electron Microscopy
Biotin-phenol
OH
O·
Streptavidin Pulldown
A
GFP
SOD2 WT
SOD2 V16A
2μm
100nm
B
SOD2WT SOD2V16A
Cx I (18 kDa)
Cx II (29 kDa)
Cx III (48 kDa)
Cx IV (22 kDa)
Cx V (54 kDa)
Actin (40 kDa)
SOD2 WT
SOD2 V16A
C
Complex/Actin Integrated Intensities (Fold Change)
2.0
1.5
1.0
0.5
0.0
Cx I
Cx II
Cx III
Cx IV
Cx V
D
Input
Pulldown
SOD2WT SOD2V16A SOD2WT SOD2V16A
ATP Citrate Synthase
Complex V
Complex IV
Complex III
Complex II
Complex I
E
Fold Enrichment (Normalized)
8
6
4
2
0
p=0.01
Cx I
Cx II
Cx III
Cx IV
Cx V
ATP CS
F
Specific Activity (Normalized)
1.5
1.0
0.5
0.0
p=0.007
Cx I
Cx III
Cx IV
G
Normalized OCR (pmols/min/RAU)
150
100
50
0
p=0.002
p=0.977
p=0.065
p=0.004
Basal
ATP-linked
Maximal
Non-Mito

Figure 3

SOD2 V16A associates with Complex IV of the mitochondria respiration chain resulting in decreased Complex IV activity and basal respiration in human arterial pulmonary endothelial cells. (A) Electron microscopy images of APEX fused SOD2 variants obtained at 100,000x magnification with JEM 1400Plus TEM. (B-C) Western blots and quantification of mitochondria respiration chain complexes in SOD2 variants. (D-E) Western blots and fold enrichment calculations of APEC-fused SOD2 variants after biotinylating and streptavidin pulldown. (F) Enzymatic activities of complexes I, III, and IV in SOD2 variants normalized to complex V activity. (G) Mitochondria respiration of cells transduced with either SOD2 variant. Results are given in mean with standard deviation.

Distribution of clinical and echo marker in SS patients by SOD2 genotype. Results are in mean (SE) unless otherwise specified.				
	AA	AG	GG	P value for linear trend
	N = 129	N = 217	N = 64	
Age	35 (1.1)	36 (0.8)	38 (1.6)	0.09
History of pulmonary embolism %	5%	3%	6%	0.82
Hemoglobin	8.9 (1.4)	8.6 (1.1)	8.5 (2.0)	0.06
MCV	94 (1.0)	93 (0.8)	93 (1.4)	0.62
Reticulocyte count	26 (1.2)	26 (0.9)	28 (1.7)	0.27
WBC count	9.7 (0.33)	10.4 (0.25)	10.4 (0.46)	0.21
Platelet count	375 (11.6)	380 (9.0)	357 (16.4)	0.37
Left ventricular e/ea'	6.8 (0.26)	7.2 (0.20)	6.8 (0.37)	0.95
Left mass index	113 (3.0)	117 (2.3)	116 (4.3)	0.52
Right atrial area	19 (0.4)	20 (0.3)	20 (0.6)	0.76
Creatinine	0.9 (0.09)	0.9 (0.07)	0.9 (0.13)	0.82
Hemolytic Index	0.4 (0.18)	0.5 (0.12)	0.9 (0.22)	0.037
LDH	493 (368)	473 (294)	506 (258)	0.39

Table 1

Baseline clinical parameters of SCD patient cohort. Distribution of clinical and ECHO marker in SS patients by SOD2 genotype. Results for LDH values are given as mean (SD). All other results are in mean (SE) unless otherwise specified. Hemolytic index is measured by a principal component analysis of four factors: aspartate transaminase (AST), LDH, absolute reticulocytes, and total bilirubin.

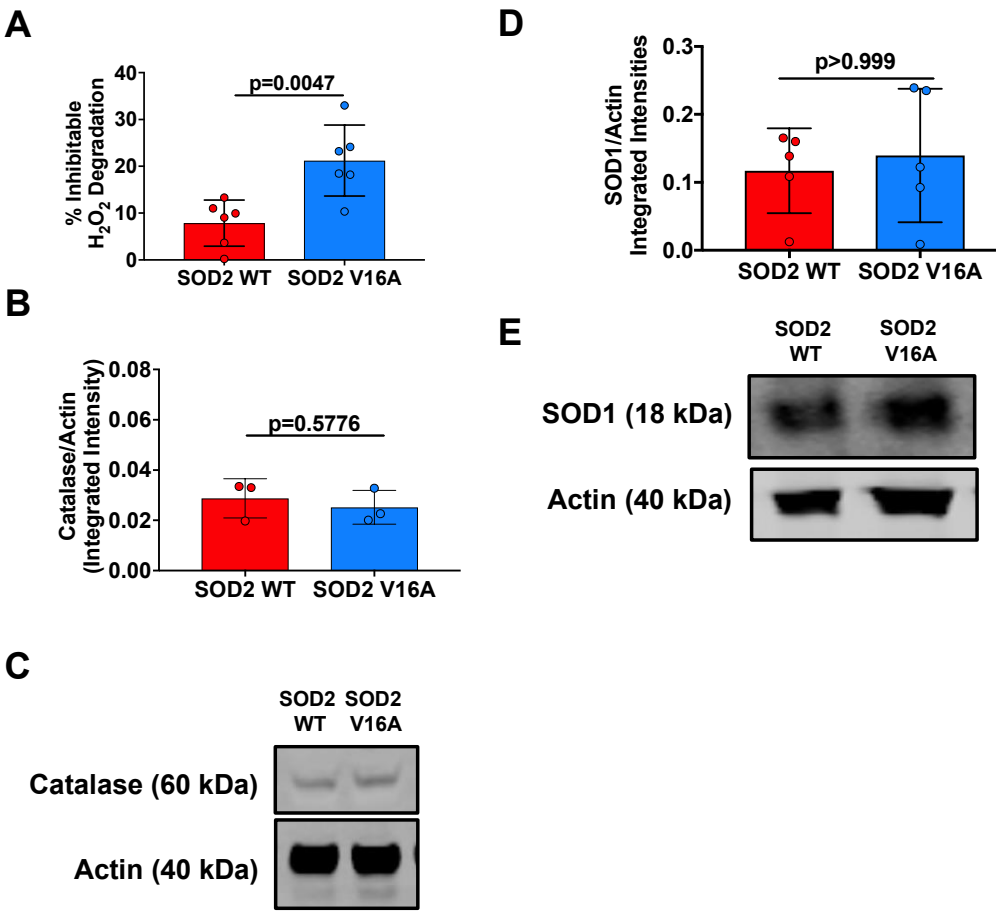

Figure 4

SOD2 V16A has increased catalase activity without changes in catalase and SOD1 protein in transduced HPAECs. (A) Hydrogen peroxide assay utilizing the catalase inhibitor amino triazole demonstrates an increase in hydrogen peroxide production inhibitable by catalase in SOD2 V16A transduced cells. (B-C) Western blot and quantification of catalase protein in SOD2 variants. (D-E) Western blot and quantification of SOD1 protein in SOD2 variants.

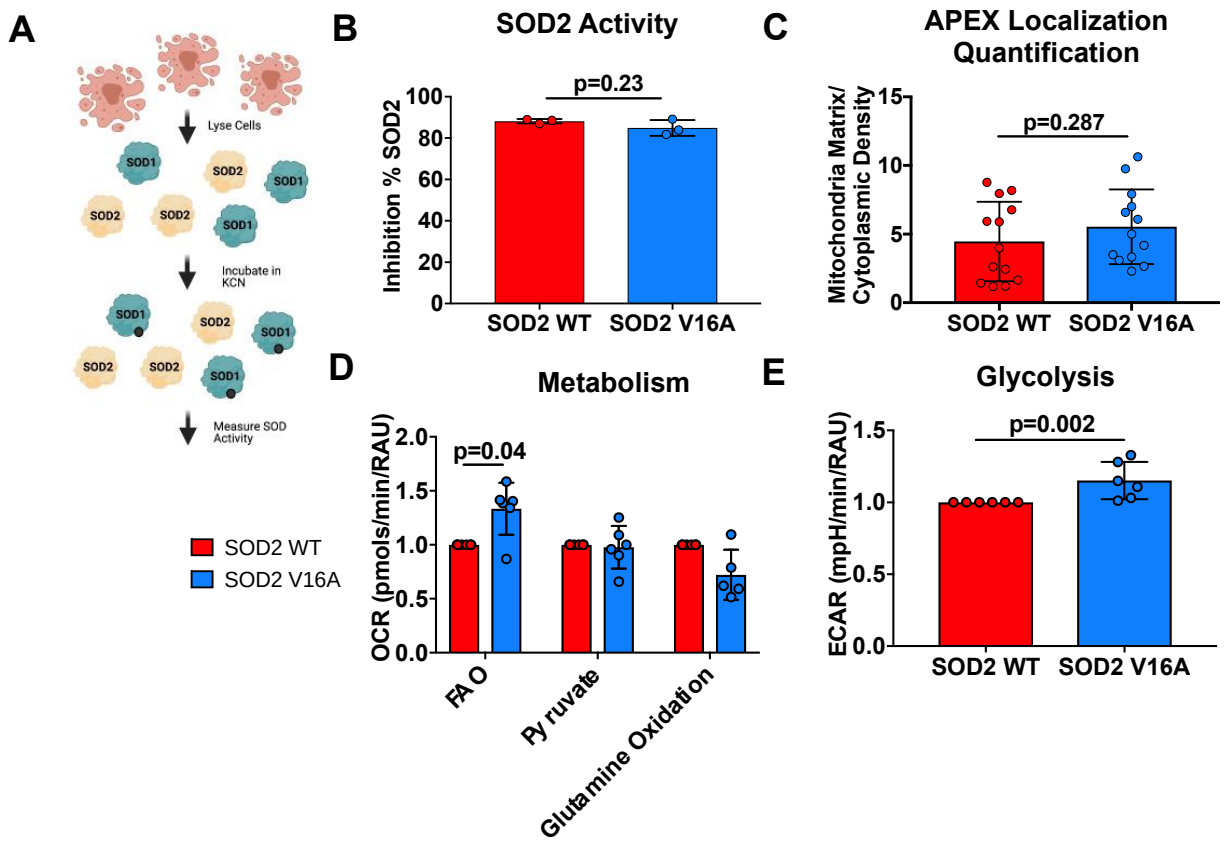

Figure 5

No change in SOD2 enzymatic activity, localization between SOD2 variants, or other metabolic pathways. (A) Schematic of experimental design to specifically measure SOD2 activity. (B) SOD2 specific activity in SOD2 variants. (C) Quantification of SOD2 APEX EM Imaging. (D, E) Increase in fatty acid oxidation (FAO) and glycolysis.

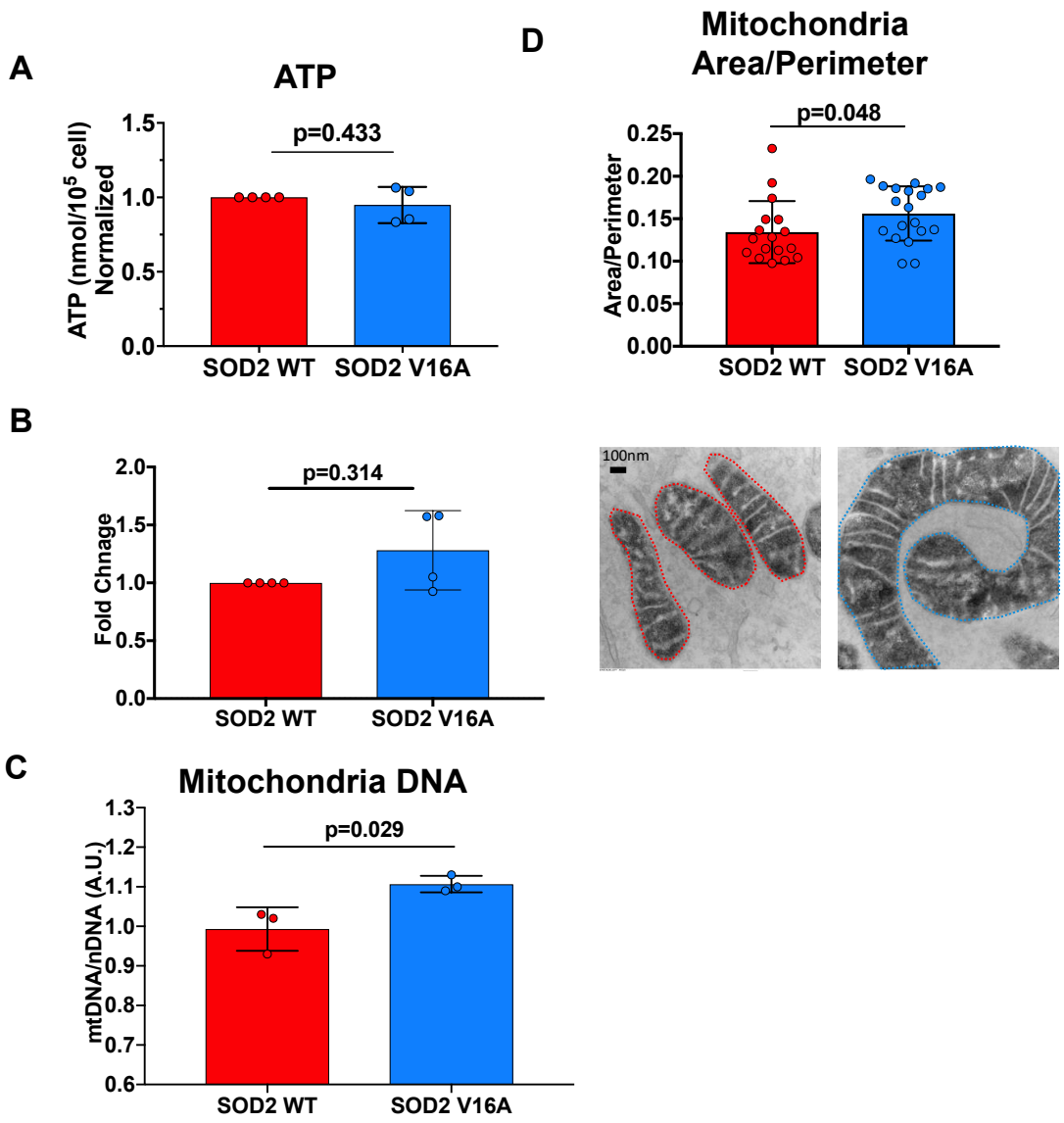

Figure 6

No changes in ATP production or mitochondria potential in SOD2 V16A transduced HPAECs. (A) ATP production, (B) mitochondria potential, and (C) mitochondria DNA in transduced HPAECs. (D) Mitochondria area normalized to perimeter, EM image taken at 100,000x magnification with JEM 1400Plus TEM.

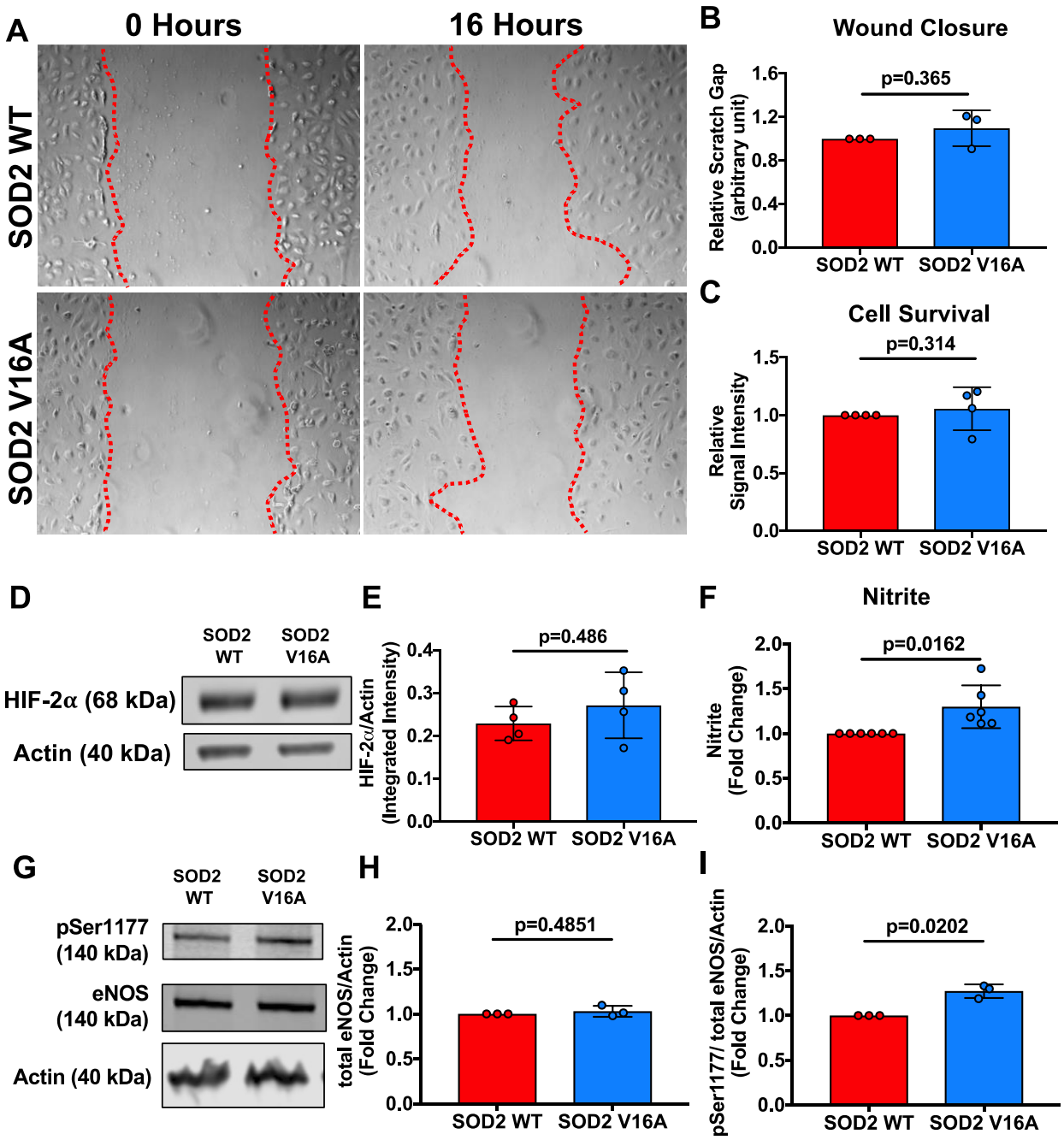

Figure 7

No change in endothelial cell function between SOD2 variants. (A, B) Representative images and quantification of *in vitro* scratch assay to measure cell proliferation and migration. No difference was appreciated between SOD2 variants. (C) Cell survival was measured by plating 22,000 transduced cells and assaying for survivability with crystal violet the next day. (D, E) Western blot and quantification of HIF-2α protein in SOD2 variants. (F) Nitrite

measurements at baseline in transduced cells. (G-I) Western blot and quantification of eNOS and eNOS pSer1177 protein in SOD2 variants.

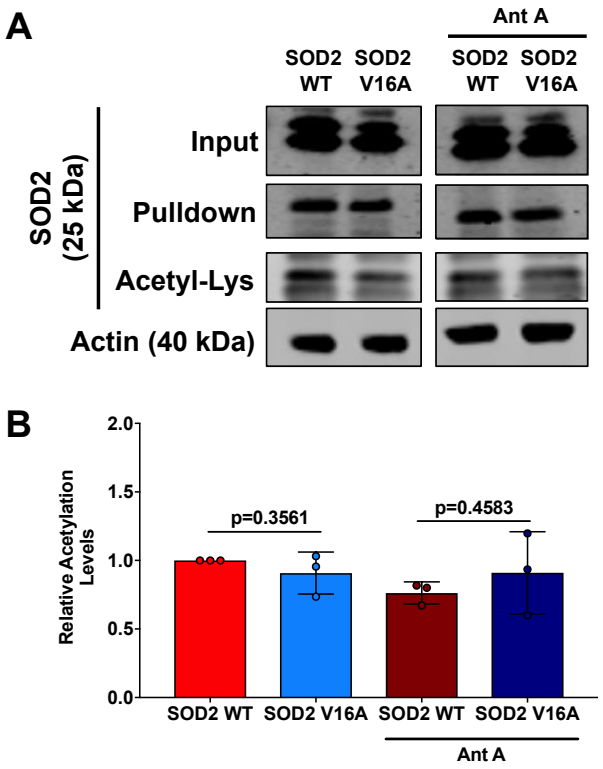

Figure 8

Increased mitochondrial superoxide production in SOD2 V16A HPAECs is not attributable to changes in acetylation. His-tag beads were used to immunoprecipitated SOD2 WT or SOD2 V16A from transduced HPAECs and degree of acetylation was measured by Western blot. No changes in acetylation were detected at baseline or after treatment with antimycin A.

3.0 Endothelial Superoxide Dismutase 2 is Decreased in Sickle Cell Disease and Regulates Fibronectin Processing

Atinuke Dosunmu-Ogunbi[1,2,3], Shuai Yuan[3], Daniel J. Shiwarski[4], Joshua W. Tashman[1,4], Michael Reynolds[3], Adam Feinberg[4,5], Enrico M. Novelli[2,3], Sruti Shiva[2,3], Adam C. Straub[2,3,6]

1 Medical Scientist Training Program, University of Pittsburgh School of Medicine, Pittsburgh, PA, USA

2 Department of Pharmacology and Chemical Biology, University of Pittsburgh School of Medicine, Pittsburgh, PA, USA

3 Heart, Lung, Blood and Vascular Medicine Institute, University of Pittsburgh, Pittsburgh, PA, USA

4 Department of Biomedical Engineering, Carnegie Mellon University, Pittsburgh, Pennsylvania, USA

5 Department of Materials Science and Engineering, Carnegie Mellon University, Pittsburgh, PA, USA

6 Center for Microvascular Research, Department of Medicine, University of Pittsburgh School of Medicine, Pittsburgh, Pennsylvania, USA

3.1 Summary

Sickle cell disease (SCD) is a genetic red blood cell disorder characterized by increased reactive oxygen species (ROS) and a concordant reduction in antioxidant capacity in the endothelium. Superoxide dismutase 2 (SOD2) is a mitochondrial-localized enzyme that catalyzes the dismutation of superoxide to hydrogen peroxide. Decreased peripheral blood expression of SOD2 is correlated with increased hemolysis and cardiomyopathy in SCD. Here, we report for the first time that endothelial cells exhibit reduced SOD2 protein expression in the pulmonary endothelium of SCD patients. To investigate the impact of decreased SOD2 expression in the

endothelium, SOD2 was knocked down in human pulmonary microvascular endothelial cells (hPMVECs). We found that SOD2 deficiency in hPMVECs results in endothelial cell dysfunction, including reduced cellular adhesion, diminished migration, integrin protein dysregulation, and disruption of permeability. Furthermore, we uncover that SOD2 mediates changes in endothelial cell function via processing of fibronectin through its inability to facilitate dimerization. These results demonstrate that endothelial cells are deficient in SOD2 expression in SCD patients and suggest a novel pathway for SOD2 in regulating fibronectin processing.

3.2 Introduction

Sickle cell disease (SCD) is an inherited hemoglobinopathy that results in sickling of deoxygenated red blood cells (RBC) due to a point mutation in the beta-globin gene[24]. In SCD, there is an increase in oxidative stress due to augmented reactive oxygen species (ROS) production from enzymatic sources such as xanthine oxidase[236] and non-enzymatic sources including Fenton chemistry[237]. Paired with this increase in ROS production is a compromised antioxidant system. Levels of both enzymatic and non-enzymatic antioxidants are diminished in sickle cell patients compared to controls[37-39]. This reduction in antioxidants leaves reactive species free to target a variety of molecules such as cysteines and lipids, leading to endothelial dysfunction, including sterile inflammation [29]. As such, activated endothelium upregulates surface adhesion molecules causing RBC adhesion and microvascular occlusion[29]. Extensive microvascular occlusions contribute to end-organ damage, which in SCD may manifest as acute chest syndrome[238], pulmonary hypertension[239-241], stroke[242,243], acute splenic sequestration[244], papillary necrosis[245,246], amongst others determined by the organ affected[247]. Pulmonary endothelial dysfunction is

responsible for pulmonary hypertension, which significantly escalates mortality of SCD patients and is thus a cause of clinical concern[239,248,249]. Both in SCD and other conditions, pulmonary hypertension is characterized by increased oxidative stress[250] and, in severe cases, a decrease in the enzymatic antioxidant superoxide dismutase 2 (SOD2)[251].

SOD2 is a mitochondrial-localized enzymatic antioxidant that functions by dismutating superoxide to hydrogen peroxide (H_2O_2)[140]. SOD2 has been shown to play an essential role in maintaining vascular function, while SOD2 deficiency increases oxidative damage and disrupts vascular homeostasis[140,234]. *In vivo*, depletion of SOD2 promotes neointimal formation through the attenuation of vascular smooth muscle cell (SMC) proliferation and migration[252]. Additionally, cardiomyocyte depletion of SOD2 in a mouse model results in the development of a dilated cardiomyopathy with isolated cardiomyocytes producing more ROS resulting in a disruption in oxidative phosphorylation[253]. However, the role of SOD2 in endothelial cells remains to be investigated.

In SCD, there is reduced peripheral blood expression of SOD2 and this decrease in SOD2 is associated with increased hemolysis, inflammation, iron overload, oxidative stress, and SCD cardiomyopathy[254]. While reduction of peripheral blood SOD2 has been reported, the study was limited due to a small sample size and select patient population. Consequently, there has been little investigation into the consequences of reduced SOD2 in SCD. More importantly, it is not clear whether vascular endothelial SOD2 is affected in SCD patients. Considering that the endothelium is a primary target for oxidative stress in SCD and that SOD2 is decreased in pulmonary vascular disease, we hypothesized that endothelial cell expression of SOD2 would be reduced in SCD lungs and that suppression of SOD2 protein levels in cultured endothelial cells would lead to mitochondria dysfunction and subsequent endothelial cell dysfunction.

3.3 Materials and Methods

Human lung tissue samples

Human lung samples were explanted from four patients with SCD and no history of lung disease. SCD patient samples were obtained through Institutional Review Board (IRB) approved protocols at the University of Pennsylvania[255]. Lung samples were formalin fixed and paraffin embedded then cut into 4- to 5-μm thick sections. Sections were then used for immunofluorescent staining. Patients were 44.2 ± 9.9 years old at the time of death and two were female. Samples from four African American controls were obtained under University of Pittsburgh CORID #451. Controls were 43±13.7 years, two were female.

Immunofluorescent staining

Tissue Histology: Lung sections were deparaffinized with xylene followed by rehydration by decreasing 100%-70% ethanol washes ending with distilled water. Sections underwent antigen retrieval in a heat mediated citric acid-based solution (H-3300, Vector Laboratories) for 20 minutes and then cooled at room temperature for 1 hour. Sections were then blocked in 10% horse serum (H1270, Millipore Sigma) in PBS for 1 hour at room temperature. Primary antibodies for von Willebrand Factor (ab11713, Abcam, 1:100) and SOD2 (ab13533, Abcam, 1:250) were diluted in 10% horse serum in PBS and incubated on sections at 4°C overnight. After primary antibody incubation, cells were washed in PBS and incubated with secondary antibodies donkey anti-rabbit Alexa Fluor 596 (A21207, Invitrogen, 1:250), and donkey anti-sheep Alexa Fluor 647 (A21448, Invitrogen, 1:250), along with preconjugated smooth muscle α-actin-FITC (ACTA2-FITC; F3777, MilliporeSigma, clone 1A4, 1:500) and DAPI (D3571, Thermo Fisher Scientific, 1:250) for 1 hour at room temperature. Sections were then washed with PBS and a coverslip was placed on after

adding Prolong Gold Antifade with DAPI reagent (P36931, Invitrogen) to each section. Lungs sections were imaged using a Nikon A1 Confocal Laser microscope at 40x magnification with 1096 x 1096 resolution at the Center for Biologic Imaging at the University of Pittsburgh. Z-stacks in 0.5μm increments were taken. Images in the figures are representative images of the maximum-intensity projections of the Z-stacks. To quantify levels of SOD2 in the endothelial cell and smooth muscle cell layers, regions of interest were drawn from the maximum intensity projection of the von Willebrand factor (endothelial cells) and ACTA2 (SMCs) and superimposed onto the maximum-intensity projection for SOD2. Raw integrated intensity per area in ImageJ was then quantified to represent the amount of SOD2 staining in the endothelial and SMC layers.

Cell Histology: hPMVECs were grown on glass coverslips, fixed with 2%PFA for 30 minutes, washed with PBS and then permeabilized in 0.1% Trypsin for 20 minutes. Following permeabilization, cells were blocked in 1% BSA in PBS/FBS for 1 hour and then primary antibody for fibronectin (E5H6X, rabbit, Cell Signaling, 1:800) was diluted in 1% BSA in PBS/FBS overnight at 4°C overnight. After primary antibody incubation, cells were washed and incubated in donkey anti-rabbit Alexa Fluor 596 (A21207, Invitrogen, 1:250) and DAPI (D3571, Thermo Fisher Scientific, 1:250) for 1 hour at room temperature. Sections were then washed with PBS and mounted with Prolong Gold Antifade with DAPI reagent (P36931, Invitrogen). hPMVECs were imaged using a Nikon A1 Confocal Laser microscope at 60x magnification with 4x zoom and 1096 x 1096 resolution at the Center for Biologic Imaging at the University of Pittsburgh. Z-stacks in 0.5μm increments were taken. Images in the figures are representative images of the maximum-intensity projections of the Z-stacks.

Mouse Strain and collection of lung specimens

All animal studies were done under a protocol approved by the Institutional Animal Care and Use Committee of the University of Pittsburgh. Homozygous male sickle and non-sickle control Townes mice were obtained from The Jackson Laboratories (Bar Harbor, ME, stock No. 013071). Mice were aged 3 months before sacrificing and collection of lung tissue. Lung tissue was flash frozen in liquid nitrogen, then ground using mortar and pestle before extracting protein and RNA for subsequent analysis. Mouse tissue was lysed in ice-cold 1x RIPA lysis supplemented with additional protease and phosphatase inhibitors (Sigma-Aldrich). Protein lysate concentrations were quantified using a BCA Protein Assay (23225, Thermo Fisher). Tissue was lysed in TRIzol reagent (15596026, Thermo Fisher). RNA from lysates were isolated according to the protocol from the Direct-zol RNA miniprep plus kit (R2051, Zymo).

Cell line, tissue culturing, and SOD2 knockdown

Human pulmonary microvascular endothelial cells (hPMVECs, CC-2527, Lonza) were cultured at 37°C in Lonza Endothelial Cell Growth Medium-2 (CC-3156) with EGM^{TM}-2 MV Microvascular Endothelial Cell Growth Medium-2 BulletKit^{TM} (CC-4147, Lonza) supplementation. Cells were passaged using Gibco Trypsin-EDTA (T4049, Sigma Aldrich) up to passage 12. To induce gene knockdown of SOD2, hPMVECs were transiently infected with SOD2 siRNA (Dharmacon) using Lipofectamine 3000 (L3000001, Thermo Fisher) transfection reagent according to the manufacturer's protocol for 48-72 hours. Control cells were similarly transfected with a non-targeting siRNA sequence (Dharmacon).

Western blotting

hPMVECs were cultured in twelve-well dishes until confluent and lysed in Laemmli sample buffer containing 1% SDS, 10% glycerol, 31.25 nM Tris-HCl, 0.005% Bromophenol Blue, and 2.5% β-Mercatoethanol. Lysates were boiled and run on 4%-12% BisTris polyacrylamide gels (Life Technologies) and transferred onto nitrocellulose membranes. Membranes were incubated in primary antibodies **(Table 2)** at 4°C overnight. Secondary antibodies **(Table 2)** were incubated for one hour at room temperature. Visualization and analyses were completed with a LI-COR Odyssey Imager and Image Studio Software.

Quantitative reverse transcription PCR

hPMVECs were cultured in twelve-well dishes until confluent and lysed in TRIzol reagent (15596026, Thermo Fisher). RNA from lysates were isolated according to the protocol from the Direct-zol RNA miniprep plus kit (R2051, Zymo). Isolated RNA was reverse transcribed to cDNA with SuperScript™ IV VILO™ Master Mix (11756050, Thermo Fisher). Quantitative PCR was performed using PowerUp SyBr Green Master Mix (A46012, Thermo Fisher) and 1 μM target primer **(Table 3)** in a QuantStudio 5 Real-Time PCR System (Thermo Fisher).

Mitochondria superoxide measurements

Transfected hPMVECs were tryspinized and then resuspended in Mg^2 and Ca^{2+} free Hank's Balanced Salt Solution (HBSS). In a 96 well plate 150,000 cells and 5 μM MitoSOX Red™ (Invitrogen) were added. Fluorescent signal (510nm/580nm) was then recorded at 37°C for 2 hours. In order to reduce variation, fluorescent intensities were averaged every 6 minutes before log phase slope was calculated to represent production rate. Results were normalized to protein concentration.

Respiratory complex activities

Respiratory complex activity assays were performed as previously described[28]. Complex activities were normalized to ATP citrate synthase activity.

Measurement of oxygen consumption rate (OCR)

Oxygen consumption rate (OCR) measurements in hPMVECs were measured using the Seahorse Extracellular Flux (XF96) Analyzer (Seahorse Bioscience, Inc., North Billercia, MA). hPMVECs were seeded and grown overnight at a density of 2.2×10^4 cells/well in standard XF24 plates. Next, growth media was replaced with DMEM and hPMVECs were consecutively treated with 2.0μM oligomycin, 0.5μM carbonyl cyanide-ρ-trifluoromethoxphenylhydrazone (FCCP), and 2.0μM Rotenone/ 2.0μM Antimycin A. Three measurements of OCR were made over 1.5 minutes after addition of the agents. OCR readings were normalized to cell number after crystal violet staining.

ATP Measurements

CellTiter-Glo® Luminescent Cell Viability Assay (Promega, G9241) was used to quantify ATP according to manufacturer's instructions.

Measurement of $\Delta\psi$

Transfected hPMVECs were incubated with 10 μg/mL JC-1 probe (ThermoFisher Scientific, T3168) for 20 minutes at 37°C then subjected to 2 color flow cytometry (514/529nm and 585/590nm). The ratio of red aggregates to green monomers was calculated and expressed relative to siNT transfected hPMVECs.

Transwell Assay

hPMVECs were grown to confluency on Transwell inserts (3450, Costar) containing 0.4 uM pores. 1 mg/mL of albumin-fluorescein isothiocyanate (66 kDa) (A9771, Sigma) was added to the media over the cells. After 30 minutes, 1 hour, 2 hours, and 4 hours 100 µL of media was extracted from below the Transwell insert and replaced with growth media. Extracted media was measured at 495 nm excitation and 519 nm emission peak wavelengths to determine endothelial cell monolayer permeability.

Electric Cell Impedance Sensing

hPMVECs were plated at 60000/cm^2 into 8-well polyethylene terephthalate arrays (8W10E+, Applied Biophysics). Measurements of transendothelial electric resistance (TEER) were obtained using an electric cell impedance sensing (ECIS) system (Applied Biophysics). Data was continuously collected every 63 seconds and recorded by computer and a Capacitance below 10nF at 64000 Hz was required for hPMVECs to be considered confluent. Baseline TEER was recorded for 1 hour and cells were serum starved for 4 hours before challenging hPMVECs with hydrogen peroxide or hemin.

In vitro wound healing assay

hPMVECs were transfected and grown to confluence in a 12 well tissue culture plate. Using a pipet tip two scratches were made within the well and an image was taken. The cells were incubated in growth factor free media for approximately 16 hours and then the scratches were reimaged. ImageJ was used to measure the area of the scratch at 0 hours and 16 hours and percent wound closure was calculated. Four measurements were made from each well and 3 wells were

plated for each condition. Figure represents average wound closures from experiments conducted on four separate days.

Adhesion assay

hPMVECs were transfected and grown to confluence in a 6 well cell culture plate. 2 mM ethylenediaminetetraacetic acid (EDTA) was used to remove the cells from the plate and then resuspended in serum free media. Approximately 8,000 cells were plated into each well of a 96 well plate. Two 96 well plates were simultaneously plated with cells and incubated at 37°C. After 20 minutes, one plate was removed from incubation, washed twice with PBS, fixed in 4% PFA, and then stained with 0.05% crystal violet. Wells were imaged using a light microscope and cells were counted. After 24 hours, the second 96 well plate was removed from incubation and cells were fixed in 4% PFA, stained with 0.05% crystal violet, and washed with deionized water. Fixed and stained cells were then dissolved with 0.1% SDS and absorbance was read at 610nm. Cell number was normalized to absorbance of wells from the 24-hour plate. 5 wells were plated for each condition in both the 20 minute and 24 hour 96 well plate. Figure represents average cell number from experiments conducted on 3 separate days normalized to the siNT cell number. To coat plates in fibronectin, 1 mg/mL fibronectin was added to each well enough to cover the surface and incubated at 37°C overnight. On the day of the experiment, fibronectin was removed from the plate and the plate was allowed to dry completely.

Fibronectin Image Analysis

Fibronectin siNT and siSOD2 3D image stacks were analyzed using the FIJI implementation of ImageJ (NIH)[256]. The fibronectin image stacks were loaded into ImageJ and a set of custom macros were executed. The first macro maximally projected the stack in Z then

segmented the fibronectin signal utilizing Phansalkar auto local thresholding. Bright pixel outliers were removed to decrease noise and the images were rotated to horizontally align the fibronectin band. The image was cropped to isolate analysis to the region containing the patterned fibronectin band of interest. Next, the image was made binary and the segmented particles were analyzed using the inbuilt particle analysis tool with circularity and other measures calculated automatically. The individual particle data and summary data were exported to Excel files. For 3D fibronectin analysis, surface objects were created in Imaris (Bitplane, v 9.5) analysis software for both the nucleus and the fibronectin channel. To minimize variability in the analysis across images and achieve consistent segmentation, the local contrast method was used for surface creation with a minimum value set to 750 for all images. The fibronectin surface was color coded using a statistic for sphericity. Image snapshots were captured and surface statistics were exported to Excel files for 3D visualization and quantification. Statistical analysis of particle data was then performed using GraphPad Prism 9 (GraphPad).

Patterning Fibronectin Lines

The fibronectin lines were fabricated using an adaptation the surface-initiated assembly technique[257,258]. Briefly, 20 μm lines with 20 μm were first designed using AutoCAD software. The CAD file was then transferred to a transparency photomask (CAD/Art Services, Inc., Bandon, OR, USA), where the spaces and the segments of the lines were dark and transparent, respectively. Square glass wafers (Fisher No. 12-543-F 45 × 50 × 2 mm) were spin-coated with Photoresist SPR-220.3 at 5000 rpm for 20 s, baked on a 115 °C hot plate for 90 s, exposed to ultraviolet (UV) light through the transparency photomask, baked on a 115 °C hot plate for 90 s, and developed for 1 min using MF-26A developer. Sylgard 184 (Dow Corning) polydimethylsiloxane (PDMS) elastomer was prepared per manufacturer's directions by mixing 10 parts base to 1 part curing agent (by

weight) using a Thinky-Conditioning mixer (Phoenix Equipment Inc., Rochester, NY, USA) for 2 min at 2000 rpm followed by 2 min of defoaming at 2000 rpm. PDMS was cast over the patterned photoresist-coated glass wafer and placed at 65 °C to cure the PDMS overnight. Square PDMS stamps ~1 cm^2 were cut out of the ~5 mm thick PDMS layer.

Prior to stamping, 25 mm circular glass coverslips (Fisher No. 12-545-86 25CIR-1D) coverslips were cleaned, spin coated with PDMS, cured overnight, and functionalized using UV/Ozone for 15 min. The PDMS stamps were sonicated in 50% ethanol for 30 min, dried with nitrogen gas, and coated with a 50 μg/mL human FN solution (Corning). After 1 h of incubation at room temperature, the FN-coated PDMS stamps were rinsed in sterile ddH_2O, dried with nitrogen, and stamped onto the PDMS coated coverslips. After 30 min, the PDMS stamps were carefully removed from the glass coverslips, leaving behind a microcontact-printed FN lines on the PDMS surface. Incubation with 1% Pluronic F-127 was performed for 15 min to prevent cells from adhering to the non-patterned PDMS. Cells were then seed onto the coverslips following previously described methods.

Statistics

Student's *t* test was used to determine significance using GraphPad Prism version 7.03 software.

3.4 Results

To determine SOD2 protein expression levels in the endothelium of patients with SCD, lung tissue samples from 4 patients (age 44.2±9.9 years, 2 female) and 4 race matched controls

(43±13.7 years, 2 female) were stained with SOD2 **(Figure 9A)**. Immunofluorescent staining analysis showed an approximately 40% reduction in SOD2 expression in SCD patient endothelial cells compared to controls (2283 ± 88.85 and 5518 ± 401.3, respectively) **(Figure 9B)**. SOD2 staining in SMC was also decreased by roughly 40% in SCD patients compared to controls (2249 ± 86.84 and 5088 ± 405.5, respectively) **(Figure 9C)**. This is the first known finding demonstrating a decrease in SOD2 protein expression in the pulmonary endothelial cells and SMCs of patients.

Next, SOD2 protein expression in the Townes transgenic sickle mouse model was investigated. mRNA and protein levels of all three SOD enzymes, as well as catalase in whole lung tissue of 3-month-old sickle (SS) and non-sickle (AA) mice, were measured. While there was no change in *sod2* mRNA expression levels **(Figure 10A)**, there was an approximately 25% decrease in SOD2 protein expression in SS mice as compared to age and gender-matched AA controls (1.914 ± 0.3504 and 3.833 ± 0.4401, respectively) **(Figure 10B, C)**. In contrast, there were no changes in either *sod1* or *sod3* mRNA or protein expression **(Figure 15)**. There was, however, a decrease in *catalase* mRNA and an increase in protein expression of catalase **(Figure 15)**. These results, in conjunction with the SCD patient data, demonstrate SOD2 protein expression is decreased as a result of sickle pathology.

To further determine the role of SOD2 in the pulmonary endothelium, siRNA was used to knockdown SOD2 in hPMVECs. While SOD2 siRNA decreased both *sod2* mRNA and SOD2 protein expression, there were no compensatory changes in *catalase* mRNA or catalase protein expression, though there was a significant decrease in SOD1 protein expression **(Figure 16)**. Next, to determine whether SOD2 knockdown affected ROS production, mitochondrial superoxide was measured and was found to be markedly increased in the absence of SOD2 **(Figure 11A)**. We next tested mitochondria complex expression and function using a Seahorse extracellular flux

technology. Mitochondria respiratory complex protein expression was first quantified, and we found that SOD2 knockdown resulted in a decrease in respiratory complex IV protein expression **(Figure 11B, C)**. However, reduced complex IV protein expression did not affect complex specific activity, mitochondria respiration, or ATP production **(Figure 11D-F)**, although the lack of SOD2 significantly decreased mitochondrial potential, indicative of damaged mitochondria **(Figure 11G)**. Taken together, these data show that SOD2 deficiency in hPMVECs causes an amplified ROS production, decreasing mitochondria membrane potential but sparing mitochondria respiratory capacity.

A primary endothelial function is to serve as a barrier to confine blood from the interstitial space. To determine whether SOD2 regulates endothelial barrier integrity, hPMVECs were plated onto porous transwell inserts, and albumin leakage was measured over time. We uncovered that SOD2-silenced hPMVECs exhibited significantly increased albumin leakage **(Figure 12A)**. Similarly, transendothelial electrical resistance measured by electric cell impedance sensing (ECIS) was decreased in SOD2 knockdown cells, indicating barrier disruption **(Figure 12B, Figure 17A).** To ascertain whether SOD2 mediated barrier disruption was due to diminished H_2O_2, siSOD2 hPMVECs were treated with H_2O_2. Decreased resistance was corrected with the addition of 4 μM H_2O_2 **(Figure 12C, Figure 17B)**, suggesting a role for H_2O_2 signaling in regulating changes in SOD2 mediated permeability pathways. SCD is characterized by episodes of increased hemolysis which elevates levels of free hemoglobin and heme in the blood[259]. Challenging sickle mice with extracellular hemin, the oxidized form of heme, triggers acute chest syndrome, a pulmonary complication of SCD characterized by increased permeability of the lung vasculature[260]. We investigated whether simulating a hemolytic crisis by challenging siSOD2 hPMVECs with hemin would exacerbate differences in permeability. However, challenging

siSOD2 hPMVECs with hemin did not further exacerbate the differences observed in permeability **(Figure 17C-E)**. These findings suggest that SOD2 maintains the endothelial barrier through H_2O_2 signaling in a hemin-independent pathway.

Another critical cellular function of the endothelium is the ability to proliferate and migrate during wound healing. One complication of SCD is the development of intractable and slow healing skin ulcers[261], indicating that there may be dysfunction in the endothelium's ability to proliferate and migrate. The scratch assay was used to measure wound closure in siSOD2 hPMVECs, and was found to be approximately half of siNT hPMVECs **(Figure 12D, E),** suggesting SOD2 is required for endothelial proliferation and migration. These data demonstrate that SOD2 is essential in the maintenance of multiple endothelial cell functions.

The assembly and turn-over of focal adhesions play essential roles in endothelial barrier integrity, proliferation, and migration[262,263]. Therefore, we examined whether SOD2 affects endothelial cell adhesion. First, adhesion of siSOD2 hPMVECs to uncoated cell culture plates was measured and was found to be decreased by 20% **(Figure 13A, B)**. Integrins are essential mediators of cell-matrix adhesion[264]. Interestingly, siSOD2 hPMVECs showed a significant decrease in integrin β3 protein expression and a significant increase in integrin β4 protein expression **(Figure 13C, D)**. Given that integrin β3 mediates cell adhesion to fibronectin[265] and that the initial stage of cell attachment is mediated by integrins[266] we hypothesized that precoating cell culture plates with fibronectin would exacerbate differences observed in adhesion **(Figure 18)**. Instead of observing a greater difference in adhesion, precoating plates with fibronectin completely corrected the defect in adhesion **(Figure 13A, B)**. Collectively, these results show that silencing of SOD2 disrupts cellular adhesion as well as diminishes integrin β3 protein expression and that

pre-coating cell culture plates with fibronectin reverses the defect in adhesion, highlighting a potential disruption in siSOD2 hPMVECs produced fibronectin.

Considering that adhesion deficiency in SOD2-silenced endothelial cells was corrected upon fibronectin addition, we hypothesized that SOD2 might be involved in fibronectin synthesis and assembly. No changes in *fibronectin* mRNA expression or total fibronectin protein expression were observed between siNT and siSOD2 hPMVECs **(Figure 19A-C).** However, there was a significant decrease in the dimer to monomer ratio in siSOD2 hPMVECs (**Figure 14A, B),** indicating that there is reduced assembly of dimerized fibronectin, an essential step in the formation of fibronectin fibrils and integration into the extracellular matrix (ECM)[104]. Meanwhile, confocal microscopy showed a reduction in the formation of fibronectin bundles seen in siNT hPMVECs **(Figure 14C)**. 3D rendering of the confocal images revealed that in SOD2 deficient hPMVECs, fibronectin is arrested within the cell **(Figure 14D)**. Measurement of fibronectin circularity and spherecity showed that fibronectin within SOD2 KD hPMVECs was more globular as opposed to linear **(Figure 14E, F)**. These results show that SOD2 plays a role in fibronectin matrix assembly.

3.5 Discussion

Decreased SOD2 protein expression has been characterized in various disease states such as SCD[254], pulmonary hypertension[251], and chronic kidney disease[267]. Given the evidence that therapeutic upregulation of SOD activity attenuates vascular dysfunction[268,269], we hypothesized that SOD2 expression may be essential in modulating disease pathogenesis in conditions in which the vasculature is a primary target such as SCD. While it has been well established that there is an

increase in oxidative stress in SCD with dysregulation of both enzymatic and non-enzymatic antioxidants[37-39,234], there is no evidence demonstrating organ downregulation of antioxidants. Our study shows for the first time that there is significant downregulation in both endothelial and SMC SOD2 protein expression in the lung tissue of SCD patients. We have also shown that this decrease in SOD2 protein expression is recapitulated in the Townes transgenic mouse model of SCD in whole lung tissue. These findings established the premise for further studies investigating the functional effect of decreased endothelial expression of SOD2.

We silenced SOD2 protein expression in hPMVECs and examined mitochondrial function. The significant increase in mitochondrial superoxide production with silencing of SOD2 **(Figure 11A)** demonstrated an essential role of SOD2 in modulating ROS levels within the mitochondria. Regardless of a 50% increase in mitochondria superoxide production, there were no deleterious effects on respiratory complex activity, mitochondrial respiration, or ATP production **(Figure 11D-F)** despite other studies having shown that oxygen consumption rate is decreased in SOD2 null HEK293T cells[270] and chondrocytes[271]. The preservation of oxygen consumption could be attributed to the more glycolytic nature of endothelial cells[272]. We did, however, observe a decrease in mitochondrial membrane potential **(Figure 11G),** which would imply the presence of mitochondrial damage[273]. Given that this impairment in mitochondrial transmembrane potential formation was not significant enough to decrease ATP production, there may be other pathways, such as glycolysis, that are able to compensate for the lack of SOD2 to maintain ATP production.

Although the effects on mitochondria function were moderate, we observed significant endothelial dysfunction. Both albumin flux and ECIS showed that knockdown of SOD2 in hPMVECs increased endothelial permeability at baseline **(Figure 12A, B, Figure 17A)**. As far as we know, this is the first study to demonstrate that SOD2 is required to maintain endothelial barrier

integrity. The impaired endothelial barrier function was reversed by H_2O_2 **(Figure 12C, Figure 17B)**. It has been well established that H_2O_2-mediated oxidation of cysteine residues is a crucial part of intracellular signaling[274]. The reversibility of impaired endothelial barrier function with H_2O_2 demonstrates that redox signaling, possibly through the modification of oxidizable amino acid residues such as cysteine, is implicit in SOD2-mediated permeability regulatory pathways. Plasma heme levels are elevated in SCD[275]. Hemin, the oxidized form of heme, is a known disruptor of endothelial barriers and has been implicated in the progression of SCD clinical complications such as acute chest syndrome [260,276,277]. We investigated whether SOD2 knockdown exacerbates hemin-induced permeability. We found no difference with hemin treatment in siSOD2 hPMVECs compared to siNT hPMVECs **(Figure 17C-E)**. One limitation of this study is the inability to monitor the effects of chronic stimulation with hemin, which would more closely model chronic hemolysis in SCD. In addition to increased permeability, endothelial migration and proliferation, measured through the *in vitro* wound healing assay, were also reduced by SOD2 siRNA (**Figure 12D, E)**. SMC mitochondria relocate to the leading edge of the cell to facilitate mobility and migration[278]. SOD2 may modulate cell migration and proliferation by facilitating H_2O_2 production at the leading edge. Future studies examining the spatial and temporal control of H_2O_2 production via SOD2 regulation are warranted.

Permeabiltiy, proliferation, and migration are all cellular functions reliant on sufficient integrity of focal adhesions[279,280]. We have shown that SOD2 deficient hPMVECs have reduced adhesion to uncoated cell culture plates **(Figure 13A, B)**. SOD2 depleted hPMVECs also had reduced integrin β3 protein expression **(Figure 13C, D)**. Considering that integrin β3 facilitates adhesion to fibronectin[265], we expected that precoating cell culture plates with fibronectin would increase adhesion differences. Surprisingly, fibronectin precoating corrected adhesion deficiency

in SOD2 knockdown cells **(Figure 13A, B)**. This would imply that the defect in focal adhesion was due to a disturbance with cell-produced fibronectin and that decreased integrin β3 protein expression was most likely a result of an issue with fibronectin. Indeed, siSOD2 hPMVECs had a reduction in the ratio of dimerized to monomeric fibronectin **(Figure 14A, B),** suggesting that SOD2 facilitates fibronectin dimerization. This disruption in fibronectin processing was visually appreciable **(Figure 14C).** Upon performing 3D rendering of the images, we observed that SOD2 is not only necessary for fibronectin dimerization but also needed for proper localization to the outside of the cell **(Figure 14D)**. Further analyses revealed that fibronectin in siSOD2 hPMVECs was more circular **(Figure 14E, F)**. This measurement further supports the finding that SOD2 is needed for the dimerization and thereby the polymerization of fibronectin. Fibronectin has multiple domains to facilitate interactions with other ECM proteins, the cell, and other fibronectin proteins[104]. Dimerized fibronectin is assembled intracellularly through oxidation of cysteine residues in the C110 region on the carboxy terminus[281,282]. Upon secretion and binding to cell surface receptors, dimers interact through disulfide bonds to cross-link into multimers[281]. Ablation of these C-terminal cysteine residues results in complete failure to dimerize, though the resultant monomeric fibronectin can still be secreted[282]. Lysyl oxidase has been identified as a catalyst for covalent cross-linking in fibrillar collagen as well as elastin[283]. Lysyl oxidase has also been shown to bind with a strong affinity to C-terminal fragments of cellular fibronectin, suggesting that it may catalyze fibronectin dimer formation [283]. No other peroxidases or oxidases have been implicated in directly or indirectly modulating fibronectin dimerization. Given the fact that mitochondria relocate to the leading edge of cells to facilitate migration [278] and that fibronectin fibrillogenesis, which is reliant on fibronectin dimerization, is essential for promoting directionality in cellular migration[284], it is probable that H_2O_2 signaling from the mitochondria affects fibronectin

processing. We propose that decreased H_2O_2 formation through knockdown of SOD2 destabilizes fibronectin dimers by decreasing oxidation of cysteine residues, thereby disrupting cellular migration. Failure of fibronectin dimerization would also decrease cellular adhesion[104] and disrupt endothelial barrier function[279]. Future studies are needed to verify whether mitochondria interact with fibronectin during dimerization and if impaired dimerization leads to physiological and pathophysiological consequences in vivo and in SCD.

In conclusion, we have shown for the first time that there is a decrease in endothelial cell SOD2 expression in SCD and that reduction in endothelial SOD2 protein expression results in disruption of fibronectin dimerization and secretion. This disruption of fibronectin processing consequently leads to decreased adhesion, migration, and proliferation, integrin protein dysregulation, as well as an increase in permeability. Taken together, these data suggest that further investigation into therapeutic treatments targeting SOD2-mediated changes in ECM protein assembly may be beneficial in SCD.

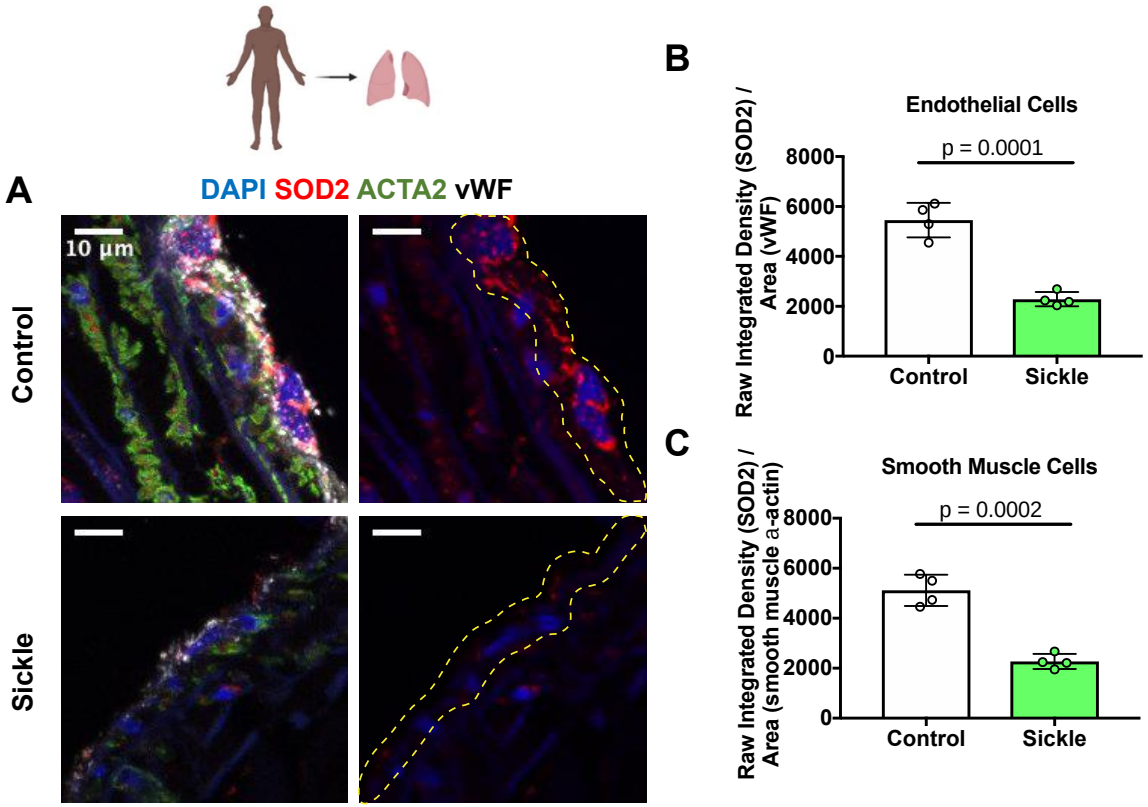

Figure 9

Sickle cell patients have a reduction in endothelial and smooth muscle SOD2 protein expression. (A) SOD2 expression was measured by immunofluorescence in lung sections from 4 patients with SCD and 4 controls without overt lung disease. Expression of SOD2 (red; smooth muscle cell stained green, von Willebrand factor stained white and DAPI stained blue) was increased in SCD patients compared to controls. (B, C) Quantification of endothelial cell or smooth muscle cell SOD2 protein expression. 3-4 regions of interests were quantified for each patient and control sample and an average was taken and graphed. Values are means ± SD. P-values determined by two tailed Student's t test. Dotted line represents endothelial cell layer.

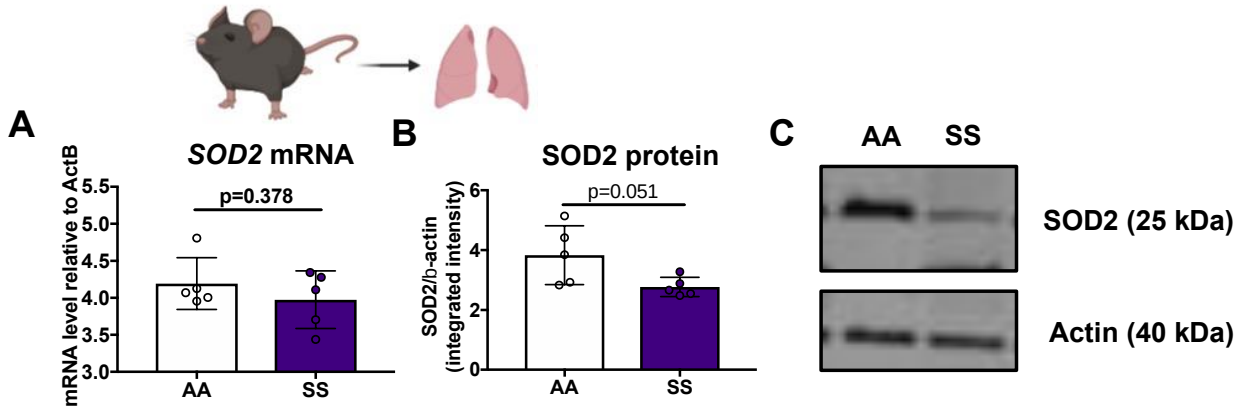

Figure 10

Townes transgenic SS mice compared to AA mice have decreased SOD2 protein expression in whole lung lysate. (A-C) Whole lung tissue of SS Townes mice (n=5) had no changes in mRNA, but increased SOD2 protein expression compared to AA Townes mice (n=5). Quantification of SOD2 band density/actin band density from western blot. Data shown are individual values with means ± SD. P-values determined by two tailed Student's t test.

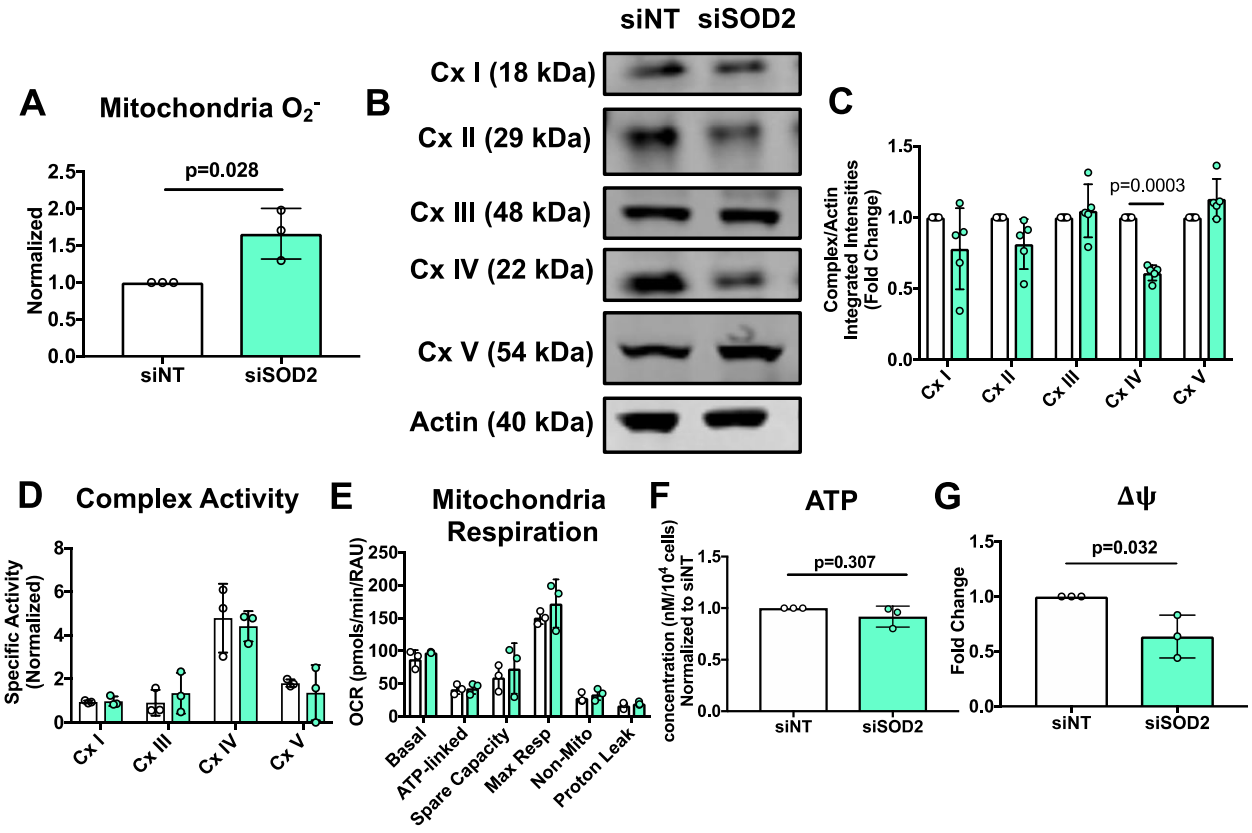

Figure 11

siSOD2 hPMVECs have increased mitochondrial superoxide production and decreased mitochondrial membrane potential. hPMVECs were transfected with non-targeting siRNA (siNT) or SOD2 siRNA to knockdown *sod2* mRNA and protein expression. Following 48 hours, experiments were conducted. (A) Mitochondria superoxide production in siNT and siSOD2 hPMVECs (n=3). (B) Cells were lysed and Western blotted for mitochondria respiratory complex proteins. (C) Quantification of Western blot (n=5). (D) Respiratory chain complex specific activity normalized to ATP citrate synthase activity in siNT and siSOD2 hPMVECs (n=3). (E) Mitochondria oxidative consumption (n=3), (F) Total ATP (n=3) and (G) Mitochondria potential (n=3) in siNT and siSOD2 hPMVECs. Data shown represent averaged values for each day of experimentation with means ± SD. P-values determined by two tailed Student's t test.

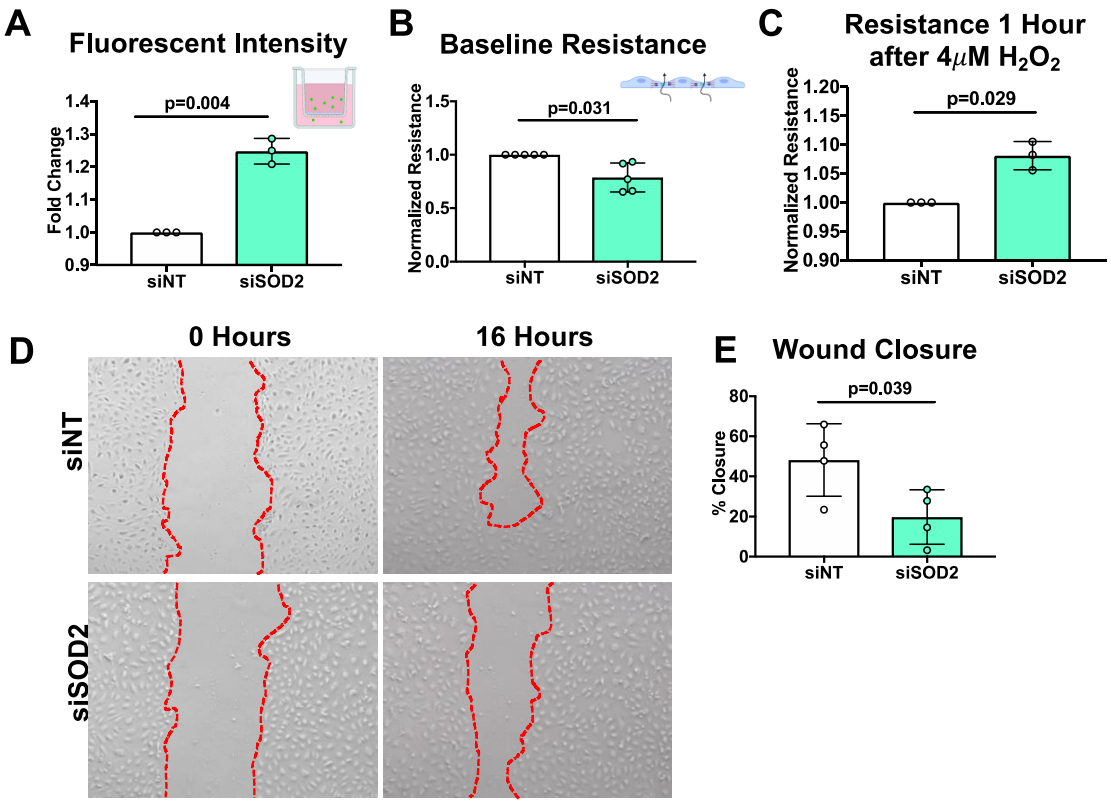

Figure 12

siSOD2 hPMVECs demonstrate increased permeability and decreased proliferation and migration. (A) siNT or siSOD2 hPMVECs were grown to a confluent monolayer on transwell filters. Albumin-fluorescein isothiocyanate was added to each well and medium from beneath the filter was collected at 1 hour and fluorescent intensity was measured (n=3). (B) siNT or siSOD2 cells were grown to a confluent monolayer on ECIS chips and baseline resistance was measured for one hour (n=5). (C) After serum starvation hPMVECs were treated with 4μM H_2O_2 while measuring resistance (n=3). (D, E) Images and quantification of siNT and siSOD2 hPMVECs wound healing assay. Images were taken 0 hours and 16 hours after wounding (n=4). Data shown represent averaged values for each day of experimentation with means ± SD. P-values determined by two tailed Student's t test.

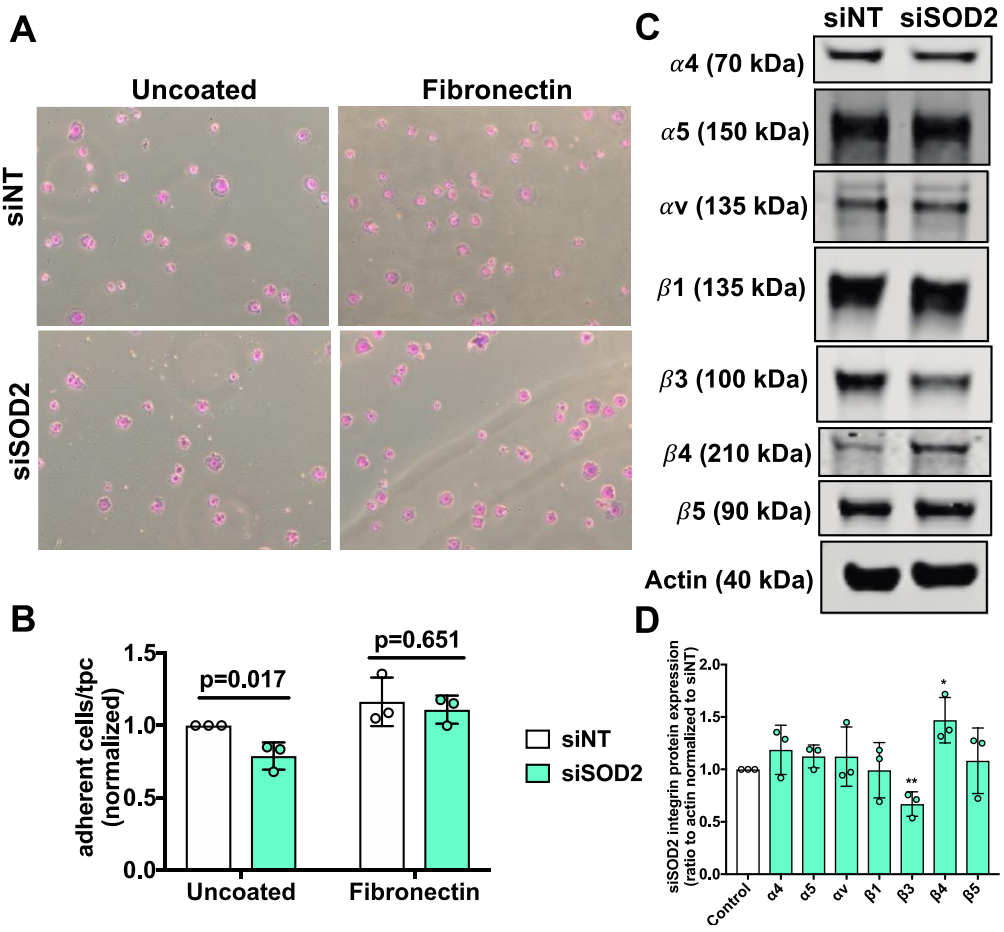

Figure 13

Decreased adhesion and integrin protein dysregulation in siSOD2 hPMVECs. (A) Representative images show attached viable siNT or siSOD2 hPMVECs in uncoated plates and plates coated with fibronectin. (B) Graphs demonstrate the number of cells per high power field (n=3). (C) Western blot image of integrins α4, α5, αV, β1, β3, β4, β5, and actin protein expression. (D) Shows quantification of Western blot above (n=3). Data shown represent averaged values for each day of experimentation with means ± SD. P-values determined by two tailed Student's t test.

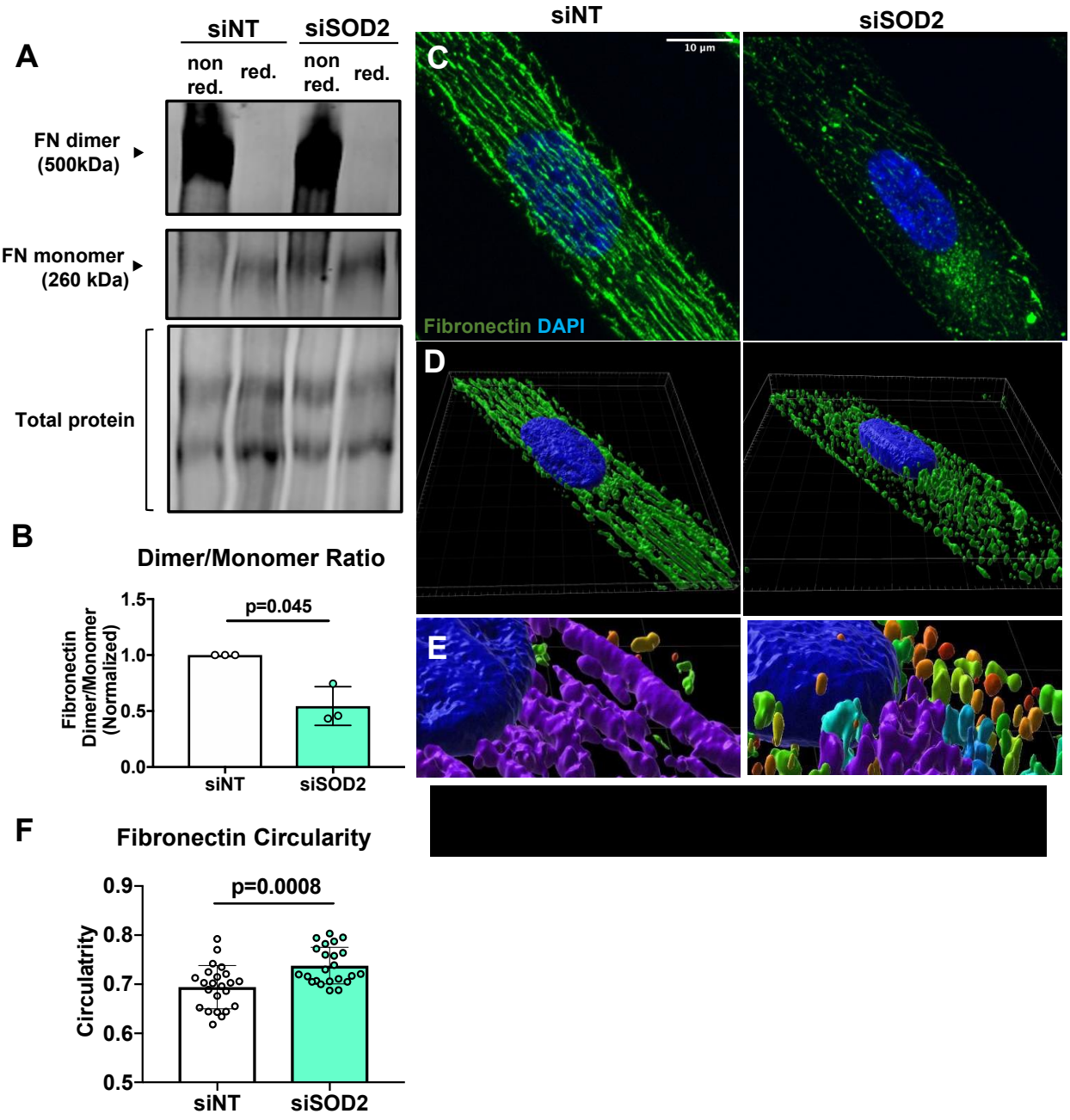

Figure 14

SOD2 knockdown disrupts fibronectin processing and trafficking. (A) Shows a Western blot image of nonreduced and reduced fibronectin and total protein. (B) Quantification of dimerized to monomeric fibronectin from above image (n=3). (C) siNT or siSOD2 hPMVECs were plated onto PDRS coverslips stamped with lines of fibronectin and then stained for fibronectin in green and nuclei in blue. (D) 3D rendering of confocal images showing fibronectin

distribution and organization. (E) 3D rendering of confocal images showing degree of spherecity of fibronectin, 0 indicating a perfect line and 1 indicating a perfect sphere (F) Quantification of fibronectin circularity (n=23). Data shown represent values with means ± SD. P-values determined by two tailed Student's t test.

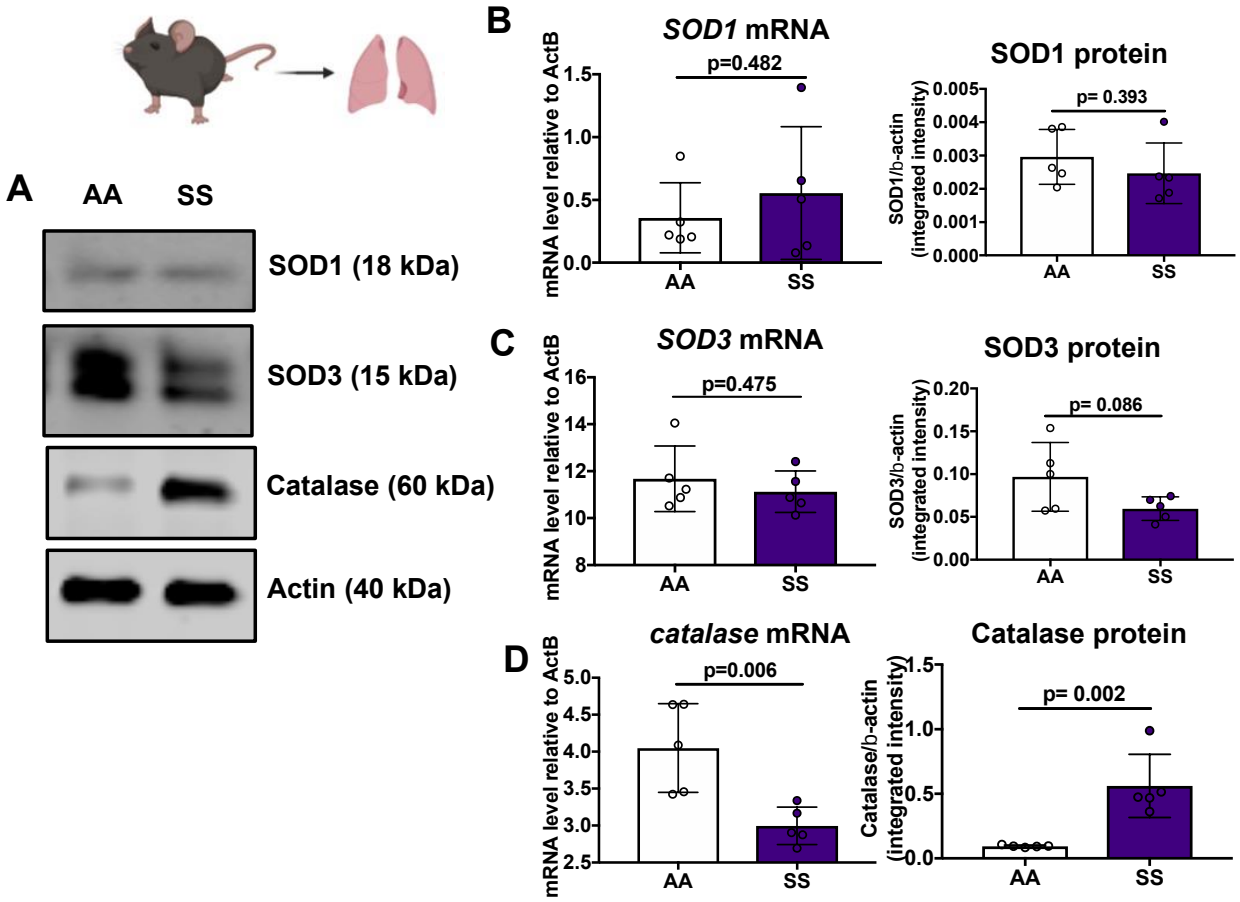

Figure 15

Townes transgenic mice show an increase in catalase protein expression in whole lung lysate and no other derangements in antioxidant protein expression. (A) Western blot of SOD1, SOD3, and catalase protein expression in SS (n=5) and AA (n=5) Townes transgenic mice. (B) SOD1, (C) SOD3, and (D) Catalase mRNA and protein expression quantification. Data shown represent values with means ± SD. P-values determined by two tailed Student's t test.

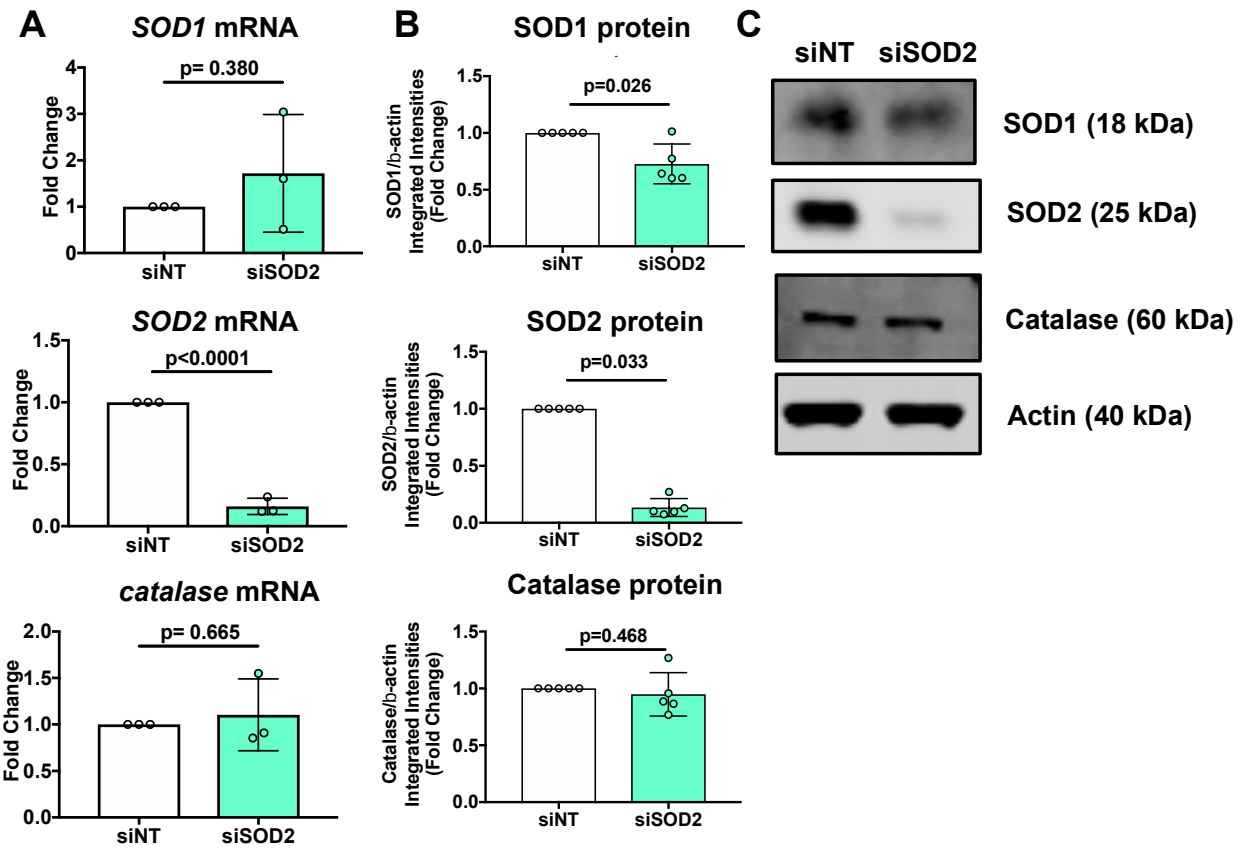

Figure 16

Knockdown of SOD2 in hPMVECs has no effect on SOD1 or catalase expression. (A) Quantification of *sod1*, *sod2*, and *catalase* mRNA in siSOD2 hPMVECs. (B, C) Quantification and western blot image of SOD1, SOD2, and catalase protein in siSOD2 hPMVECs (n=5). Data shown represent averaged values for each day of experimentation with means ± SD. P-values determined by two tailed Student's t test.

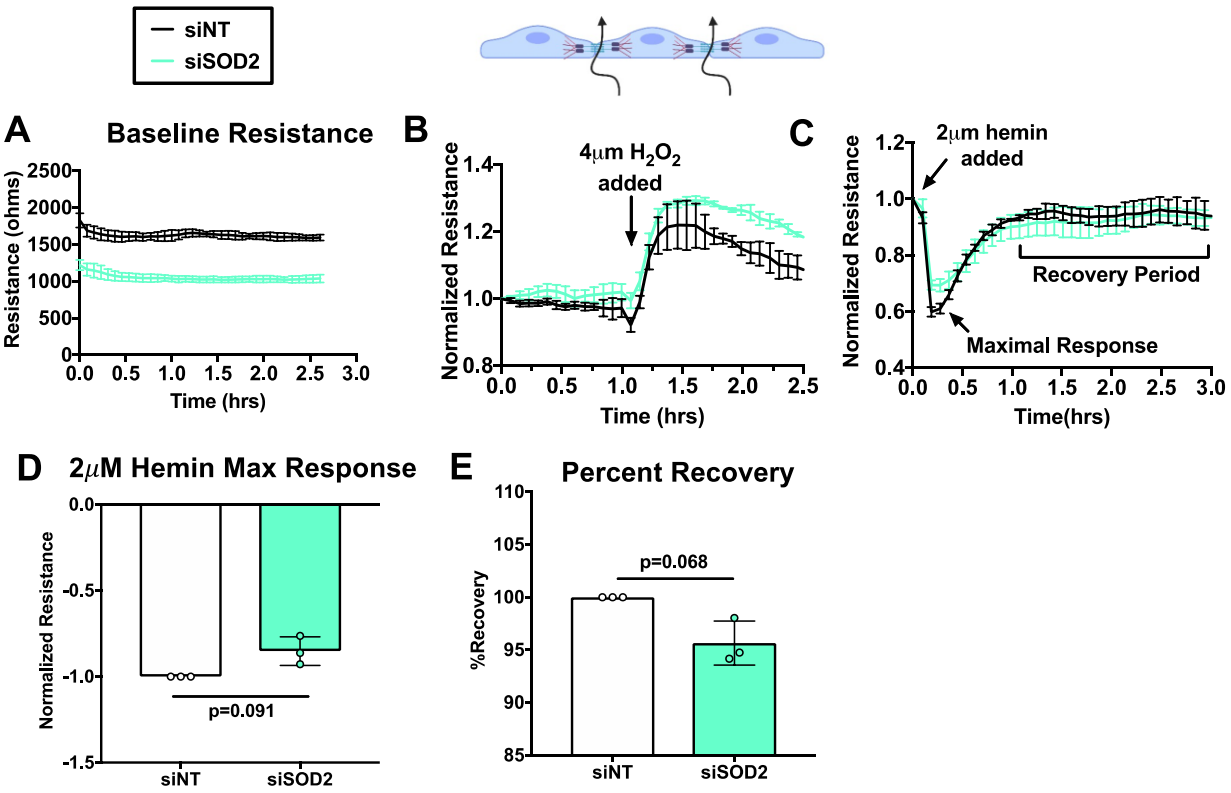

Figure 17

No difference in permeability in siSOD2 hPMVECs with treatment with 2μM hemin. (A) siNT and siSOD2 hPMVECs ECIS tracings of baseline resistance over two and a half hours (n=7-8), (B) After treatment with 4μM H_2O_2 (n=3), and (C) With treatment with 2μM hemin (n=3). (D) Maximum change in resistance and (E) Percent recovery after treatment with 2μM hemin. Data shown represent averaged values for each day of experimentation with means ± SD. P-values determined by two tailed Student's t test.

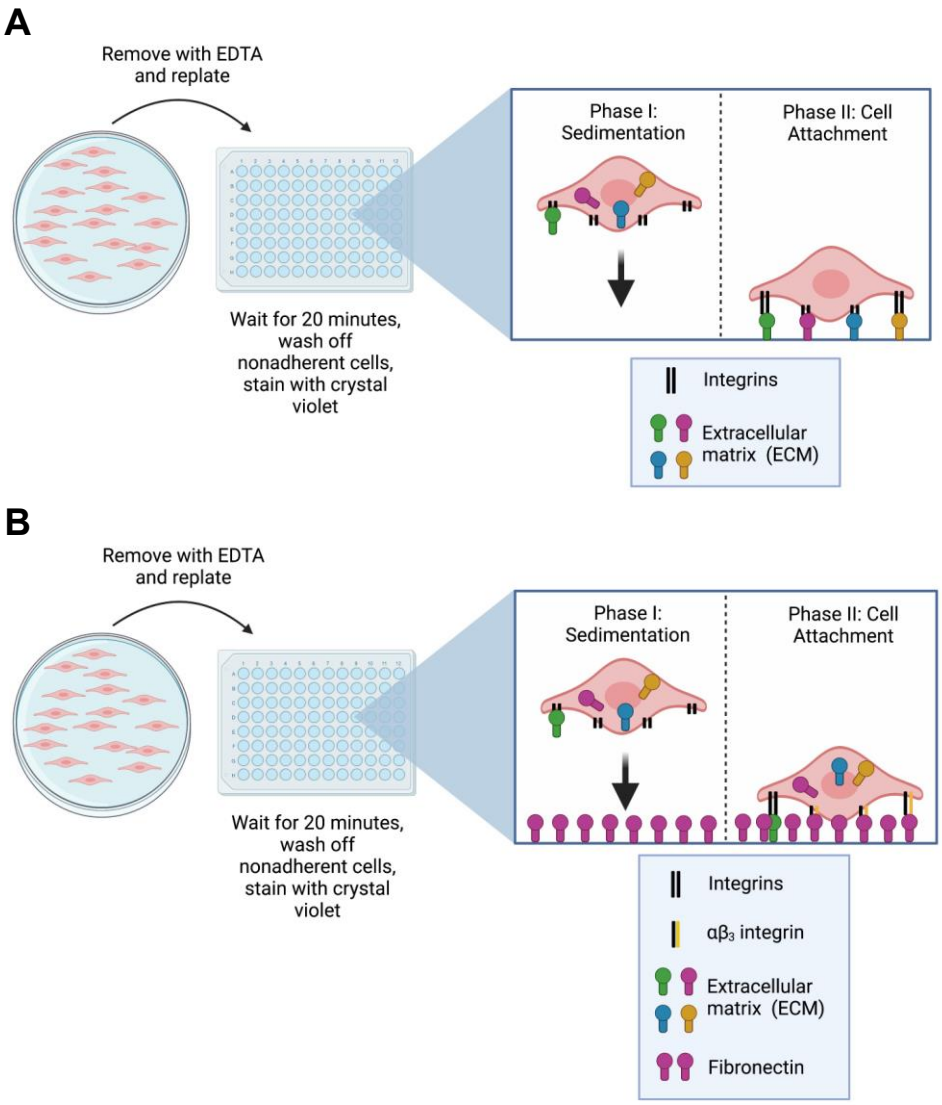

Figure 18

Schematic of adhesion assay using uncoated and fibronectin coated cell culture plates. (A) To perform the adhesion assay, hPMVECs are removed from a plate using EDTA and then replated into wells of a 96 well cell culture plate. After waiting 20 minutes nonadherent hPMVECs are washed off with PBS and the remaining cells are stained with crystal violet. As a control another 96 well cell culture plate is plated at the same time and cells are grown for 24 hours. hPMVECs counted in the 20 minute plate are normalized to the protein from the 24 hours plate. Within 20 minutes, the adhesion process undergoes two phases. In phase I the cells initially attach to the plate via electrostatic interactions, this is sedimentation. Because cells are removed with EDTA, the cells have on their outer membrane integrins as well as some extracellular matrix (ECM) proteins. The second phase of adhesion is when integrins bind

to ECM proteins. Since the plates we use are uncoated, hPMVECs will use ECM proteins carried on its outer membrane or secrete its own for integrin proteins to bind to. (B) After sedimentation, cells should be able to more efficiently bind to fibronectin coated cell culture plates by using β3 integrins. Because we obesrved a decrease in β3integrin protein expression in siSOD2 hPMVECs, they will not be able to use the fibronectin coating as efficiently as the siNT hPMVECs which have normal levels of β3 integrin.

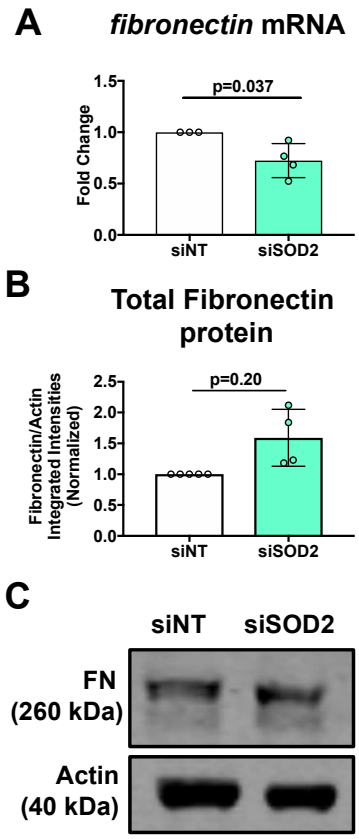

Figure 19

Total fibronectin protein is unchanged in siSOD2 hPMVECs. (A) *Fibronectin* mRNA from siNT and siSOD2 hPMVECs (n=3-4), (B) Western blot of total fibronectin and actin from siNT and siSOD2 hPMVECs. (C) Quantification of total fibronectin (n=4). Student's t test was used to determine significance for all measurements. Data shown represent values with means ± SD. P-values determined by two tailed Student's t test.

Table 2 Catalogue of primary and secondary antibodies

Antibody	Species	Catalog No	Company
SOD1	Rabbit	2770	Cell Signaling
SOD2	Rabbit	ab13533	Abcam
SOD3	Mouse	sc-271170	Santa Cruz Biotechnology
Catalase	Rabbit	12980	Cell Signaling
Fibronectin	Rabbit	E5H6X	Cell Signaling
Integrin Anitbody Sampler Kit	Rabbit	4749	Cell Signaling
Total OXPHOS Human WB Antibody Cocktail	Mouse	ab110411	Abcam
Actin	Mouse	sc-47778	Santa Cruz Biotechnology
IRDye® 680RD Donkey	Mouse	926-68072	Li-Cor
IRDye® 800CW Donkey	Rabbit	926-32213	Li-Cor
Revert 700 Total Protein Stain Kit	N/A	926-11010	Li-Cor

Table 3 Catalogue of PCR primers used

Gene Name	Species	Sequence
Catalase Fwd	Mouse	CTCGTTCAGGATGTGGTTTTC
Catalase Rev	Mouse	CTTTCCCTTGGAGTATCTGGTG
Catalase Fwd	Human	CAGATAGCCTTCGACCCAAG
Catalase Rev	Human	GTAGGGACAGTTCACAGGTATATG
SOD1 Fwd	Mouse	TGTGTCCATTGAAGATCGTGTG
SOD1 Rev	Mouse	TCCCAGCATTTCCAGTCTTTG
SOD1 Fwd	Human	GTCCTCACTTTAATCCTCTATCCAG
SOD1 Rev	Human	AGTCACATTGCCCAAGTCTC
SOD3 Fwd	Mouse	GAGAGCCAGACAAAGGAGC
SOD3 Rev	Mouse	CCTGGAGACATCTATGCGTG
SOD3 Fwd	Human	CTCTTGGAGGAGCTGGAAAG
SOD3 Rev	Human	CATGTCTCGGATCCACTCC
SOD2 Fwd	Mouse	TGCTCTAATCAGGACCCATTG
SOD2 Rev	Mouse	CATTCTCCCAGTTGATTACATTCC
SOD2 Fwd	Human	CCTGGAACCTCACATCAACG
SOD2 Rev	Human	GCTATCTGGGCTGTAACATCTC

4.0 Conclusions and Future Directions

4.1 Conclusions of Our Work

Within this dissertation, the work of myself and my colleagues has demonstrated several new findings which have critical basic science and clinical applications for the fields of sickle cell disease, fibronectin regulation and antioxidant biology. Our hypothesis was to identify SOD2 as a biomarker modulating sickle cell disease pathology. To this end in Aim 1, we have investigated the polymorphism SOD2 V16A which is found in approximately 40% of the general population. We found that this SNP was associated with pulmonary and cardiac dysfunction in sickle cell patients. Further investigation revealed that SOD2 V16A overassociates with complex IV of the respiratory chain in cultured HPAECs, decreases complex IV activity and basal respiration. This also resulted in an increase in reactive oxygen species production at baseline and exacerbated ROS production when the mitochondria respiratory complex was stressed with antimycin A. In Aim 2 we next investigated the role of SOD2 in the endothelium and found that SOD2 is greatly diminished within pulmonary endothelial and smooth muscle cells of SCD patients. The Townes sickle transgenic mouse model also had diminished SOD2 protein expression within whole lung protein lysates, a finding that was unique to SOD2 and not found with SOD1 or SOD3 highlighting a unique role for SOD2 in SCD. *In vitro* investigations using SOD2 knockdown HPMVECs revealed that SOD2 is necessary for the maintenance of endothelial cell permeability and is a key driver of proliferation and migration. These processes were found to be linked to decreased adherence of siSOD2 HPMVECs due to a disruption in

fibronectin dimerization most likely due to reduced H_2O_2 signaling. Taken together our work demonstrate a novel role of SOD2 as a modulator of SCD pathophysiology.

Future directions for Aim1 should be to generate a sickle mouse model with the SOD2 V16A polymorphism to determine whether the complications found in the SCD patient population, increased tricuspid regurgitant velocities, increased systolic blood pressure, decreased exercise tolerance, and increased right ventricular hypertrophy, can be recapitulated in the mouse model. Generation of a mouse model would allow for the ability to test therapeutics that could be then used in a patient population. Also, further investigation into the mechanisms by which SOD2 V16A overassociates with complex IV of the respiratory chain should be conducted. Namely, the role of the mitochondrial leader sequence after it has been cleaved from SOD2. Either variant's sequence could be overexpressed in HPAECs and the localization of $SOD2^{WT}$ and production of ROS determined. Future directions for Aim 2 should be pointed towards the investigation of the *in vivo* consequences of endothelial SOD2 depletion in mouse models. Based upon our data in Chapter 3 showing decreased migration and proliferation and fibronectin dysregulation in SOD2 deficient hPMVECs, it is hypothesized that endothelial SOD2 deficient mice may also experience deficiencies in migration and proliferation which could be assayed using the *in vivo* wound healing assay. However, fibroblasts are the primary secretor of fibronectin during wound healing[285] therefore it is possible that any deficiencies in endothelial fibronectin assembly can be compensated for by fibroblasts. SOD2 null mice succumb by three weeks of age primarily due to the development of cardiomyopathies[187] suggesting that SOD2 is highly expressed in SMCs. We also observe a significant decrease in SMC expression of SOD2 in SCD patients in Chapter 3. Thus, there would be translational and clinical significance in exploring the consequences of SMC SOD2 depletion *in vitro* and *in vivo*.

4.2 Additional Mechanisms by which SOD2 could be Modulating SCD Pathology

Oxidative stress is a well-established component of various diseases such as diabetes[286], cancer[287], chronic kidney disease[288], cardiovascular disease[289], and neurodegenerative diseases[290,291]. Given its localization to the mitochondria, SOD2 is a critical part of the antioxidant defense system in metabolically active tissues[292]. The most metabolically active tissues in healthy adults are the brain, heart, kidneys, and liver[293], however sickle patients have a 15%-20% increase in overall energy expenditure[294]. This increased resting energy expenditure escalates metabolic demand in all tissues and the mitochondria within them, increasing electron leak from the respiratory chain and superoxide formation[295]. Indeed, SCD patients have reportedly an increase in mitochondrial superoxide production in reticulocytes[296] and platlets[297]. Additionally, hemin can directly lead to mitochondrial dysfunction within endothelial cells[298]. These findings further highlight the role of SOD2 in modulating SCD pathology, most likely through management of mitochondrial ROS.

Armenis et al[254] found that in a group of 21 sickle cell patients, peripheral blood expression of SOD2 was reduced by 25% compared to matched controls. This reduction is SOD2 correlated with platelet count, reticulocyte count, red blood cell count, and ferritin[254]. Interestingly, those SCD patients with elevated tricuspid regurgitant velocities, an echocardiographic indication of pulmonary hypertension, had lower SOD2 expression levels than SCD patients with lower tricuspid regurgitant velocities[254]. This finding further supports our data in Chapter 2 where we found that a polymorphism of SOD2, SOD2 V16A, was associated with increased tricuspid regurgitant velocities. Furthermore, in a heritable type of pulmonary arterial hypertension the enhancer region of SOD2 is hypermethylated downregulating its expression[299]. This genetic

reduction of SOD2 creates apoptosis-resistant, proliferative pulmonary artery smooth muscle cells through the impairment of H_2O_2 redox signaling and activation of HIF-1α[299]. SOD2 protein expression is also decreased in an obstructive sleep apnea/chronic intermittent hypoxia (OSA/CIH) model of pulmonary hypertension[300]. The mechanism by which loss of SOD2 promotes OSA/CIH-mediated pulmonary hypertension was found to be due to superoxide activation of the nod-like receptor pyrin domain containing 3 (NLRP3) inflammasome complex and over proliferation of apoptosis-resistant pulmonary arterial smooth muscle cells[300]. These data can serve to inform us on potential mechanisms by which loss of SOD2 leads to the development of pulmonary hypertension in SCD patients.

SOD2 has also been implicated in wound healing. Negative pressure wound therapy is a treatment used for large, persistent wounds as well as complicated, acute wounds[301]. In this therapy, wounds are completely sealed, and a negative pressure is applied[301]. Healing is thought to be promoted through promotion of blood circulation[301]. Wound tissue derived from patients undergoing this treatment have an increase in SOD2 protein and enzymatic activity with no changes in SOD1 protein or catalytic activity[302]. Topical treatment of wounds on mice with an SOD2 mimetic accelerated wound closure detailing a role for SOD2 and mitochondria in promoting wound healing[302]. Notably, upregulation of SOD2 is linked to aggressive breast carcinomas by promoting cell migration and proliferation[303,304]. SOD2 has also been implicated in the regulation of vascular smooth muscle cell migration and proliferation in a balloon-injured rat carotid arteries[252]. Taken together these data suggest that topical treatment of skin ulcers with SOD2 mimetics may accelerate wound healing in SCD patients by repleting SOD2 locally to promote revascularization.

4.3 Other Genetic Modifiers of SCD

The study of genetic modifiers of SCD is not novel. Others have identified that the clinical heterogeneity found amongst SCD is indicative of other potential genotypic factors playing a role in modulating the disease presentation. A primary contributing genetic factor is homozygosity or heterozygosity for HbS and other hemoglobin variants such as β thalassemia or HbC, sickle heterozygous patients typically have milder symptoms due to a reduction in the concentration of HbS[305]. However, even amongst homozygous HbS SCD patients there is great variance in presentation.

While fetal hemoglobin (HbF) is found primarily within neonates switching to predominately adult hemoglobin within the first two months of life, SCD patients typically have a delayed switch and HbF levels are frequently elevated throughout life[305]. The degree by which HbF is elevated is variable and depends upon other genetic factors[306]. Genotype-phenotype association studies have shown that elevated HbF concentrations are associated with increased longevity[307], reduced rate of vaso-occlusive crises[308] and acute chest syndrome[238], and fewer leg ulcers[309] in SCD patients. A genetic condition termed gene deletion hereditary persistence of HbF (HPFH) in which the fetal hemoglobin genes are not effectively silenced results in the persistent production of HbF[310]. SCD patients who carry this genotype (HbS-HPFH) are typically asymptomatic due to HbF's ability to disrupt HbS polymerization[305]. One of the effects of hydroxyurea is stimulation of production of HbF though this effect can vary from nonexistent to a 10-fold increase[305]. Variation in HbF response to hydroxyurea is also thought to be related to genetic modifiers in hydroxyurea metabolism and erythroid progenitor proliferation pathways[311]. Co-inheritance of α-thalassemia with SCD, which occurs in approximately 30% of SCD

patients[312], begets a reduction of intracellular HbS concentration diminishing HbS-induced hemolysis[305]. This reduction in hemolysis translates clinically as a reduced risk of stroke[313], leg ulcers[309], and splenic sequestration[314]. Unfortunately, these patients often have an increased risk of painful episodes[315] and osteonecrosis[316] due to an increase in blood viscosity[305].

Genome wide sequencing has brought to light the extent of human genetic variability. Employing this and similar techniques to survey variations in biological pathways and how they associate with disease severity has highlighted several candidate genes and pathways that warrant further investigation. Wonkam et al identified that glutamate and oxidative stress biosynthesis pathways were enriched in SCD patients aged over 40 while genes associated with increased complement and blood coagulation cascade activity were significant in SCD patients who had experienced at least one episode of stroke[317]. Another study investigating genetic polymorphism in children with SCD and risk of stroke also revealed multiple candidates including TNF (-308), VCAM1 (-1594), and ILR4 503P[318]. SNPs in the TGF-beta/BMP signaling pathway which regulates angiogenesis and wound healing were associated with leg ulcers[309]. Identification of these new genetic modifiers not only creates a new potential druggable target, but also identifies what clinical complications clinicians needs to screen and monitor more frequently in each patient.

4.4 Antioxidants in Therapeutics and Opportunities Moving Forward

Despite the evidence of increased ROS in disease processes, the use of antioxidants in therapeutics is complicated by the necessity of maintaining physiological levels of oxygen and free radicals [319]. The current status and future directions of the clinical use of antioxidant drugs have been reviewed elsewhere [320]. Briefly, excitement in the 1980s and 1990s surrounding the use of

antioxidant therapies to modulate disease processes was dampened as the newly developed drugs struggled to make it past clinical trials. The few notable antioxidants that have been approved for clinical use include *N*-acetylcysteine for acetaminophen overdose and dry eye syndrome, α-lipoic acid for diabetic nephropathy, and the flavonoids baicalein and catechins for use in osteoarthritis[320]. Explanations for why antioxidant therapy has not been as resounding a success as it was hoped to be include the following: 1) oxidative stress may not be the only or the primary cause of the disease; 2) patients may not equally benefit from antioxidant therapy; 3) the target is not well selected; and 4) the antioxidant chosen may have poor selectivity for the target[320]. It is then crucial for more focused research to describe how specific antioxidants play a role in modulating diseases.

There are currently no studies investigating the benefits of SOD2 therapy in SCD. The use of SOD2 targeted therapeutics has, however, been studied for over 30 years. Therapies aimed at alleviating oxidative stress and superoxide levels through increasing SOD2 have been studied in inflammation reduction, protection from irradiation, transplantation immunosuppression, and fibrosis[321-323]. In 1983, it was shown that in patients undergoing radiation, lysosome encapsulated SOD was able to prevent inflammation and fibrosis[321]. In 1994, intravenous administration of human recombinant SOD decreased the number of acute and chronic rejection events in recipients of cadaveric renal transplants. More recently in 2013, oral administration of human recombinant SOD2 reduced liver fibrosis and portal pressure in cirrhotic rats [322,323]. Administration of SOD2 as a drug has been complicated by the short 6-minute half-life of the enzyme due to rapid renal clearance[324]. In order to circumvent this limitation, SOD2 plasmid containing liposomes[325] and small molecule mimetics[326,327] are being developed. The recent availability of improved

formulations of SOD2 extends its therapeutic potential; this along with the history of efficacy paves the way for clinical trials in SCD.

Increased reactive oxygen species and decreased antioxidant capacity in SCD overwhelms RBCs and mitochondria and damages endothelial cells and tissues, promoting pathology. SOD2, a significant component of the enzymatic antioxidant defense system, is both transcriptionally and post-transcriptionally regulated. Upregulation of SOD2 in SCD comes with increased ROS, though this response is impaired due to decreased Nrf2 activation and posttranslational downregulation of SOD2 by RNS. The importance of increasing the antioxidant response, in particular SOD2, is underscored by increased clinical complications found with the decreased SOD2 activity of the Val-16-Ala polymorphism [193]. The role of SOD2 in maintaining vascular homeostasis [166] also contributes to the vital part it plays in modulating SCD pathology. Further exploration of the events that lead to SOD2 activity regulation in SCD will provide a clearer understanding of SOD2's role in the progression of SCD pathology and potentially produce improvement in clinical outcomes. In particular, the importance of SOD2 in the vascular wall has not been thoroughly investigated. We anticipate that SOD2 supplementation would confer protection to the endothelium during acute and chronic oxidative stress events, potentially reducing the incidence of pulmonary hypertension associated with SCD.

In this era of precision medicine, it is important to consider disease in context of the patient and their own innate antioxidant defense systems. Increased oxidative stress is commonly found in a wide array of diseases and the antioxidant response between patients is not uniform. Investigation of the patient's own antioxidant expression levels and known polymorphisms that may alter activity levels will lead to more informed clinical decision making.

Bibliography

1.Modell B, Darlison M. Global epidemiology of haemoglobin disorders and derived service indicators. *Bull World Health Organ*. 2008;86(6):480-487.

2.Kohne E. Hemoglobinopathies: clinical manifestations, diagnosis, and treatment. *Dtsch Arztebl Int*. 2011;108(31-32):532-540.

3.Weatherall DJ. Thalassemia as a global health problem: recent progress toward its control in the developing countries. *Ann N Y Acad Sci*. 2010;1202:17-23.

4.Steinberg MH. Sickle cell anemia, the first molecular disease: overview of molecular etiology, pathophysiology, and therapeutic approaches. *ScientificWorldJournal*. 2008;8:1295-1324.

5.Pauling L, Itano HA, et al. Sickle cell anemia a molecular disease. *Science*. 1949;110(2865):543-548.

6.Marengo-Rowe AJ. Structure-function relations of human hemoglobins. *Proc (Bayl Univ Med Cent)*. 2006;19(3):239-245.

7.Hempe JM, Craver RD. Laboratory diagnosis of structural hemoglobinopathies and thalassemias by capillary isoelectric focusing. *Methods Mol Med*. 1999;27:81-98.

8.Hardison RC. Evolution of hemoglobin and its genes. *Cold Spring Harb Perspect Med*. 2012;2(12):a011627.

9.Kaufman DP, Khattar J, Lappin SL. Physiology, Fetal Hemoglobin. StatPearls. Treasure Island (FL); 2021.

10.Kaeda JS, Prasad K, Howard RJ, Mehta A, Vulliamy T, Luzzatto L. Management of pregnancy when maternal blood has a very high level of fetal haemoglobin. *Br J Haematol*. 1994;88(2):432-434.

11.Kato GJ, Piel FB, Reid CD, et al. Sickle cell disease. *Nat Rev Dis Primers*. 2018;4:18010.

12.Wastnedge E, Waters D, Patel S, et al. The global burden of sickle cell disease in children under five years of age: a systematic review and meta-analysis. *J Glob Health*. 2018;8(2):021103.

13.Sedrak A, Kondamudi NP. Sickle Cell Disease. StatPearls. Treasure Island (FL); 2021.

14.Campbell A, Cong Z, Agodoa I, et al. The Economic Burden of End-Organ Damage Among Medicaid Patients with Sickle Cell Disease in the United States: A Population-Based Longitudinal Claims Study. *J Manag Care Spec Pharm*. 2020;26(9):1121-1129.

15.Holdford D, Vendetti N, Sop DM, Johnson S, Smith WR. Indirect Economic Burden of Sickle Cell Disease. *Value Health*. 2021;24(8):1095-1101.

16.Lubeck D, Agodoa I, Bhakta N, et al. Estimated Life Expectancy and Income of Patients With Sickle Cell Disease Compared With Those Without Sickle Cell Disease. *JAMA Netw Open*. 2019;2(11):e1915374.

17.Stotesbury H, Kawadler JM, Hales PW, Saunders DE, Clark CA, Kirkham FJ. Vascular Instability and Neurological Morbidity in Sickle Cell Disease: An Integrative Framework. *Front Neurol*. 2019;10:871.

18.Fadugbagbe AO, Gurgel RQ, Mendonca CQ, Cipolotti R, dos Santos AM, Cuevas LE. Ocular manifestations of sickle cell disease. *Ann Trop Paediatr*. 2010;30(1):19-26.

19.Miller AC, Gladwin MT. Pulmonary complications of sickle cell disease. *Am J Respir Crit Care Med*. 2012;185(11):1154-1165.

20.Gladwin MT. Cardiovascular complications in patients with sickle cell disease. *Hematology Am Soc Hematol Educ Program*. 2017;2017(1):423-430.

21.Nath KA, Hebbel RP. Sickle cell disease: renal manifestations and mechanisms. *Nat Rev Nephrol*. 2015;11(3):161-171.

22.Aguilar C, Vichinsky E, Neumayr L. Bone and joint disease in sickle cell disease. *Hematol Oncol Clin North Am*. 2005;19(5):929-941, viii.

23.Hamideh D, Alvarez O. Sickle cell disease related mortality in the United States (1999-2009). *Pediatr Blood Cancer*. 2013;60(9):1482-1486.

24.Ashley-Koch A, Yang Q, Olney RS. Sickle hemoglobin (HbS) allele and sickle cell disease: a HuGE review. *Am J Epidemiol*. 2000;151(9):839-845.

25.Hoover R, Rubin R, Wise G, Warren R. Adhesion of normal and sickle erythrocytes to endothelial monolayer cultures. *Blood*. 1979;54(4):872-876.

26.Hebbel RP, Yamada O, Moldow CF, Jacob HS, White JG, Eaton JW. Abnormal adherence of sickle erythrocytes to cultured vascular endothelium: possible mechanism for microvascular occlusion in sickle cell disease. *J Clin Invest*. 1980;65(1):154-160.

27.Telen MJ. Role of adhesion molecules and vascular endothelium in the pathogenesis of sickle cell disease. *Hematology Am Soc Hematol Educ Program*. 2007:84-90.

28.Cardenes N, Corey C, Geary L, et al. Platelet bioenergetic screen in sickle cell patients reveals mitochondrial complex V inhibition, which contributes to platelet activation. *Blood*. 2014;123(18):2864-2872.

29.Chirico EN, Pialoux V. Role of oxidative stress in the pathogenesis of sickle cell disease. *IUBMB Life*. 2012;64(1):72-80.

30.Nur E, Biemond BJ, Otten HM, Brandjes DP, Schnog JJ, Group CS. Oxidative stress in sickle cell disease; pathophysiology and potential implications for disease management. *Am J Hematol*. 2011;86(6):484-489.

31.Ware RE, de Montalembert M, Tshilolo L, Abboud MR. Sickle cell disease. *Lancet*. 2017;390(10091):311-323.

32.Nader E, Grau M, Fort R, et al. Hydroxyurea therapy modulates sickle cell anemia red blood cell physiology: Impact on RBC deformability, oxidative stress, nitrite levels and nitric oxide synthase signalling pathway. *Nitric Oxide*. 2018;81:28-35.

33.Almeida CB, Franco-Penteado C, Saad ST, Costa FF, Conran N. Sickle cell disease serum induces NADPH enzyme subunit expression and oxidant production in leukocytes. *Hematology*. 2010;15(6):422-429.

34.Fibach E, Rachmilewitz E. The role of oxidative stress in hemolytic anemia. *Curr Mol Med*. 2008;8(7):609-619.

35.Schieber M, Chandel NS. ROS function in redox signaling and oxidative stress. *Curr Biol*. 2014;24(10):R453-462.

36.Sies H. Oxidative stress: a concept in redox biology and medicine. *Redox Biol*. 2015;4:180-183.

37.Ray D, Deshmukh P, Goswami K, Garg N. Antioxidant vitamin levels in sickle cell disorders. *Natl Med J India*. 2007;20(1):11-13.

38.Biswal S, Rizwan H, Pal S, Sabnam S, Parida P, Pal A. Oxidative stress, antioxidant capacity, biomolecule damage, and inflammation symptoms of sickle cell disease in children. *Hematology*. 2019;24(1):1-9.

39.Al-Naama LM, Hassan MK, Mehdi JK. Association of erythrocytes antioxidant enzymes and their cofactors with markers of oxidative stress in patients with sickle cell anemia. *Qatar Med J*. 2015;2015(2):14.

40.Ren H, Ghebremeskel K, Okpala I, Lee A, Ibegbulam O, Crawford M. Patients with sickle cell disease have reduced blood antioxidant protection. *Int J Vitam Nutr Res*. 2008;78(3):139-147.

41.Lachant NA, Tanaka KR. Antioxidants in sickle cell disease: the in vitro effects of ascorbic acid. *Am J Med Sci*. 1986;292(1):3-10.

42.Ohnishi ST, Ohnishi T. In vitro effects of aged garlic extract and other nutritional supplements on sickle erythrocytes. *J Nutr*. 2001;131(3s):1085S-1092S.

43.Kaul DK, Liu XD, Zhang X, Ma L, Hsia CJ, Nagel RL. Inhibition of sickle red cell adhesion and vasoocclusion in the microcirculation by antioxidants. *Am J Physiol Heart Circ Physiol*. 2006;291(1):H167-175.

44.Kaddam L, Fadl-Elmula I, Eisawi OA, et al. Gum Arabic as novel anti-oxidant agent in sickle cell anemia, phase II trial. *BMC Hematol*. 2017;17:4.

45.Yarbro JW. Mechanism of action of hydroxyurea. *Semin Oncol*. 1992;19(3 Suppl 9):1-10.

46.Torres Lde S, da Silva DG, Belini Junior E, et al. The influence of hydroxyurea on oxidative stress in sickle cell anemia. *Rev Bras Hematol Hemoter*. 2012;34(6):421-425.

47.Niihara Y, Miller ST, Kanter J, et al. A Phase 3 Trial of l-Glutamine in Sickle Cell Disease. *N Engl J Med*. 2018;379(3):226-235.

48.Niihara Y, Zerez CR, Akiyama DS, Tanaka KR. Oral L-glutamine therapy for sickle cell anemia: I. Subjective clinical improvement and favorable change in red cell NAD redox potential. *Am J Hematol*. 1998;58(2):117-121.

49.Matschke J, Riffkin H, Klein D, et al. Targeted Inhibition of Glutamine-Dependent Glutathione Metabolism Overcomes Death Resistance Induced by Chronic Cycling Hypoxia. *Antioxid Redox Signal*. 2016;25(2):89-107.

50.Frimat M, Boudhabhay I, Roumenina LT. Hemolysis Derived Products Toxicity and Endothelium: Model of the Second Hit. *Toxins (Basel)*. 2019;11(11).

51.Uzunova VV, Pan W, Galkin O, Vekilov PG. Free heme and the polymerization of sickle cell hemoglobin. *Biophys J*. 2010;99(6):1976-1985.

52.Eberhardt RT, McMahon L, Duffy SJ, et al. Sickle cell anemia is associated with reduced nitric oxide bioactivity in peripheral conduit and resistance vessels. *Am J Hematol*. 2003;74(2):104-111.

53.Gladwin MT, Schechter AN, Ognibene FP, et al. Divergent nitric oxide bioavailability in men and women with sickle cell disease. *Circulation*. 2003;107(2):271-278.

54.Reiter CD, Wang X, Tanus-Santos JE, et al. Cell-free hemoglobin limits nitric oxide bioavailability in sickle-cell disease. *Nat Med*. 2002;8(12):1383-1389.

55.Gladwin MT, Ofori-Acquah SF. Erythroid DAMPs drive inflammation in SCD. *Blood*. 2014;123(24):3689-3690.

56.Fortes GB, Alves LS, de Oliveira R, et al. Heme induces programmed necrosis on macrophages through autocrine TNF and ROS production. *Blood*. 2012;119(10):2368-2375.

57.Belcher JD, Chen C, Nguyen J, et al. Heme triggers TLR4 signaling leading to endothelial cell activation and vaso-occlusion in murine sickle cell disease. *Blood*. 2014;123(3):377-390.

58.Chen G, Zhang D, Fuchs TA, Manwani D, Wagner DD, Frenette PS. Heme-induced neutrophil extracellular traps contribute to the pathogenesis of sickle cell disease. *Blood*. 2014;123(24):3818-3827.

59.Santiago RP, Guarda CC, Figueiredo CVB, et al. Serum haptoglobin and hemopexin levels are depleted in pediatric sickle cell disease patients. *Blood Cells Mol Dis*. 2018;72:34-36.

60.Yalamanoglu A, Deuel JW, Hunt RC, et al. Depletion of haptoglobin and hemopexin promote hemoglobin-mediated lipoprotein oxidation in sickle cell disease. *Am J Physiol Lung Cell Mol Physiol*. 2018;315(5):L765-L774.

61.Kim JY, Yenari MA. The immune modulating properties of the heat shock proteins after brain injury. *Anat Cell Biol*. 2013;46(1):1-7.

62.Zhang Y, Dai Y, Wen J, et al. Detrimental effects of adenosine signaling in sickle cell disease. *Nat Med*. 2011;17(1):79-86.

63.Bennett HS, Luft JH, Hampton JC. Morphological classifications of vertebrate blood capillaries. *Am J Physiol*. 1959;196(2):381-390.

64.Florey. The endothelial cell. *Br Med J*. 1966;2(5512):487-490.

65.Feletou M. The Endothelium: Part 1: Multiple Functions of the Endothelial Cells-Focus on Endothelium-Derived Vasoactive Mediators. San Rafael (CA); 2011.

66.Aird WC. Phenotypic heterogeneity of the endothelium: I. Structure, function, and mechanisms. *Circ Res*. 2007;100(2):158-173.

67.Satchell SC, Braet F. Glomerular endothelial cell fenestrations: an integral component of the glomerular filtration barrier. *Am J Physiol Renal Physiol*. 2009;296(5):F947-956.

68.Risau W. Development and differentiation of endothelium. *Kidney Int Suppl*. 1998;67:S3-6.

69.Becker BF, Heindl B, Kupatt C, Zahler S. Endothelial function and hemostasis. *Z Kardiol*. 2000;89(3):160-167.

70.Sandoo A, van Zanten JJ, Metsios GS, Carroll D, Kitas GD. The endothelium and its role in regulating vascular tone. *Open Cardiovasc Med J*. 2010;4:302-312.

71.Sukriti S, Tauseef M, Yazbeck P, Mehta D. Mechanisms regulating endothelial permeability. *Pulm Circ*. 2014;4(4):535-551.

72.Monaghan-Benson E, Wittchen ES. In vitro analyses of endothelial cell permeability. *Methods Mol Biol*. 2011;763:281-290.

73.Radi ZA, Kehrli ME, Jr., Ackermann MR. Cell adhesion molecules, leukocyte trafficking, and strategies to reduce leukocyte infiltration. *J Vet Intern Med*. 2001;15(6):516-529.

74.Rao RM, Yang L, Garcia-Cardena G, Luscinskas FW. Endothelial-dependent mechanisms of leukocyte recruitment to the vascular wall. *Circ Res*. 2007;101(3):234-247.

75.Risau W. Angiogenesis and endothelial cell function. *Arzneimittelforschung*. 1994;44(3A):416-417.

76.Munoz-Chapuli R, Quesada AR, Angel Medina M. Angiogenesis and signal transduction in endothelial cells. *Cell Mol Life Sci*. 2004;61(17):2224-2243.

77.Gale AJ. Continuing education course #2: current understanding of hemostasis. *Toxicol Pathol*. 2011;39(1):273-280.

78.van Hinsbergh VW. Endothelium--role in regulation of coagulation and inflammation. *Semin Immunopathol*. 2012;34(1):93-106.

79.Watson SP. Platelet activation by extracellular matrix proteins in haemostasis and thrombosis. *Curr Pharm Des*. 2009;15(12):1358-1372.

80.Jackson SP. The growing complexity of platelet aggregation. *Blood*. 2007;109(12):5087-5095.

81.Heemskerk JW, Bevers EM, Lindhout T. Platelet activation and blood coagulation. *Thromb Haemost*. 2002;88(2):186-193.

82.Katritsis D, Kaiktsis L, Chaniotis A, Pantos J, Efstathopoulos EP, Marmarelis V. Wall shear stress: theoretical considerations and methods of measurement. *Prog Cardiovasc Dis*. 2007;49(5):307-329.

83.Shav D, Gotlieb R, Zaretsky U, Elad D, Einav S. Wall shear stress effects on endothelial-endothelial and endothelial-smooth muscle cell interactions in tissue engineered models of the vascular wall. *PLoS One*. 2014;9(2):e88304.

84.Sakariassen KS, Nievelstein PF, Coller BS, Sixma JJ. The role of platelet membrane glycoproteins Ib and IIb-IIIa in platelet adherence to human artery subendothelium. *Br J Haematol*. 1986;63(4):681-691.

85.Yun SH, Sim EH, Goh RY, Park JI, Han JY. Platelet Activation: The Mechanisms and Potential Biomarkers. *Biomed Res Int*. 2016;2016:9060143.

86.Belhassen L, Pelle G, Sediame S, et al. Endothelial dysfunction in patients with sickle cell disease is related to selective impairment of shear stress-mediated vasodilation. *Blood*. 2001;97(6):1584-1589.

87.Chen K, Pittman RN, Popel AS. Nitric oxide in the vasculature: where does it come from and where does it go? A quantitative perspective. *Antioxid Redox Signal*. 2008;10(7):1185-1198.

88.Moncada S, Higgs EA. The discovery of nitric oxide and its role in vascular biology. *Br J Pharmacol*. 2006;147 Suppl 1:S193-201.

89.Morris CR, Kato GJ, Poljakovic M, et al. Dysregulated arginine metabolism, hemolysis-associated pulmonary hypertension, and mortality in sickle cell disease. *JAMA*. 2005;294(1):81-90.

90.Kato GJ, Wang Z, Machado RF, Blackwelder WC, Taylor JGt, Hazen SL. Endogenous nitric oxide synthase inhibitors in sickle cell disease: abnormal levels and correlations with pulmonary hypertension, desaturation, haemolysis, organ dysfunction and death. *Br J Haematol*. 2009;145(4):506-513.

91.Mackman N. Role of tissue factor in hemostasis, thrombosis, and vascular development. *Arterioscler Thromb Vasc Biol*. 2004;24(6):1015-1022.

92.Solovey A, Gui L, Key NS, Hebbel RP. Tissue factor expression by endothelial cells in sickle cell anemia. *J Clin Invest*. 1998;101(9):1899-1904.

93.Key NS, Slungaard A, Dandelet L, et al. Whole blood tissue factor procoagulant activity is elevated in patients with sickle cell disease. *Blood*. 1998;91(11):4216-4223.

94.Faes C, Sparkenbaugh EM, Pawlinski R. Hypercoagulable state in sickle cell disease. *Clin Hemorheol Microcirc*. 2018;68(2-3):301-318.

95.Nasimuzzaman M, Malik P. Role of the coagulation system in the pathogenesis of sickle cell disease. *Blood Adv*. 2019;3(20):3170-3180.

96.Stevens T, Garcia JG, Shasby DM, Bhattacharya J, Malik AB. Mechanisms regulating endothelial cell barrier function. *Am J Physiol Lung Cell Mol Physiol*. 2000;279(3):L419-422.

97.Rodrigues SF, Granger DN. Blood cells and endothelial barrier function. *Tissue Barriers*. 2015;3(1-2):e978720.

98.Dejana E. Endothelial cell-cell junctions: happy together. *Nat Rev Mol Cell Biol*. 2004;5(4):261-270.

99.Kumar NM, Gilula NB. The gap junction communication channel. *Cell*. 1996;84(3):381-388.

100.Giannotta M, Trani M, Dejana E. VE-cadherin and endothelial adherens junctions: active guardians of vascular integrity. *Dev Cell*. 2013;26(5):441-454.

101.Sohl G, Willecke K. Gap junctions and the connexin protein family. *Cardiovasc Res*. 2004;62(2):228-232.

102.Zihni C, Mills C, Matter K, Balda MS. Tight junctions: from simple barriers to multifunctional molecular gates. *Nat Rev Mol Cell Biol*. 2016;17(9):564-580.

103.Jayadev R, Sherwood DR. Basement membranes. *Curr Biol*. 2017;27(6):R207-R211.

104.Singh P, Carraher C, Schwarzbauer JE. Assembly of fibronectin extracellular matrix. *Annu Rev Cell Dev Biol*. 2010;26:397-419.

105.Wu C. Focal adhesion: a focal point in current cell biology and molecular medicine. *Cell Adh Migr*. 2007;1(1):13-18.

106.Lampugnani MG, Resnati M, Dejana E, Marchisio PC. The role of integrins in the maintenance of endothelial monolayer integrity. *J Cell Biol*. 1991;112(3):479-490.

107.Porto BN, Alves LS, Fernandez PL, et al. Heme induces neutrophil migration and reactive oxygen species generation through signaling pathways characteristic of chemotactic receptors. *J Biol Chem*. 2007;282(33):24430-24436.

108.He P, Talukder MAH, Gao F. Oxidative Stress and Microvessel Barrier Dysfunction. *Front Physiol*. 2020;11:472.

109.Wagener FA, Eggert A, Boerman OC, et al. Heme is a potent inducer of inflammation in mice and is counteracted by heme oxygenase. *Blood*. 2001;98(6):1802-1811.

110.Ghosh S, Tan F, Ofori-Acquah SF. Spatiotemporal dysfunction of the vascular permeability barrier in transgenic mice with sickle cell disease. *Anemia*. 2012;2012:582018.

111.Karlsson EA, Oguin TH, Meliopoulos V, et al. Vascular Permeability Drives Susceptibility to Influenza Infection in a Murine Model of Sickle Cell Disease. *Sci Rep*. 2017;7:43308.

112.Dutta D, Methe B, Amar S, Morris A, Lim SH. Intestinal injury and gut permeability in sickle cell disease. *J Transl Med*. 2019;17(1):183.

113.Mai J, Virtue A, Shen J, Wang H, Yang XF. An evolving new paradigm: endothelial cells--conditional innate immune cells. *J Hematol Oncol*. 2013;6:61.

114.Beutler B. Innate immunity: an overview. *Mol Immunol*. 2004;40(12):845-859.

115.Flajnik MF, Kasahara M. Origin and evolution of the adaptive immune system: genetic events and selective pressures. *Nat Rev Genet*. 2010;11(1):47-59.

116.Gupta SK, Lysko PG, Pillarisetti K, Ohlstein E, Stadel JM. Chemokine receptors in human endothelial cells. Functional expression of CXCR4 and its transcriptional regulation by inflammatory cytokines. *J Biol Chem*. 1998;273(7):4282-4287.

117.Faure E, Equils O, Sieling PA, et al. Bacterial lipopolysaccharide activates NF-kappaB through toll-like receptor 4 (TLR-4) in cultured human dermal endothelial cells. Differential expression of TLR-4 and TLR-2 in endothelial cells. *J Biol Chem*. 2000;275(15):11058-11063.

118.Anand AR, Cucchiarini M, Terwilliger EF, Ganju RK. The tyrosine kinase Pyk2 mediates lipopolysaccharide-induced IL-8 expression in human endothelial cells. *J Immunol*. 2008;180(8):5636-5644.

119.Marelli-Berg FM, Jarmin SJ. Antigen presentation by the endothelium: a green light for antigen-specific T cell trafficking? *Immunol Lett*. 2004;93(2-3):109-113.

120.Ebong WW. Acute osteomyelitis in Nigerians with sickle cell disease. *Ann Rheum Dis*. 1986;45(11):911-915.

121.Bansil NH, Kim TY, Tieu L, Barcega B. Incidence of serious bacterial infections in febrile children with sickle cell disease. *Clin Pediatr (Phila)*. 2013;52(7):661-666.

122.Chenou F, Azevedo J, Leal HF, Goncalves MS, Reis JN. Bacterial meningitis in patients with sickle cell anemia in Salvador, Bahia, Brazil: a report on ten cases. *Hematol Transfus Cell Ther*. 2020;42(2):139-144.

123.Chukwu BF, Okafor HU, Ikefuna AN. Asymptomatic bacteriuria in children with sickle cell anemia at The University of Nigeria teaching hospital, Enugu, South East, Nigeria. *Ital J Pediatr*. 2011;37:45.

124.Falcao RP, Donadi EA. [Infection and immunity in sickle cell disease]. *AMB Rev Assoc Med Bras*. 1989;35(2):70-74.

125.de Azevedo JTC, Malmegrim KCR. Immune mechanisms involved in sickle cell disease pathogenesis: current knowledge and perspectives. *Immunol Lett*. 2020;224:1-11.

126.Pober JS, Sessa WC. Evolving functions of endothelial cells in inflammation. *Nat Rev Immunol*. 2007;7(10):803-815.

127.Lamalice L, Le Boeuf F, Huot J. Endothelial cell migration during angiogenesis. *Circ Res*. 2007;100(6):782-794.

128.Mongiat M, Andreuzzi E, Tarticchio G, Paulitti A. Extracellular Matrix, a Hard Player in Angiogenesis. *Int J Mol Sci*. 2016;17(11).

129.Cheresh DA, Stupack DG. Regulation of angiogenesis: apoptotic cues from the ECM. *Oncogene*. 2008;27(48):6285-6298.

130.Lopes FC, Traina F, Almeida CB, et al. Key endothelial cell angiogenic mechanisms are stimulated by the circulating milieu in sickle cell disease and attenuated by hydroxyurea. *Haematologica*. 2015;100(6):730-739.

131.Sun K, Xia Y. New insights into sickle cell disease: a disease of hypoxia. *Curr Opin Hematol*. 2013;20(3):215-221.

132.Cimmino F, Avitabile M, Lasorsa VA, et al. HIF-1 transcription activity: HIF1A driven response in normoxia and in hypoxia. *BMC Med Genet*. 2019;20(1):37.

133.Haddy TB. Erythropoietin in sickle cell disease: relation of erythropoietin levels to crisis and other complications. *Am J Pediatr Hematol Oncol*. 1982;4(2):191-196.

134.Brittain JE, Hulkower B, Jones SK, et al. Placenta growth factor in sickle cell disease: association with hemolysis and inflammation. *Blood*. 2010;115(10):2014-2020.

135.Duits AJ, Rodriguez T, Schnog JJ, Group CS. Serum levels of angiogenic factors indicate a pro-angiogenic state in adults with sickle cell disease. *Br J Haematol*. 2006;134(1):116-119.

136.Lopes FC, Ferreira R, Albuquerque DM, et al. In vitro and in vivo anti-angiogenic effects of hydroxyurea. *Microvasc Res*. 2014;94:106-113.

137.McCord JM, Fridovich I. Superoxide dismutase. An enzymic function for erythrocuprein (hemocuprein). *J Biol Chem*. 1969;244(22):6049-6055.

138.Miao L, St Clair DK. Regulation of superoxide dismutase genes: implications in disease. *Free Radic Biol Med*. 2009;47(4):344-356.

139.Borgstahl GE, Parge HE, Hickey MJ, Beyer WF, Jr., Hallewell RA, Tainer JA. The structure of human mitochondrial manganese superoxide dismutase reveals a novel tetrameric interface of two 4-helix bundles. *Cell*. 1992;71(1):107-118.

140.Fukai T, Ushio-Fukai M. Superoxide dismutases: role in redox signaling, vascular function, and diseases. *Antioxid Redox Signal*. 2011;15(6):1583-1606.

141.Jagadeeswaran R, Vazquez BA, Thiruppathi M, et al. Pharmacological inhibition of LSD1 and mTOR reduces mitochondrial retention and associated ROS levels in the red blood cells of sickle cell disease. *Exp Hematol*. 2017;50:46-52.

142.Maehara K, Oh-Hashi K, Isobe KI. Early growth-responsive-1-dependent manganese superoxide dismutase gene transcription mediated by platelet-derived growth factor. *FASEB J*. 2001;15(11):2025-2026.

143.Zelko IN, Mariani TJ, Folz RJ. Superoxide dismutase multigene family: a comparison of the CuZn-SOD (SOD1), Mn-SOD (SOD2), and EC-SOD (SOD3) gene structures, evolution, and expression. *Free Radic Biol Med*. 2002;33(3):337-349.

144.Visner GA, Chesrown SE, Monnier J, Ryan US, Nick HS. Regulation of manganese superoxide dismutase: IL-1 and TNF induction in pulmonary artery and microvascular endothelial cells. *Biochem Biophys Res Commun*. 1992;188(1):453-462.

145.Iida R, Yasuda T, Tsubota E, et al. M-LP, Mpv17-like protein, has a peroxisomal membrane targeting signal comprising a transmembrane domain and a positively charged loop and up-regulates expression of the manganese superoxide dismutase gene. *J Biol Chem*. 2003;278(8):6301-6306.

146.Iida R, Yasuda T, Tsubota E, et al. A novel alternative spliced Mpv17-like protein isoform localizes in cytosol and is expressed in a kidney- and adult-specific manner. *Exp Cell Res*. 2005;302(1):22-30.

147.Das KC, Guo XL, White CW. Protein kinase Cdelta-dependent induction of manganese superoxide dismutase gene expression by microtubule-active anticancer drugs. *J Biol Chem*. 1998;273(51):34639-34645.

148.Kannan P, Buettner R, Chiao PJ, Yim SO, Sarkiss M, Tainsky MA. N-ras oncogene causes AP-2 transcriptional self-interference, which leads to transformation. *Genes Dev*. 1994;8(11):1258-1269.

149.Zhu CH, Huang Y, Oberley LW, Domann FE. A family of AP-2 proteins down-regulate manganese superoxide dismutase expression. *J Biol Chem*. 2001;276(17):14407-14413.

150.Zou X, Ratti BA, O'Brien JG, et al. Manganese superoxide dismutase (SOD2): is there a center in the universe of mitochondrial redox signaling? *J Bioenerg Biomembr*. 2017;49(4):325-333.

151.Candas D, Fan M, Nantajit D, et al. CyclinB1/Cdk1 phosphorylates mitochondrial antioxidant MnSOD in cell adaptive response to radiation stress. *J Mol Cell Biol*. 2013;5(3):166-175.

152.Tao R, Coleman MC, Pennington JD, et al. Sirt3-mediated deacetylation of evolutionarily conserved lysine 122 regulates MnSOD activity in response to stress. *Mol Cell*. 2010;40(6):893-904.

153.Chen Y, Zhang J, Lin Y, et al. Tumour suppressor SIRT3 deacetylates and activates manganese superoxide dismutase to scavenge ROS. *EMBO Rep*. 2011;12(6):534-541.

154.Redondo-Horcajo M, Romero N, Martinez-Acedo P, et al. Cyclosporine A-induced nitration of tyrosine 34 MnSOD in endothelial cells: role of mitochondrial superoxide. *Cardiovasc Res*. 2010;87(2):356-365.

155.Akashi M, Hachiya M, Paquette RL, Osawa Y, Shimizu S, Suzuki G. Irradiation increases manganese superoxide dismutase mRNA levels in human fibroblasts. Possible mechanisms for its accumulation. *J Biol Chem*. 1995;270(26):15864-15869.

156.Arumugam T, Pillay Y, Ghazi T, Nagiah S, Abdul NS, Chuturgoon AA. Fumonisin B1-induced oxidative stress triggers Nrf2-mediated antioxidant response in human hepatocellular carcinoma (HepG2) cells. *Mycotoxin Res*. 2019;35(1):99-109.

157.Lin G, Field JJ, Yu JC, et al. NF-kappaB is activated in CD4+ iNKT cells by sickle cell disease and mediates rapid induction of adenosine A2A receptors. *PLoS One*. 2013;8(10):e74664.

158.Belcher JD, Chen C, Nguyen J, et al. Control of Oxidative Stress and Inflammation in Sickle Cell Disease with the Nrf2 Activator Dimethyl Fumarate. *Antioxid Redox Signal*. 2017;26(14):748-762.

159.Wang Q, Chuikov S, Taitano S, et al. Dimethyl Fumarate Protects Neural Stem/Progenitor Cells and Neurons from Oxidative Damage through Nrf2-ERK1/2 MAPK Pathway. *Int J Mol Sci*. 2015;16(6):13885-13907.

160.Go YM, Jones DP. Cysteine/cystine redox signaling in cardiovascular disease. *Free Radic Biol Med*. 2011;50(4):495-509.

161.Ushio-Fukai M. Compartmentalization of redox signaling through NADPH oxidase-derived ROS. *Antioxid Redox Signal*. 2009;11(6):1289-1299.

162.Connor KM, Subbaram S, Regan KJ, et al. Mitochondrial H2O2 regulates the angiogenic phenotype via PTEN oxidation. *J Biol Chem*. 2005;280(17):16916-16924.

163.Cassano S, Agnese S, D'Amato V, et al. Reactive oxygen species, Ki-Ras, and mitochondrial superoxide dismutase cooperate in nerve growth factor-induced differentiation of PC12 cells. *J Biol Chem*. 2010;285(31):24141-24153.

164.Archer SL, Gomberg-Maitland M, Maitland ML, Rich S, Garcia JG, Weir EK. Mitochondrial metabolism, redox signaling, and fusion: a mitochondria-ROS-HIF-1alpha-Kv1.5 O2-sensing pathway at the intersection of pulmonary hypertension and cancer. *Am J Physiol Heart Circ Physiol*. 2008;294(2):H570-578.

165.Ohashi M, Runge MS, Faraci FM, Heistad DD. MnSOD deficiency increases endothelial dysfunction in ApoE-deficient mice. *Arterioscler Thromb Vasc Biol*. 2006;26(10):2331-2336.

166.Wenzel P, Schuhmacher S, Kienhofer J, et al. Manganese superoxide dismutase and aldehyde dehydrogenase deficiency increase mitochondrial oxidative stress and aggravate age-dependent vascular dysfunction. *Cardiovasc Res*. 2008;80(2):280-289.

167.Armenis I, Kalotychou V, Tzanetea R, et al. Reduced peripheral blood superoxide dismutase 2 expression in sickle cell disease. *Ann Hematol*. 2019.

168.Wang Y, Branicky R, Noe A, Hekimi S. Superoxide dismutases: Dual roles in controlling ROS damage and regulating ROS signaling. *J Cell Biol*. 2018;217(6):1915-1928.

169.Brand MD, Affourtit C, Esteves TC, et al. Mitochondrial superoxide: production, biological effects, and activation of uncoupling proteins. *Free Radic Biol Med*. 2004;37(6):755-767.

170.Brown GC. Nitric oxide and mitochondria. *Front Biosci*. 2007;12:1024-1033.

171.Radi R, Beckman JS, Bush KM, Freeman BA. Peroxynitrite oxidation of sulfhydryls. The cytotoxic potential of superoxide and nitric oxide. *J Biol Chem*. 1991;266(7):4244-4250.

172.Schmidt HM, Kelley EE, Straub AC. The impact of xanthine oxidase (XO) on hemolytic diseases. *Redox Biol*. 2019;21:101072.

173.Aslan M, Ryan TM, Adler B, et al. Oxygen radical inhibition of nitric oxide-dependent vascular function in sickle cell disease. *Proc Natl Acad Sci U S A*. 2001;98(26):15215-15220.

174.Osarogiagbon UR, Choong S, Belcher JD, Vercellotti GM, Paller MS, Hebbel RP. Reperfusion injury pathophysiology in sickle transgenic mice. *Blood*. 2000;96(1):314-320.

175.Musicki B, Liu T, Sezen SF, Burnett AL. Targeting NADPH oxidase decreases oxidative stress in the transgenic sickle cell mouse penis. *J Sex Med*. 2012;9(8):1980-1987.

176.George A, Pushkaran S, Konstantinidis DG, et al. Erythrocyte NADPH oxidase activity modulated by Rac GTPases, PKC, and plasma cytokines contributes to oxidative stress in sickle cell disease. *Blood*. 2013;121(11):2099-2107.

177.Wood KC, Hebbel RP, Granger DN. Endothelial cell NADPH oxidase mediates the cerebral microvascular dysfunction in sickle cell transgenic mice. *FASEB J*. 2005;19(8):989-991.

178.Bank N, Aynedjian HS, Qiu JH, et al. Renal nitric oxide synthases in transgenic sickle cell mice. *Kidney Int*. 1996;50(1):184-189.

179.Chandel NS, Maltepe E, Goldwasser E, Mathieu CE, Simon MC, Schumacker PT. Mitochondrial reactive oxygen species trigger hypoxia-induced transcription. *Proc Natl Acad Sci U S A*. 1998;95(20):11715-11720.

180.Wood KC, Hsu LL, Gladwin MT. Sickle cell disease vasculopathy: a state of nitric oxide resistance. *Free Radic Biol Med*. 2008;44(8):1506-1528.

181.Hebbel RP, Morgan WT, Eaton JW, Hedlund BE. Accelerated autoxidation and heme loss due to instability of sickle hemoglobin. *Proc Natl Acad Sci U S A*. 1988;85(1):237-241.

182.Moestrup SK, Moller HJ. CD163: a regulated hemoglobin scavenger receptor with a role in the anti-inflammatory response. *Ann Med*. 2004;36(5):347-354.

183.Wood KC, Hebbel RP, Lefer DJ, Granger DN. Critical role of endothelial cell-derived nitric oxide synthase in sickle cell disease-induced microvascular dysfunction. *Free Radic Biol Med*. 2006;40(8):1443-1453.

184.Kato GJ, Martyr S, Blackwelder WC, et al. Levels of soluble endothelium-derived adhesion molecules in patients with sickle cell disease are associated with pulmonary hypertension, organ dysfunction, and mortality. *Br J Haematol*. 2005;130(6):943-953.

185.Setty BN, Stuart MJ. Vascular cell adhesion molecule-1 is involved in mediating hypoxia-induced sickle red blood cell adherence to endothelium: potential role in sickle cell disease. *Blood*. 1996;88(6):2311-2320.

186.Sultana C, Shen Y, Rattan V, Johnson C, Kalra VK. Interaction of sickle erythrocytes with endothelial cells in the presence of endothelial cell conditioned medium induces oxidant stress leading to transendothelial migration of monocytes. *Blood*. 1998;92(10):3924-3935.

187.Lebovitz RM, Zhang H, Vogel H, et al. Neurodegeneration, myocardial injury, and perinatal death in mitochondrial superoxide dismutase-deficient mice. *Proc Natl Acad Sci U S A*. 1996;93(18):9782-9787.

188.Friedman JS, Rebel VI, Derby R, et al. Absence of mitochondrial superoxide dismutase results in a murine hemolytic anemia responsive to therapy with a catalytic antioxidant. *J Exp Med*. 2001;193(8):925-934.

189.Mohanty JG, Nagababu E, Friedman JS, Rifkind JM. SOD2 deficiency in hematopoietic cells in mice results in reduced red blood cell deformability and increased heme degradation. *Exp Hematol*. 2013;41(3):316-321.

190.Fidler TP, Rowley JW, Araujo C, et al. Superoxide Dismutase 2 is dispensable for platelet function. *Thromb Haemost*. 2017;117(10):1859-1867.

191.Shao J, Chen L, Marrs B, et al. SOD2 polymorphisms: unmasking the effect of polymorphism on splicing. *BMC Med Genet*. 2007;8:7.

192.Iida R, Tsubota E, Takeshita H, Yasuda T. Multiplex single base extension method for simultaneous genotyping of non-synonymous SNP in the three human SOD genes. *Electrophoresis*. 2008;29(23):4788-4794.

193.Farias ICC, Mendonca-Belmont TF, da Silva AS, et al. Association of the SOD2 Polymorphism (Val16Ala) and SOD Activity with Vaso-occlusive Crisis and Acute Splenic Sequestration in Children with Sickle Cell Anemia. *Mediterr J Hematol Infect Dis*. 2018;10(1):e2018012.

194.Martin RC, Li Y, Liu Q, et al. Manganese superoxide dismutase V16A single-nucleotide polymorphism in the mitochondrial targeting sequence is associated with reduced enzymatic activity in cryopreserved human hepatocytes. *DNA Cell Biol*. 2009;28(1):3-7.

195.Bastaki M, Huen K, Manzanillo P, et al. Genotype-activity relationship for Mn-superoxide dismutase, glutathione peroxidase 1 and catalase in humans. *Pharmacogenet Genomics*. 2006;16(4):279-286.

196.Lek M, Karczewski KJ, Minikel EV, et al. Analysis of protein-coding genetic variation in 60,706 humans. *Nature*. 2016;536(7616):285-291.

197.Ganini D, Santos JH, Bonini MG, Mason RP. Switch of Mitochondrial Superoxide Dismutase into a Prooxidant Peroxidase in Manganese-Deficient Cells and Mice. *Cell Chem Biol*. 2018;25(4):413-425 e416.

198.van Beers EJ, Yang Y, Raghavachari N, et al. Iron, inflammation, and early death in adults with sickle cell disease. *Circ Res*. 2015;116(2):298-306.

199.Alachkar H, Fulton N, Sanford B, et al. Expression and polymorphism (rs4880) of mitochondrial superoxide dismutase (SOD2) and asparaginase induced hepatotoxicity in adult patients with acute lymphoblastic leukemia. *Pharmacogenomics J*. 2017;17(3):274-279.

200.Hassani S, Ghaffari P, Chahardouli B, et al. Disulfiram/copper causes ROS levels alteration, cell cycle inhibition, and apoptosis in acute myeloid leukaemia cell lines with modulation in the expression of related genes. *Biomed Pharmacother*. 2018;99:561-569.

201.Zhang H, Li L, Li M, et al. Combination of betulinic acid and chidamide inhibits acute myeloid leukemia by suppression of the HIF1alpha pathway and generation of reactive oxygen species. *Oncotarget*. 2017;8(55):94743-94758.

202.Barr PM, Miller TP, Friedberg JW, et al. Phase 2 study of imexon, a prooxidant molecule, in relapsed and refractory B-cell non-Hodgkin lymphoma. *Blood*. 2014;124(8):1259-1265.

203.Dikalova AE, Itani HA, Nazarewicz RR, et al. Sirt3 Impairment and SOD2 Hyperacetylation in Vascular Oxidative Stress and Hypertension. *Circ Res*. 2017;121(5):564-574.

204.Rodriguez-Iturbe B, Sepassi L, Quiroz Y, Ni Z, Wallace DC, Vaziri ND. Association of mitochondrial SOD deficiency with salt-sensitive hypertension and accelerated renal senescence. *J Appl Physiol (1985)*. 2007;102(1):255-260.

205.Mehari A, Gladwin MT, Tian X, Machado RF, Kato GJ. Mortality in adults with sickle cell disease and pulmonary hypertension. *JAMA*;307(12):1254-1256.

206.Parent F, Bachir D, Inamo J, et al. A hemodynamic study of pulmonary hypertension in sickle cell disease. *N Engl J Med*. 2011;365(1):44-53.

207.Talahma M, Strbian D, Sundararajan S. Sickle cell disease and stroke. *Stroke*. 2014;45(6):e98-100.

208.Domingos IF, Pereira-Martins DA, Borges-Medeiros RL, et al. Evaluation of oxidative stress-related genetic variants for predicting stroke in patients with sickle cell anemia. *J Neurol Sci*. 2020;414:116839.

209.Sutton A, Imbert A, Igoudjil A, et al. The manganese superoxide dismutase Ala16Val dimorphism modulates both mitochondrial import and mRNA stability. *Pharmacogenet Genomics*. 2005;15(5):311-319.

210.Machado RF, Barst RJ, Yovetich NA, et al. Hospitalization for pain in patients with sickle cell disease treated with sildenafil for elevated TRV and low exercise capacity. *Blood*. 2011;118(4):855-864.

211.Richards TJ, Park C, Chen Y, et al. Allele-specific transactivation of matrix metalloproteinase 7 by FOXA2 and correlation with plasma levels in idiopathic pulmonary fibrosis. *Am J Physiol Lung Cell Mol Physiol*. 2012;302(8):L746-754.

212.Gurtu V, Yan G, Zhang G. IRES bicistronic expression vectors for efficient creation of stable mammalian cell lines. *Biochem Biophys Res Commun*. 1996;229(1):295-298.

213.Lee SY, Kang MG, Park JS, Lee G, Ting AY, Rhee HW. APEX Fingerprinting Reveals the Subcellular Localization of Proteins of Interest. *Cell Rep*. 2016;15(8):1837-1847.

214.Rigo A, Viglino P, Rotilio G. Kinetic study of O-2 DISMUTATION BY BOVINE SUPEROXIDE DISMUTASE. Evidence for saturation of the catalytic sites by O-2. *Biochem Biophys Res Commun*. 1975;63(4):1013-1018.

215.Kolesar JE, Kaufman BA. Using Two-Dimensional Intact Mitochondrial DNA (mtDNA) Agarose Gel Electrophoresis (2D-IMAGE) to Detect Changes in Topology Associated with Mitochondrial Replication, Transcription, and Damage. *Methods Mol Biol*. 2020;2119:25-42.

216.Ware SA, Desai N, Lopez M, et al. An automated, high-throughput methodology optimized for quantitative cell-free mitochondrial and nuclear DNA isolation from plasma. *J Biol Chem*. 2020;295(46):15677-15691.

217.Xu W, Cardenes N, Corey C, Erzurum SC, Shiva S. Platelets from Asthmatic Individuals Show Less Reliance on Glycolysis. *PLoS One*. 2015;10(7):e0132007.

218.Galley JC, Durgin BG, Miller MP, et al. Antagonism of Forkhead Box Subclass O Transcription Factors Elicits Loss of Soluble Guanylyl Cyclase Expression. *Mol Pharmacol*. 2019;95(6):629-637.

219.Yuan S, Patel RP, Kevil CG. Working with nitric oxide and hydrogen sulfide in biological systems. *Am J Physiol Lung Cell Mol Physiol*. 2015;308(5):L403-415.

220.Kato GJ, McGowan V, Machado RF, et al. Lactate dehydrogenase as a biomarker of hemolysis-associated nitric oxide resistance, priapism, leg ulceration, pulmonary hypertension, and death in patients with sickle cell disease. *Blood*. 2006;107(6):2279-2285.

221.Jovanovic P, Zoric L, Stefanovic I, et al. Lactate dehydrogenase and oxidative stress activity in primary open-angle glaucoma aqueous humour. *Bosn J Basic Med Sci*. 2010;10(1):83-88.

222.Sheng Y, Abreu IA, Cabelli DE, et al. Superoxide dismutases and superoxide reductases. *Chem Rev*. 2014;114(7):3854-3918.

223.Kadenbach B. Complex IV - The regulatory center of mitochondrial oxidative phosphorylation. *Mitochondrion*. 2021;58:296-302.

224.Rolland SG, Motori E, Memar N, et al. Impaired complex IV activity in response to loss of LRPPRC function can be compensated by mitochondrial hyperfusion. *Proc Natl Acad Sci U S A*. 2013;110(32):E2967-2976.

225.Thomas SR, Chen K, Keaney JF, Jr. Hydrogen peroxide activates endothelial nitric-oxide synthase through coordinated phosphorylation and dephosphorylation via a phosphoinositide 3-kinase-dependent signaling pathway. *J Biol Chem*. 2002;277(8):6017-6024.

226.Suthammarak W, Somerlot BH, Opheim E, Sedensky M, Morgan PG. Novel interactions between mitochondrial superoxide dismutases and the electron transport chain. *Aging Cell*. 2013;12(6):1132-1140.

227.Caruana NJ, Stroud DA. The road to the structure of the mitochondrial respiratory chain supercomplex. *Biochem Soc Trans*. 2020;48(2):621-629.

228.Huttemann M, Kadenbach B, Grossman LI. Mammalian subunit IV isoforms of cytochrome c oxidase. *Gene*. 2001;267(1):111-123.

229.Kim HJ, Khalimonchuk O, Smith PM, Winge DR. Structure, function, and assembly of heme centers in mitochondrial respiratory complexes. *Biochim Biophys Acta*. 2012;1823(9):1604-1616.

230.He C, Danes JM, Hart PC, et al. SOD2 acetylation on lysine 68 promotes stem cell reprogramming in breast cancer. *Proc Natl Acad Sci U S A*. 2019;116(47):23534-23541.

231.Ghezzi D, Viscomi C, Ferlini A, et al. Paroxysmal non-kinesigenic dyskinesia is caused by mutations of the MR-1 mitochondrial targeting sequence. *Hum Mol Genet*. 2009;18(6):1058-1064.

232.Nicolay K, Laterveer FD, van Heerde WL. Effects of amphipathic peptides, including presequences, on the functional integrity of rat liver mitochondrial membranes. *J Bioenerg Biomembr*. 1994;26(3):327-334.

233.Vona R, Sposi NM, Mattia L, Gambardella L, Straface E, Pietraforte D. Sickle Cell Disease: Role of Oxidative Stress and Antioxidant Therapy. *Antioxidants (Basel)*. 2021;10(2).

234.Dosunmu-Ogunbi AM, Wood KC, Novelli EM, Straub AC. Decoding the role of SOD2 in sickle cell disease. *Blood Adv*. 2019;3(17):2679-2687.

235.Murphy MP, Hartley RC. Mitochondria as a therapeutic target for common pathologies. *Nat Rev Drug Discov*. 2018;17(12):865-886.

236.Schmidt HM, Wood KC, Lewis SE, et al. Xanthine Oxidase Drives Hemolysis and Vascular Malfunction in Sickle Cell Disease. *Arterioscler Thromb Vasc Biol*. 2021;41(2):769-782.

237.Thomas C, Mackey MM, Diaz AA, Cox DP. Hydroxyl radical is produced via the Fenton reaction in submitochondrial particles under oxidative stress: implications for diseases associated with iron accumulation. *Redox Rep*. 2009;14(3):102-108.

238.Castro O, Brambilla DJ, Thorington B, et al. The acute chest syndrome in sickle cell disease: incidence and risk factors. The Cooperative Study of Sickle Cell Disease. *Blood*. 1994;84(2):643-649.

239.Gladwin MT, Sachdev V, Jison ML, et al. Pulmonary hypertension as a risk factor for death in patients with sickle cell disease. *N Engl J Med*. 2004;350(9):886-895.

240.Ataga KI, Moore CG, Jones S, et al. Pulmonary hypertension in patients with sickle cell disease: a longitudinal study. *Br J Haematol*. 2006;134(1):109-115.

241.De Castro LM, Jonassaint JC, Graham FL, Ashley-Koch A, Telen MJ. Pulmonary hypertension associated with sickle cell disease: clinical and laboratory endpoints and disease outcomes. *Am J Hematol*. 2008;83(1):19-25.

242.Ohene-Frempong K, Weiner SJ, Sleeper LA, et al. Cerebrovascular accidents in sickle cell disease: rates and risk factors. *Blood*. 1998;91(1):288-294.

243.Adams RJ, McKie VC, Carl EM, et al. Long-term stroke risk in children with sickle cell disease screened with transcranial Doppler. *Ann Neurol*. 1997;42(5):699-704.

244.Brousse V, Elie C, Benkerrou M, et al. Acute splenic sequestration crisis in sickle cell disease: cohort study of 190 paediatric patients. *Br J Haematol*. 2012;156(5):643-648.

245.Zadeii G, Lohr JW. Renal papillary necrosis in a patient with sickle cell trait. *J Am Soc Nephrol*. 1997;8(6):1034-1039.

246.Eckert DE, Jonutis AJ, Davidson AJ. The incidence and manifestations of urographic papillary abnormalities in patients with S hemoglobinopathies. *Radiology*. 1974;113(1):59-63.

247.Bender MA. Sickle Cell Disease. In: Adam MP, Ardinger HH, Pagon RA, et al., eds. GeneReviews((R)). Seattle (WA); 1993.

248.Sutton LL, Castro O, Cross DJ, Spencer JE, Lewis JF. Pulmonary hypertension in sickle cell disease. *Am J Cardiol*. 1994;74(6):626-628.

249.Klinger JR, Abman SH, Gladwin MT. Nitric oxide deficiency and endothelial dysfunction in pulmonary arterial hypertension. *Am J Respir Crit Care Med*. 2013;188(6):639-646.

250.Novelli EM, Little-Ihrig L, Knupp HE, et al. Vascular TSP1-CD47 signaling promotes sickle cell-associated arterial vasculopathy and pulmonary hypertension in mice. *Am J Physiol Lung Cell Mol Physiol*. 2019;316(6):L1150-L1164.

251.Bowers R, Cool C, Murphy RC, et al. Oxidative stress in severe pulmonary hypertension. *Am J Respir Crit Care Med*. 2004;169(6):764-769.

252.Wang JN, Shi N, Chen SY. Manganese superoxide dismutase inhibits neointima formation through attenuation of migration and proliferation of vascular smooth muscle cells. *Free Radic Biol Med*. 2012;52(1):173-181.

253.Sharma S, Bhattarai S, Ara H, et al. SOD2 deficiency in cardiomyocytes defines defective mitochondrial bioenergetics as a cause of lethal dilated cardiomyopathy. *Redox Biol*. 2020;37:101740.

254.Armenis I, Kalotychou V, Tzanetea R, et al. Reduced peripheral blood superoxide dismutase 2 expression in sickle cell disease. *Ann Hematol*. 2019;98(7):1561-1572.

255.Mehari A, Alam S, Tian X, et al. Hemodynamic predictors of mortality in adults with sickle cell disease. *Am J Respir Crit Care Med*. 2013;187(8):840-847.

256.Schindelin J, Arganda-Carreras I, Frise E, et al. Fiji: an open-source platform for biological-image analysis. *Nat Methods*. 2012;9(7):676-682.

257.Feinberg AW, Parker KK. Surface-initiated assembly of protein nanofabrics. *Nano Lett*. 2010;10(6):2184-2191.

258.Shiwarski DJ, Tashman JW, Tsamis A, et al. Fibronectin-based nanomechanical biosensors to map 3D surface strains in live cells and tissue. *Nat Commun*. 2020;11(1):5883.

259.Santaterra VAG, Fiusa MML, Hounkpe BW, et al. Endothelial Barrier Integrity Is Disrupted In Vitro by Heme and by Serum From Sickle Cell Disease Patients. *Front Immunol*. 2020;11:535147.

260.Ghosh S, Adisa OA, Chappa P, et al. Extracellular hemin crisis triggers acute chest syndrome in sickle mice. *J Clin Invest*. 2013;123(11):4809-4820.

261.Minniti CP, Eckman J, Sebastiani P, Steinberg MH, Ballas SK. Leg ulcers in sickle cell disease. *Am J Hematol*. 2010;85(10):831-833.

262.Sarelius IH, Glading AJ. Control of vascular permeability by adhesion molecules. *Tissue Barriers*. 2015;3(1-2):e985954.

263.Houreld NN, Ayuk SM, Abrahamse H. Cell Adhesion Molecules are Mediated by Photobiomodulation at 660 nm in Diabetic Wounded Fibroblast Cells. *Cells*. 2018;7(4).

264.Boettiger D. Mechanical control of integrin-mediated adhesion and signaling. *Curr Opin Cell Biol*. 2012;24(5):592-599.

265.Boettiger D, Lynch L, Blystone S, Huber F. Distinct ligand-binding modes for integrin alpha(v)beta(3)-mediated adhesion to fibronectin versus vitronectin. *J Biol Chem*. 2001;276(34):31684-31690.

266.Khalili AA, Ahmad MR. A Review of Cell Adhesion Studies for Biomedical and Biological Applications. *Int J Mol Sci*. 2015;16(8):18149-18184.

267.Krueger K, Shen J, Maier A, Tepel M, Scholze A. Lower Superoxide Dismutase 2 (SOD2) Protein Content in Mononuclear Cells Is Associated with Better Survival in Patients with Hemodialysis Therapy. *Oxid Med Cell Longev*. 2016;2016:7423249.

268.Vendrov AE, Stevenson MD, Alahari S, et al. Attenuated Superoxide Dismutase 2 Activity Induces Atherosclerotic Plaque Instability During Aging in Hyperlipidemic Mice. *J Am Heart Assoc*. 2017;6(11).

269.Liu Z, Gou Y, Zhang H, et al. Estradiol improves cardiovascular function through up-regulation of SOD2 on vascular wall. *Redox Biol*. 2014;3:88-99.

270.Cramer-Morales K, Heer CD, Mapuskar KA, Domann FE. SOD2 targeted gene editing by CRISPR/Cas9 yields Human cells devoid of MnSOD. *Free Radic Biol Med*. 2015;89:379-386.

271.Koike M, Nojiri H, Ozawa Y, et al. Mechanical overloading causes mitochondrial superoxide and SOD2 imbalance in chondrocytes resulting in cartilage degeneration. *Sci Rep*. 2015;5:11722.

272.Leung SWS, Shi Y. The glycolytic process in endothelial cells and its implications. *Acta Pharmacol Sin*. 2021.

273.Zorova LD, Popkov VA, Plotnikov EY, et al. Mitochondrial membrane potential. *Anal Biochem*. 2018;552:50-59.

274.Garcia-Santamarina S, Boronat S, Hidalgo E. Reversible cysteine oxidation in hydrogen peroxide sensing and signal transduction. *Biochemistry*. 2014;53(16):2560-2580.

275.Louie JE, Anderson CJ, Fayaz MFK, et al. Case series supporting heme detoxification via therapeutic plasma exchange in acute multiorgan failure syndrome resistant to red blood cell exchange in sickle cell disease. *Transfusion*. 2018;58(2):470-479.

276.Singla S, Sysol JR, Dille B, Jones N, Chen J, Machado RF. Hemin Causes Lung Microvascular Endothelial Barrier Dysfunction by Necroptotic Cell Death. *Am J Respir Cell Mol Biol*. 2017;57(3):307-314.

277.Noubouossie D, Key NS, Ataga KI. Coagulation abnormalities of sickle cell disease: Relationship with clinical outcomes and the effect of disease modifying therapies. *Blood Rev*. 2016;30(4):245-256.

278.Nguyen EK, Koval OM, Noble P, et al. CaMKII (Ca(2+)/Calmodulin-Dependent Kinase II) in Mitochondria of Smooth Muscle Cells Controls Mitochondrial Mobility, Migration, and Neointima Formation. *Arterioscler Thromb Vasc Biol*. 2018;38(6):1333-1345.

279.Alexander JS, Elrod JW. Extracellular matrix, junctional integrity and matrix metalloproteinase interactions in endothelial permeability regulation. *J Anat*. 2002;200(6):561-574.

280.Oharazawa H, Ibaraki N, Lin LR, Reddy VN. The effects of extracellular matrix on cell attachment, proliferation and migration in a human lens epithelial cell line. *Exp Eye Res*. 1999;69(6):603-610.

281.McDonald JA. Extracellular matrix assembly. *Annu Rev Cell Biol*. 1988;4:183-207.

282.Schwarzbauer JE. Identification of the fibronectin sequences required for assembly of a fibrillar matrix. *J Cell Biol*. 1991;113(6):1463-1473.

283.Fogelgren B, Polgar N, Szauter KM, et al. Cellular fibronectin binds to lysyl oxidase with high affinity and is critical for its proteolytic activation. *J Biol Chem*. 2005;280(26):24690-24697.

284.Missirlis D, Haraszti T, Kessler H, Spatz JP. Fibronectin promotes directional persistence in fibroblast migration through interactions with both its cell-binding and heparin-binding domains. *Sci Rep*. 2017;7(1):3711.

285.Beyeler J, Katsaros C, Chiquet M. Impaired Contracture of 3D Collagen Constructs by Fibronectin-Deficient Murine Fibroblasts. *Front Physiol*. 2019;10:166.

286.Giacco F, Brownlee M. Oxidative stress and diabetic complications. *Circ Res*. 2010;107(9):1058-1070.

287.Reuter S, Gupta SC, Chaturvedi MM, Aggarwal BB. Oxidative stress, inflammation, and cancer: how are they linked? *Free Radic Biol Med*. 2010;49(11):1603-1616.

288.Daenen K, Andries A, Mekahli D, Van Schepdael A, Jouret F, Bammens B. Oxidative stress in chronic kidney disease. *Pediatr Nephrol*. 2019;34(6):975-991.

289.Dhalla NS, Temsah RM, Netticadan T. Role of oxidative stress in cardiovascular diseases. *J Hypertens*. 2000;18(6):655-673.

290.Liguori I, Russo G, Curcio F, et al. Oxidative stress, aging, and diseases. *Clin Interv Aging*. 2018;13:757-772.

291.Barnham KJ, Masters CL, Bush AI. Neurodegenerative diseases and oxidative stress. *Nat Rev Drug Discov*. 2004;3(3):205-214.

292.Flynn JM, Melov S. SOD2 in mitochondrial dysfunction and neurodegeneration. *Free Radic Biol Med*. 2013;62:4-12.

293.Wang Z, Ying Z, Bosy-Westphal A, et al. Specific metabolic rates of major organs and tissues across adulthood: evaluation by mechanistic model of resting energy expenditure. *Am J Clin Nutr*. 2010;92(6):1369-1377.

294.Akohoue SA, Shankar S, Milne GL, et al. Energy expenditure, inflammation, and oxidative stress in steady-state adolescents with sickle cell anemia. *Pediatr Res*. 2007;61(2):233-238.

295.Jastroch M, Divakaruni AS, Mookerjee S, Treberg JR, Brand MD. Mitochondrial proton and electron leaks. *Essays Biochem*. 2010;47:53-67.

296.Martino S, Arlet JB, Odievre MH, et al. Deficient mitophagy pathways in sickle cell disease. *Br J Haematol*. 2021;193(5):988-993.

297.Gbotosho OT, Kapetanaki MG, Kato GJ. The Worst Things in Life are Free: The Role of Free Heme in Sickle Cell Disease. *Front Immunol*. 2020;11:561917.

298.Higdon AN, Benavides GA, Chacko BK, et al. Hemin causes mitochondrial dysfunction in endothelial cells through promoting lipid peroxidation: the protective role of autophagy. *Am J Physiol Heart Circ Physiol*. 2012;302(7):H1394-1409.

299.Archer SL, Marsboom G, Kim GH, et al. Epigenetic attenuation of mitochondrial superoxide dismutase 2 in pulmonary arterial hypertension: a basis for excessive cell proliferation and a new therapeutic target. *Circulation*. 2010;121(24):2661-2671.

300.Fu C, Hao S, Liu Z, et al. SOD2 ameliorates pulmonary hypertension in a murine model of sleep apnea via suppressing expression of NLRP3 in CD11b(+) cells. *Respir Res*. 2020;21(1):9.

301.Peinemann F, Sauerland S. Negative-pressure wound therapy: systematic review of randomized controlled trials. *Dtsch Arztebl Int*. 2011;108(22):381-389.

302.Bellot GL, Dong X, Lahiri A, et al. MnSOD is implicated in accelerated wound healing upon Negative Pressure Wound Therapy (NPWT): A case in point for MnSOD mimetics as adjuvants for wound management. *Redox Biol*. 2019;20:307-320.

303.Kumar AP, Loo SY, Shin SW, et al. Manganese superoxide dismutase is a promising target for enhancing chemosensitivity of basal-like breast carcinoma. *Antioxid Redox Signal*. 2014;20(15):2326-2346.

304.Loo SY, Hirpara JL, Pandey V, et al. Manganese Superoxide Dismutase Expression Regulates the Switch Between an Epithelial and a Mesenchymal-Like Phenotype in Breast Carcinoma. *Antioxid Redox Signal*. 2016;25(6):283-299.

305.Steinberg MH, Sebastiani P. Genetic modifiers of sickle cell disease. *Am J Hematol*. 2012;87(8):795-803.

306.Garner C, Tatu T, Reittie JE, et al. Genetic influences on F cells and other hematologic variables: a twin heritability study. *Blood*. 2000;95(1):342-346.

307.Platt OS, Brambilla DJ, Rosse WF, et al. Mortality in sickle cell disease. Life expectancy and risk factors for early death. *N Engl J Med*. 1994;330(23):1639-1644.

308.Platt OS, Thorington BD, Brambilla DJ, et al. Pain in sickle cell disease. Rates and risk factors. *N Engl J Med*. 1991;325(1):11-16.

309.Nolan VG, Adewoye A, Baldwin C, et al. Sickle cell leg ulcers: associations with haemolysis and SNPs in Klotho, TEK and genes of the TGF-beta/BMP pathway. *Br J Haematol*. 2006;133(5):570-578.

310.Wilber A, Nienhuis AW, Persons DA. Transcriptional regulation of fetal to adult hemoglobin switching: new therapeutic opportunities. *Blood*. 2011;117(15):3945-3953.

311.Ma Q, Wyszynski DF, Farrell JJ, et al. Fetal hemoglobin in sickle cell anemia: genetic determinants of response to hydroxyurea. *Pharmacogenomics J*. 2007;7(6):386-394.

312.Steinberg MH, Embury SH. Alpha-thalassemia in blacks: genetic and clinical aspects and interactions with the sickle hemoglobin gene. *Blood*. 1986;68(5):985-990.

313.Flanagan JM, Frohlich DM, Howard TA, et al. Genetic predictors for stroke in children with sickle cell anemia. *Blood*. 2011;117(24):6681-6684.

314.De Ceulaer K, Serjeant GR. Acute splenic sequestration in Jamaican adults with homozygous sickle cell disease: a role of alpha thalassaemia. *Br J Haematol*. 1991;77(4):563-564.

315.Darbari DS, Onyekwere O, Nouraie M, et al. Markers of severe vaso-occlusive painful episode frequency in children and adolescents with sickle cell anemia. *J Pediatr*. 2012;160(2):286-290.

316.Milner PF, Kraus AP, Sebes JI, et al. Sickle cell disease as a cause of osteonecrosis of the femoral head. *N Engl J Med*. 1991;325(21):1476-1481.

317.Wonkam A, Chimusa ER, Mnika K, et al. Genetic modifiers of long-term survival in sickle cell anemia. *Clin Transl Med*. 2020;10(4):e152.

318.Hoppe C, Klitz W, Cheng S, et al. Gene interactions and stroke risk in children with sickle cell anemia. *Blood*. 2004;103(6):2391-2396.

319.Day BJ. Antioxidant therapeutics: Pandora's box. *Free Radic Biol Med*. 2014;66:58-64.

320.Firuzi O, Miri R, Tavakkoli M, Saso L. Antioxidant therapy: current status and future prospects. *Curr Med Chem*. 2011;18(25):3871-3888.

321.Emerit J, Michelson AM, Robert HG, et al. [Superoxide dismutase treatment of 2 cases of radiation-induced sclerosis]. *Sem Hop*. 1983;59(4):277-281.

322.Land W, Schneeberger H, Schleibner S, et al. The beneficial effect of human recombinant superoxide dismutase on acute and chronic rejection events in recipients of cadaveric renal transplants. *Transplantation*. 1994;57(2):211-217.

323.Guillaume M, Rodriguez-Vilarrupla A, Gracia-Sancho J, et al. Recombinant human manganese superoxide dismutase reduces liver fibrosis and portal pressure in CCl4-cirrhotic rats. *J Hepatol*. 2013;58(2):240-246.

324.Turrens JF, Crapo JD, Freeman BA. Protection against oxygen toxicity by intravenous injection of liposome-entrapped catalase and superoxide dismutase. *J Clin Invest*. 1984;73(1):87-95.

325.Tarhini AA, Belani CP, Luketich JD, et al. A phase I study of concurrent chemotherapy (paclitaxel and carboplatin) and thoracic radiotherapy with swallowed manganese superoxide dismutase plasmid liposome protection in patients with locally advanced stage III non-small-cell lung cancer. *Hum Gene Ther*. 2011;22(3):336-342.

326.Coudriet GM, Delmastro-Greenwood MM, Previte DM, et al. Treatment with a Catalytic Superoxide Dismutase (SOD) Mimetic Improves Liver Steatosis, Insulin Sensitivity, and Inflammation in Obesity-Induced Type 2 Diabetes. *Antioxidants (Basel)*. 2017;6(4).

327.Shrishrimal S, Kosmacek EA, Chatterjee A, Tyson MJ, Oberley-Deegan RE. The SOD Mimic, MnTE-2-PyP, Protects from Chronic Fibrosis and Inflammation in Irradiated Normal Pelvic Tissues. *Antioxidants (Basel)*. 2017;6(4).